약학박사 학위논문

Angular Dihydropyranocoumarins from *Peucedanum japonicum* Roots

식방풍의 angular dihydropyranocoumarin 화합물

2017 년 8 월

서울대학교 대학원

약학과 생약학전공

홍 민 지

Angular Dihydropyranocoumarins

from *Peucedanum japonicum* Roots

식방풍의 angular dihydropyranocoumarin 화합물

지도 교수 김 진 웅

이 논문을 약학박사 학위논문으로 제출함

2017 년 5 월

서울대학교 대학원

약학과 생약학전공

홍 민 지

홍민지의 약학박사 학위논문을 인준함

2017 년 6 월

위 원 장 _____ (인)

부위원장 _____ (인)

위 원 _____ (인)

위 원 _____ (인)

위 원 _____ (인)

Abstract

Peucedanum japonicum Thunberg, belongs to Umbelliferae family, was distributed in southern and eastern Asian countries. Its roots were traditionally used as a medicine for cold and neuralgic diseases in Korea and Taiwan.

It was reported that the roots of this plant contained coumarins, chromones, polyacetylenes, sugar alcohols, and steroid glycosides. Pharmacological researches revealed that *P. japonicum* roots showed antioxidative, anti-inflammatory, antifungal activity and cytotoxic effect against lymphocytic leukaemia.

In this study, sixteen new angular dihydropyranocoumarins (**1-16**) and three new angular monohydromonohydroxyfuranocoumarins (**41-43**) were isolated along with forty-five known compounds from the *n*-hexane and $CHCl_3$ fractions of the *P. japonicum* roots. The known compounds were characterized as angular dihydropyranocoumarins (**17-40**), linear furanocoumarins (**44-47**), an angular dihydrofuranocoumarin (**48**), a linear dihydropyranocoumarin (**49**), simple coumarins (**50-58**), a chromone (**59**), ferulic acid derivatives (**60-61**), a lignan (**62**), a phenylpropanoid (**63**), and an indole alkaloid (**64**).

Isolated angular dihydropyranocoumarins (khellactones) included monoacyl- and diacyl-type khellactone esters. In the case of monoacylkhellactones, the absolute configuration was easily determined by the Mosher method. However, the absolute configuration of diacyl khellactone esters was difficult to assign due to the absence of free hydroxyl group. Therefore, partial alkaline hydrolysis prior to MTPA derivatization and X-ray diffraction analysis were applied to determine the absolute configurations at 3'- and 4'-positions. Because the success of partial hydrolysis and single crystallization was very difficult, ECD spectroscopy was suggested to confirm the absolute configuration of most of the compounds.

Interestingly, a few enantiomers were discovered and isolated by enantio-selective column. Enantiomers were usually detected and isolated using chiral column. However, RP-HPLC analysis with MTPA reaction products could be alternative method to confirm enantiomer existence without testing a number of

chiral-selective columns. In the case of *cis*-monoacylkhellactones, the interconversion of substituents at 3'- and 4'-position was observed. The major MS fragment peak of khellactone esters was detected without a C-4' substituent. Thus, the position of substituents at 3' and 4' could be determined by MS fragmentation analysis without HMBC measurement.

The NO production inhibitory activity of isolated compounds were tested using Griess assay in LPS-induced RAW264.7 cells. As a result, **1**, **3-6**, **22**, **31**, and **36-38** showed significant activity without cytotoxicity. The isobutyryl, senecioyl, 2-methylbutyryl, and isovaleryl moieties at 3' position played more important role than the acetyl and angeloyl groups.

In conclusion, the absolute configuration of isolated compounds were assigned by various methods. Those methods will become useful guide to solve similar structures. The isolated compounds which significantly inhibited NO production were suggested as anti-inflammatory candidates from natural resources.

Keyword : *Peucedanum japonicum*, angular dihydropyranocoumarins, khellactone esters, partial hydrolysis, X-ray crystallography, and Circular dichroism (CD)
Student Number : 2012-31116

Table of Contents

List of Schemes

List of Tables

List of Figures

List of Abbreviations

ACN	: acetonitrile
$[\alpha]_D$	: specific rotation
br s	: broad singlet
n-BuOH	: *n*-buthanol
CC	: column chromatography
CD	: circular dichroism
$CHCl_3$	: chloroform
CI	: chemical ionization
COSY	: correlation spectroscopy
d	: doublet
dd	: doublet of doublet
DMAP	: 4-dimethylaminopyridine
DMEM	: Dulbecco's modified Eagle's medium
DMSO	: dimethyl sulfoxide
dt	: doublet of triplet
ECD	: electronic circular dichroism
ESI	: electrospray ionization
EtOAc	: ethyl acetate
fr.	: fraction
HMBC	: heteronuclear multiple bond correlation
HPLC	: high performance liquid chromatography
HSQC	: heteronuclear single quantum coherence
Hz	: hertz
IC_{50}	: the half maximal inhibitory concentration
IR	: infrared absorption
LPS	: lipopolysaccharide
m	: multiplet
MeOH	: methanol
MS	: mass spectrometry

MTPA : α-methoxy-α-trifluoromethylphenylacetyl

MTT : 3-(4,5-dimethylthiazol-2-yl)-2,5-diphenyltetrazolium bromide

NEDHC : N-1-naphtylethylenediamine dihydrochloride

NMR : nuclear magnetic resonance

NO : nitric oxide

NOESY : nuclear overhauser effect spectroscopy

ODS : octadecyl silane

q : quartet

qd : quartet of doublet

Q-TOF : quadrupole-time of flight

qui : quintet

RP : reverse phase

rt : room temperature

s : singlet

sep : septet

sxt : sextet

t : triplet

TLC : thin layer chromatography

t_R : retention time

UV : ultraviolet absorption spectroscopy

Chapter 1. Introduction

1.1. Study Background

1.1.1. The genus *Peucedanum and Peucedanum japonicum* Thunberg

The genus *Peucedanum* belongs to Umbelliferae (Apiaceae) and there are more than 120 species, which are distributed in Europe, Asia, Africa, and North America. The major constituents of most *Peucedanum* plants are coumarins and essential oils like most plants of the Umbelliferae family and they are important for their pharmacological activities of *Peucedanum* species (Sarkhail 2014). Among the *Peucedanum* species, the most frequently studied species are *P. praeruptorum*, *P. japonicum*, and *P. decursivum*.

Peucedanum japonicum Thunberg is widely distributed in southern and eastern Asian countries. The roots of *P. japonicum* are cone or spindle shaped, are 5-15 cm long, and have 2-4 lateral roots (Whang et al. 2001). In Korea, Japan, China, and Taiwan, they have been traditionally used for cold and headache (Gan 1965; Bae 2001). Pharmacological studies reported that *P. japonicum* roots had antioxidative, anti-inflammatory (Kim et al. 2009; Choi et al. 1999), antifungal (Bae 2002), hypoglycemic (Lee et al. 2004), and antiplatelet aggregation activities (Hsiao et al. 1998; Chen et al. 1996). In addition, this plant also had vasorelaxant effect (Lee et al. 2002), MAO inhibitory activity (Huong et al. 1999), topoisomerase I inhibitory activity (Lee et al. 2000), cytotoxic effect against lymphocytic leukaemia (Duh et al. 1992), and chemopreventive effect against colon carcinogenesis (Morioka et al. 2004). It has been reported that coumarins (Chen et al. 1996; Ikeshiro et al. 1994, 1993, 1992; Duh et al. 1992), chromones, polyacetylenes (Lee et al. 2000), sugar alcohols (Lee et al. 2004), and steroid glycosides (Shin et al. 1992) were isolated from the roots of *P. japonicum*. Phytochemical studies proved that *P. japonicum* leaves possess coumarins (Jang et al. 2008; Hisamoto et al. 2003), flavonoids, phenylpropanoid glycosides (Hisamoto et al. 2004), phenol derivatives, C_{13} norisoprenoid glycosides, nucleosides, nucleobases, amino acids, and benzofuran glycosides. Based on the literature survey, it was revealed that the angular

dihydropyranocoumarins are major constituents of *P. japonicum* roots.

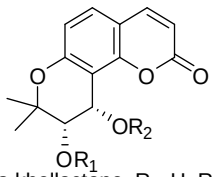

(-)-*cis*-khellactone, R_1=H, R_2=H
peujaponisinol A, R_1=Sen, R_2=H
peujaponisinol B, R_1=H, R_2=Sen
peujaponisin, R_1=Sen, R_2=*i*-Val
praeruptorin A, R_1=Ang, R_2=Ac
3'(*S*),4'(*S*)-diisovaleryloxy-3',4'-di hydroseselin, R_1=*i*-Val, R_2=*i*-Val
3'(*S*),4'(*S*)-disenecioyloxy-3',4'-di hydroseselin, R_1=Sen, R_2=Sen
(+)-anomalin, R_1=Ang, R_2=Ang
(+)-samidin, R_1=Sen, R_2=Ac
(-)-visnadin, R_1=MeBu, R_2=Ac
(+)-pteryxin, R_1=Ac, R_2=Ang

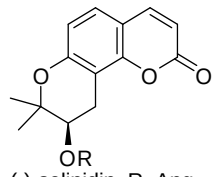

(-)-selinidin, R=Ang

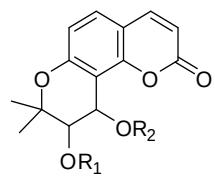

(±)-*cis*-3'-acetyl-4'-tigloylkhellactone, R_1=Ac, R_2=Tig
(±)-*cis*-4'-tigloylkhellactone, R_1=H, R_2=Tig

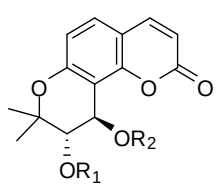

(+)-peucedanocoumarin III, R_1=Ac, R_2=Tig

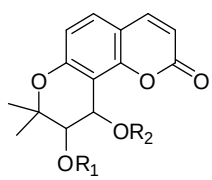

<Absolute configuration unknown>

(-)-*trans*-3'-acetyl-4'-senecioyl khellactone, R_1=Ac, R_2=Sen
(+)-*trans*-4'-tigloylkhellactone, R_1=H, R_2=Tig

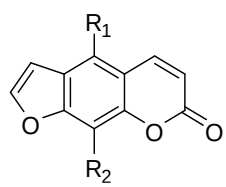

psoralen, R_1,R_2=H
xanthotoxin, R_1=H, R_2=OCH_3
bergapten, R_1=OCH_3, R_2=H
xanthotoxol, R_1=H, R_2=OH
isopimpinellin, R_1,R_2=OCH_3
imperatorin, R_1=H, R_2=OCH_2-CH=C-$(CH_3)_2$
isoimperatorin, R_1=OCH_2-CH=C-$(CH_3)_2$, R_2=H
cnidilin, R_1=OCH_2-CH=C-$(CH_3)_2$, R_2=OCH_3
(+)-oxypeucedanin hydrate, R_1=OCH_2-CH(OH)-C-$(CH_3)_2$(OH), R_2=H

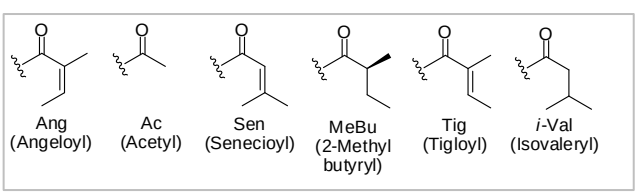

Figure 1. Chemical constituents reported from the roots of *P. japonicum* (continued)

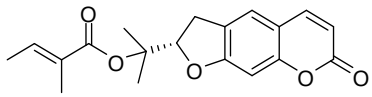

(-)-deltoin

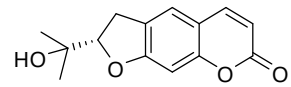

(+)-marmesin

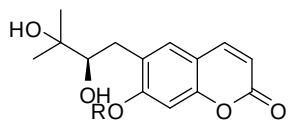

(+)-peucedanol, R=H
peucedanol 7-*O*-*β*-$_D$-glucopyranoside, R=*β*-$_D$-glc
peujaponiside, R=*β*-$_D$-glc-(6→1)-*β*-$_D$-api

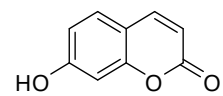

umbelliferone

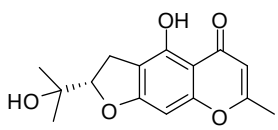

(+)-visamminol

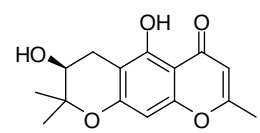

(-)-hamaudol

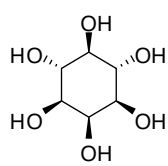

myo-inositol

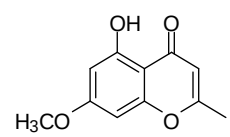

eugenin

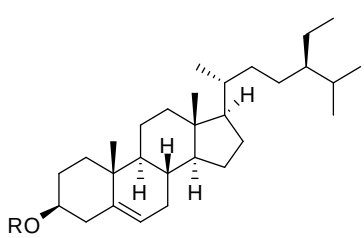

β-sitosterol-3-*O*-*β*-$_D$-glucopyranoside, R=*β*-$_D$-glc

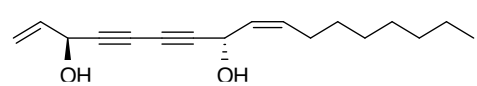

falcarindiol

Figure 1. Chemical constituents reported from the roots of *P. japonicum*

1.1.2. Angular dihydropyranocoumarins

Coumarins are divided into 4 sub-types including simple coumarins, furanocoumarins, pyranocoumarins, and pyrone-substituted coumarins. Pyranocoumarins contain a six membered ring which is connected to coumarin and there are two types, linear (xanthyletin type) and angular (seselin type), depending on the connection method. Angular-type pyranocoumarins possess khellactone skeleton (dihydroseselin) and the substituents are attached at the two stereocenters, C-3' and C-4'. According to their relative configurations, *cis*-khellactones are generally divided into the (3'*R*,4'*R*)- and (3'*S*,4'*S*)-khellactone esters. In addition, enantiomers and diastereomers could occur (Sarkhail 2014). Angular dihydropyranocoumarins were isolated mainly from the genera *Peucedanum*, *Angelica*, and *Seseli*, which belong to the Umbelliferae family (Lee et al. 2015; Chun et al. 2016; Jung et al. 2012). It was reported that the khellactone esters showed anti-inflammatory effect (Yu et al. 2012), antibacterial activity (Lu et al. 2001), tracheal relaxant activity (Zhao et al. 1999), monoamine oxidase inhibitory activity (Huong et al. 1999), antiplatelet aggregation activity (Jong et al. 1992), and anti-tumor activity (Duh et al. 1991).

1.1.3. Inflammation and the role of nitric oxdie

Inflammation is a complex mechanism, which occurred to protect host tissue from injurious agents. Acute inflammation is a beneficial defense process particularly during infectious challenges. However, if the inflammation is persisted chronically, it could cause inflammatory diseases. Chronic inflammation is related to the infiltration of mononuclear cells, such as macrophages and lymphocytes (Kaplanski et al. 2003).

Microbial products such as lipopolysaccharide (LPS) and proinflammatory cytokines such as interleukins, tumor necrosis factor-α (TNF-α), and interferon-γ (IFN-γ) triggers the gene expression of iNOS (inducible nitric oxide synthase) in various inflammatory and tissue cells (Molloy et al. 1993; Korhonen et al. 2005). Nitric oxide (NO) mediates and regulates the inflammatory responses. Its cytotoxic

effect is aimed to protect host against invading pathogens, but it can also be harmful to host tissues. If NO interacts with molecular oxygen and superoxide anion, it can produce reactive nitrogen species. Cellular functions could be modified and it can play important role in inflammation (Korhonen et al. 2005).

1.2. Purpose of Research

The khellactone moiety was easily indicated by typical NMR patterns such as chemical shift and coupling constant. Based on the *J* value and NOESY correlation, the relative configuration cold be suggested. However, Mosher method or X-ray crystallography was required to determine the absolute configuration. Especially, in the case of diacyl angular dihydropyranocoumarin, pretreatment step was needed to produce a free 4'-OH for the Mosher method. In addition, it is difficult to make a fine crystal for X-ray diffraction analysis. Therefore, most of the literatures ambiguously reported the absolute configuration and there are few helpful references. In the early years, comparing the optical rotation of hydrolysate with authentic sample was common way to define the absolute configuration (Ikeshiro et al. 1993). Recently, the studies about enantioseparation and ECD measurement were reported (Song et al. 2012; Song et al. 2014b; Lou et al. 2004). In this study, partial hydrolysis prior to MTPA method, X-ray crystallography, and ECD calculation were applied to unambiguously determine the absolute configuration of khellactone esters.

Although *P. japonicum* roots were traditionally used as a cold medicine, there is a lack of research on anti-inflammatory activities at compound level. Because, a lot of khellactone esters were isolated in this study, the bioactivity screening of compounds could help to suggest anti-inflammatory candidates from natural resources.

Chapter 2. Structure Elucidation of Khellactone Esters

2.1. Compound 1

Compound **1** was obtained as colorless needles with molecular formula $C_{23}H_{28}O_7$ based on the *m/z* 417.1912 $[M+H]^+$ in HRCIMS. The proton signals of an α-pyrone [δ_H 6.20 (1H, d, *J* = 9.5 Hz, H-3) and 7.57 (1H, d, *J* = 9.5 Hz, H-4)] and an ortho disubstituted benzene [δ_H 7.33 (1H, d, *J* = 8.6 Hz, H-5) and 6.78 (1H, d, *J* = 8.6 Hz, H-6)] revealed the presence of coumarin moiety (Figure 2). Two methines at δ_H 5.30 (1H, d, *J* = 4.8 Hz, H-3') and 6.53 (1H, d, *J* = 4.8 Hz, H-4') and geminal dimethyls at δ_H 1.38 and 1.43 (each 3H, s, H-5', H-6') indicated an angular dihydropyran ring in this structure. The signals of an isobutyryl group were observed at δ_H 2.55 (1H, sep, *J* = 7.0 Hz, H-2''), 1.18, and 1.17 (each 3H, d, *J* = 7.0 Hz, H-3'', H-4''), and that of 2-methylbutyryl group at δ_H 2.37 (1H, sxt, *J* = 7.0 Hz, H-2'''), 1.71, 1.44 (each 1H, m, H-3'''), 0.91 (3H, t, *J* = 7.4 Hz, H-4'''), and 1.19 (3H, d, *J* = 7.0 Hz, H-5'''). The linkages between isobutyryl group (C-1'') and H-3' (δ_H 5.30), 2-methylbutyryl (C-1''') group and H-4' (δ_H 6.53) were confirmed by HMBC (Figure 3). Based on the *J* value (4.8 Hz) (Macias et al. 1989; Song et al. 2012) and NOESY correlation between H-3' and H-4' (Figure 4), the relative configuration at C-3' and C-4' was identified as *cis*-orientation. To determine the absolute configuration, partial alkaline hydrolysis was performed to produce a hydroxyl group which is necessary to the MTPA (*α*-methoxy-*α*-trifluoromethylphenylacetyl) reaction. During alkaline hydrolysis, three products (**1a-1c**) were obtained (Scheme 6). Due to the inversion at 4'-position, the partial hydrolyzed product (**1a**) was identified as *trans* configuration based on the coupling constant between H-3' and H-4' (3.9 Hz). Based on NMR and optical rotation, the other products were assigned as (+)-*trans*-khellactone (**1b**) and (-)-*cis*-khellactone (**1c**). The hydrolysate **1a** was treated with the Mosher reagents to give (*S*)- and (*R*)-MTPA esters (**1aa** and **1ab**). As a result, the absolute configuration of **1a** was identified as 3'*S* and 4'*R* due to the *trans*

orientation (Figure 5) and that of **1** was assigned as (3'*S*,4'*S*) in consideration of the epimerization at the 4' position. Furthermore, the (3'*S*,4'*S*) configuration was confirmed based on the crystal structure of **1**, which is obtained by single-crystal X-ray diffraction (Figure 6). The calculated ECD spectrum of **1** was in good agreement with the experimental ECD spectrum of **1** (Figure 7). Compound **1** was isolated for the first time from nature and assigned to be (3'*S*,4'*S*)-3'-*O*-isobutyryl-4'-*O*-(2-methylbutyryl)khellactone.

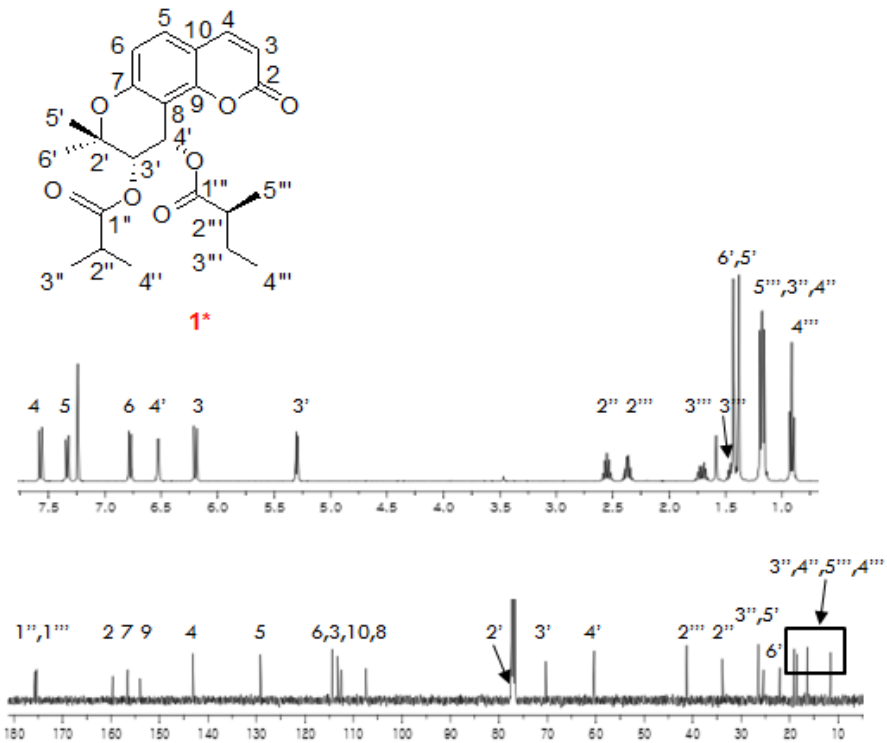

Figure 2. ^{1}H and ^{13}C NMR spectra of compound **1** (400/100 MHz, $CDCl_3$)

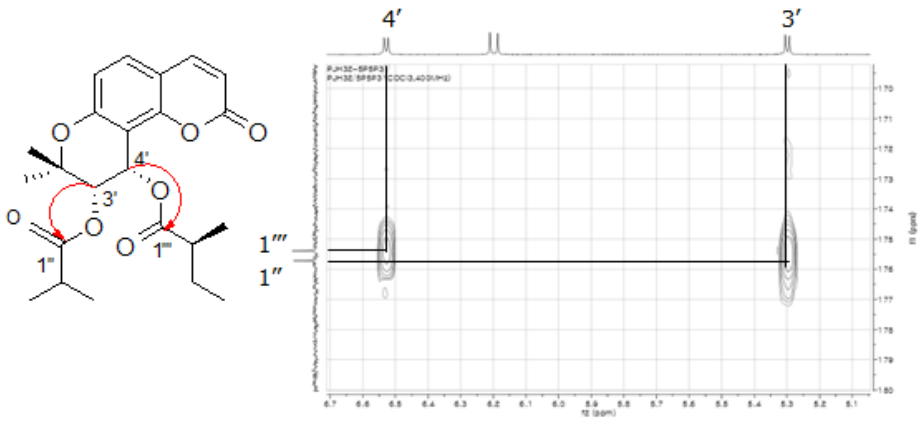

Figure 3. HMBC spectrum of compound **1** (400 MHz, $CDCl_3$)

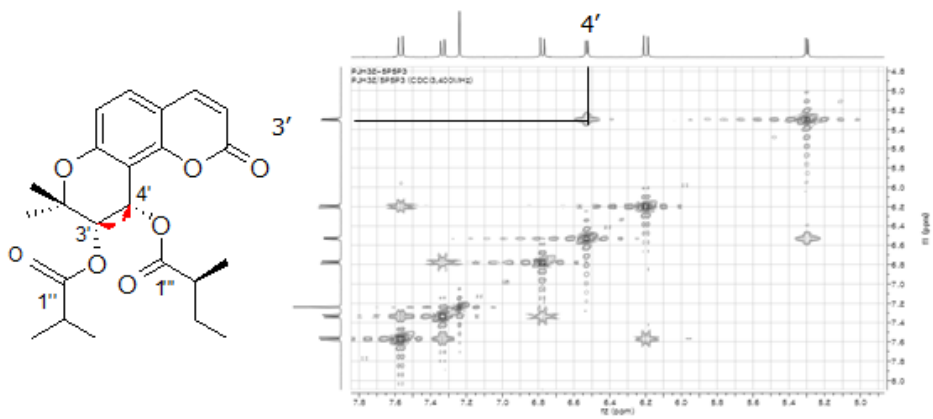

Figure 4. NOESY spectrum of compound **1** (400 MHz, $CDCl_3$)

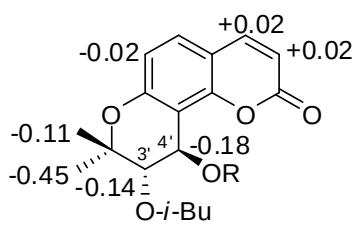

1aa R=(*S*)-MTPA ester
1ab R=(*R*)-MTPA ester

Figure 5. $\Delta\delta$ (δ_S-δ_R) values obtained from MTPA esters for partial hydrolysis product **1a**

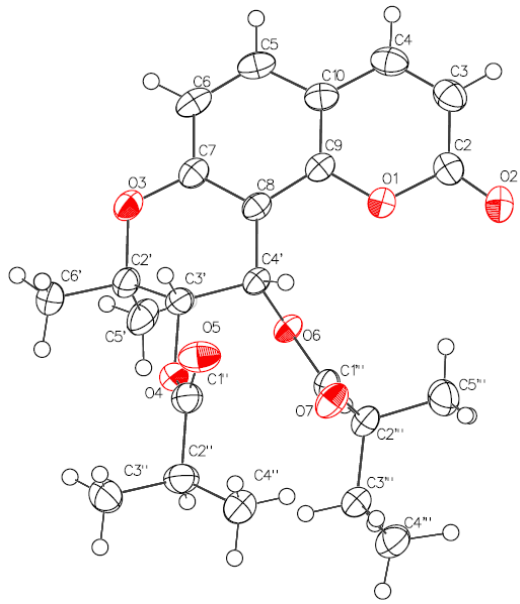

Figure 6. X-ray crystallographic structure of **1** (ORTEP drawing)

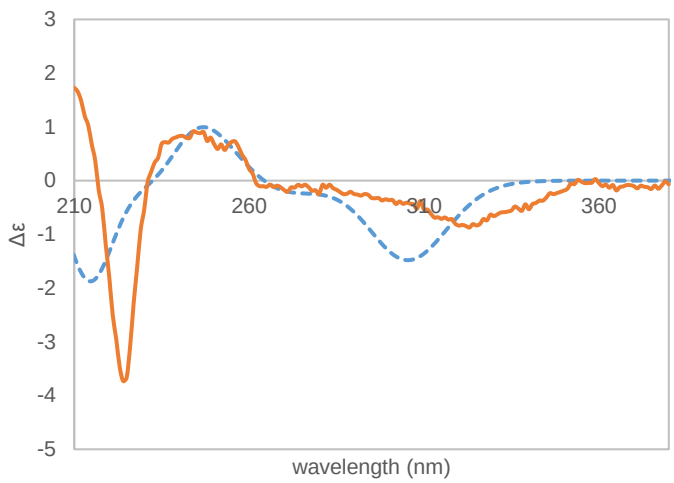

Figure 7. Calculated (dashed) and experimental (solid) ECD spectra of **1**.

2.2. Compound 2

Compound **2** was isolated as colorless needles. The molecular formula of **2** was determined to be $C_{19}H_{20}O_6$ by HRESIMS. The ^{1}H NMR spectrum of **2** was similar to **1**, except for the 3'- and 4'-substituents. The signal of an acetyl moiety was observed at δ_H 2.07 (3H, s, H-2''), and that of senecioyl group at δ_H 5.62 (1H, s, H-2'''), 2.21 (3H, s, H-4'''), and 1.87 (3H, s, H-5''') (Figure 8). Based on HMBC spectrum, acetyl (C-1'' (δ_C 169.9)) and senecioyl (C-1''' (δ_C 165.2)) moieties were connected to H-3' (δ_H 5.29) and H-4' (δ_H 6.56), respectively (Figure 9). The *cis*-orientation at C-3' and C-4' was determined by *J* value (4.8 Hz) and NOESY interaction (Figure 10). Based on single-crystal X-ray diffraction analysis, the absolute configuration of compound **2** was identified as (3'*S*,4'*S*) (Figure 11). The ECD spectrum of **2** exhibited similar pattern with **1** (Figure 12). Compound **2** was isolated for the first time from nature and named (3'*S*,4'*S*)-3'-*O*-acetyl-4'-*O*-senecioylkhellactone.

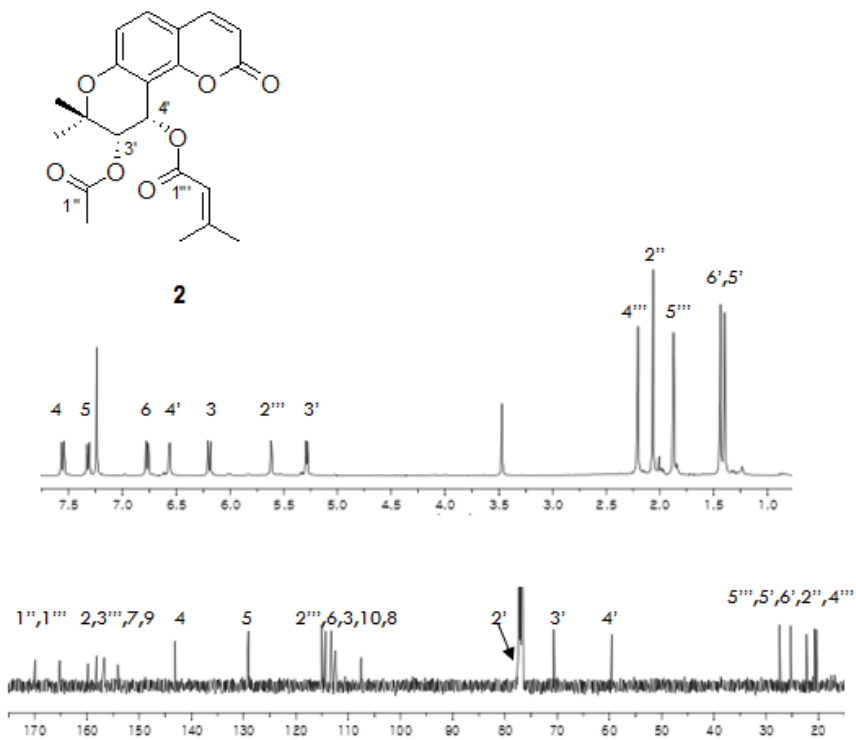

Figure 8. ^{1}H and ^{13}C NMR spectra of compound **2** (400/100 MHz, $CDCl_3$)

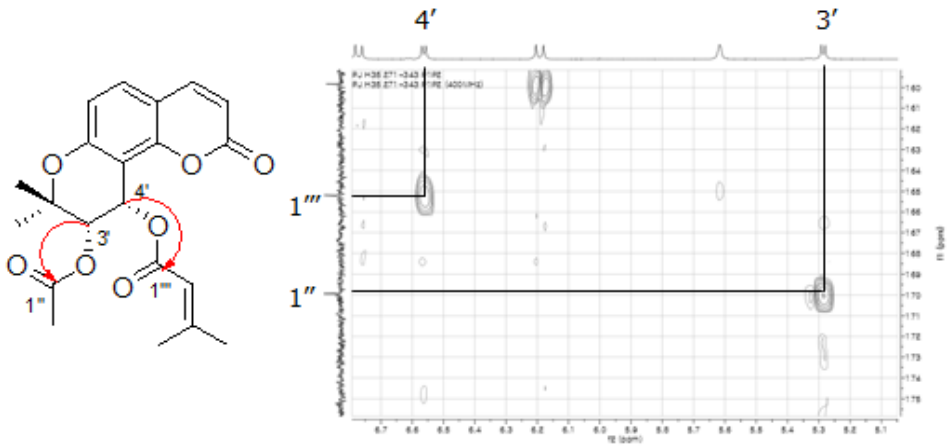

Figure 9. HMBC spectrum of compound **2** (400 MHz, $CDCl_3$)

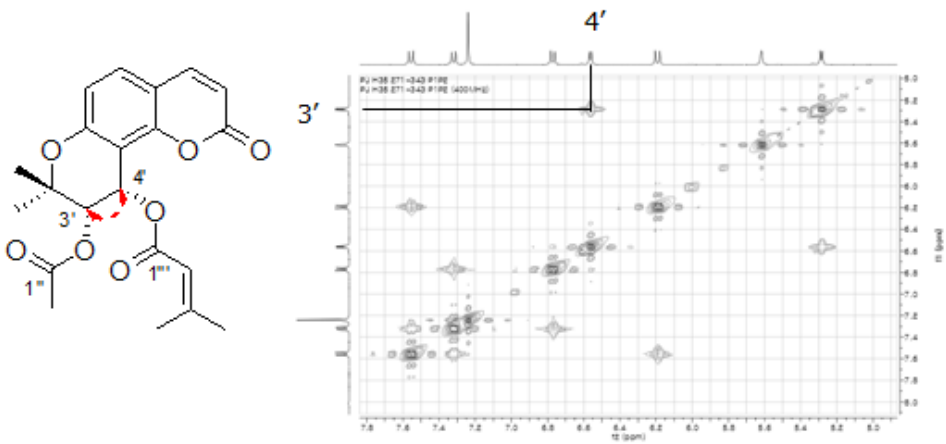

Figure 10. NOESY spectrum of compound **2** (400 MHz, $CDCl_3$)

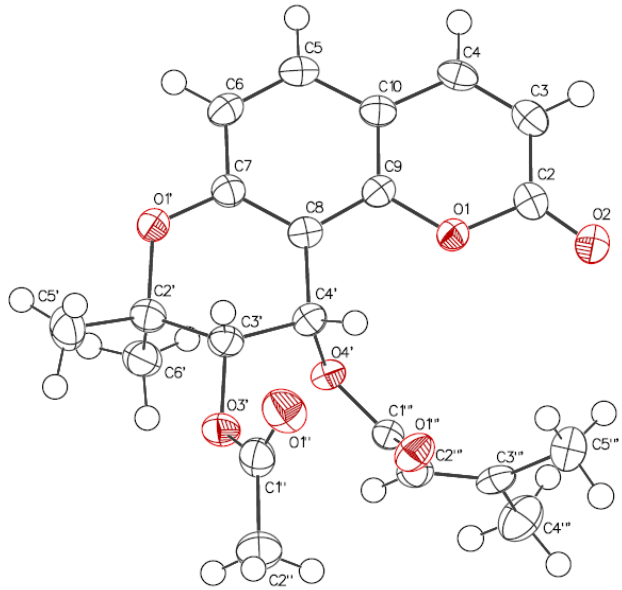

Figure 11. X-ray crystallographic structure of **2** (ORTEP drawing)

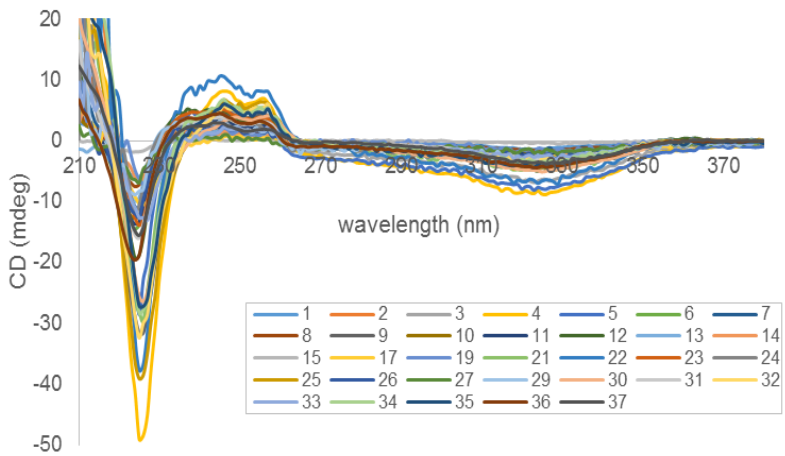

Figure 12. ECD curves of **1-15**, **17**, **19**, **21-27**, and **29-37**

2.3. Compound 9

The molecular formula of **9** was determined as $C_{24}H_{28}O_7$ by HRESIMS. The ^1H and ^{13}C NMR spectra of **9** indicated the presence of khellactone moiety. In the ^1H NMR, **9** exhibited the signals of an isovaleryl moiety at δ_H 2.21 (1H, d, *J* = 7.4 Hz, H-2''a), 2.20 (1H, d, *J* = 6.9 Hz, H-2''b), 2.08 (1H, m, H-3''), 0.94 (3H, d, *J* = 6.6 Hz, H-4''), and 0.93 (3H, d, *J* = 6.6 Hz, H-5''), and that of angeloyl group at δ_H 6.01 (1H, q, *J* = 7.3 Hz, H-3'''), 1.98 (3H, d, *J* = 7.3 Hz, H-4'''), and 1.84 (3H, s, H-5''') (Figure 13). The connection between isovaleryl (C-1'') group and H-3', and angeloyl (C-1''') group and H-4' was confirmed by HMBC correlations (Figure 14). The configuration between 3' and 4' position was assigned as *cis* based on the *J* value (4.9 Hz) and the presence of NOESY correlation (Figure 15). The ECD spectrum of **9** was in good agreement with the ECD spectra of **1** and **2** (Figure 12). Therefore, the absolute configuration of **9** could be determined as 3'*S* and 4'*S*. Compound **9** was newly isolated from nature and named (3'*S*,4'*S*)-4'-*O*-angeloyl-3'-*O*-isovalerylkhellactone.

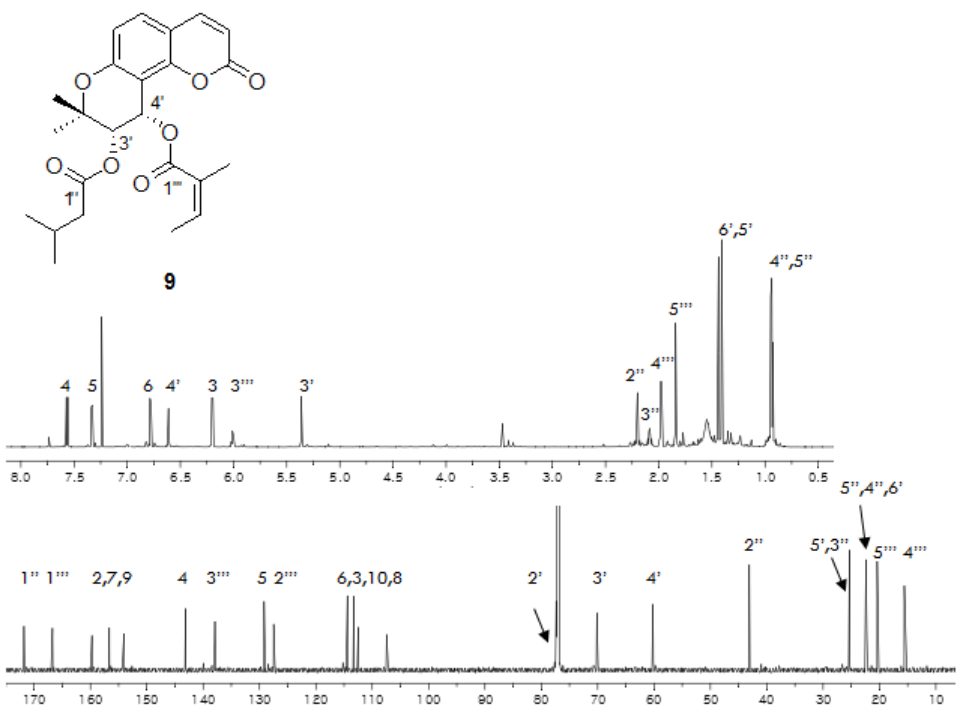

Figure 13. ^1H and ^{13}C NMR spectra of compound **9** (800/200 MHz, $CDCl_3$)

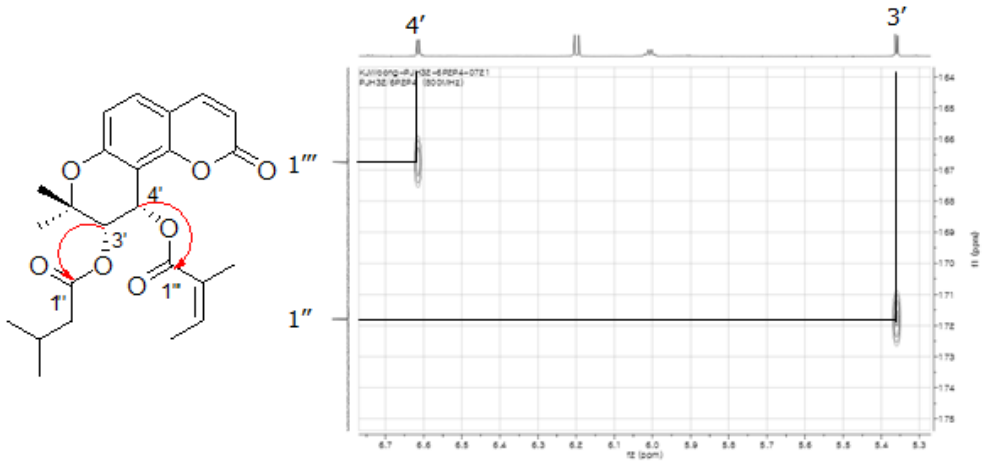

Figure 14. HMBC spectrum of compound **9** (800 MHz, $CDCl_3$)

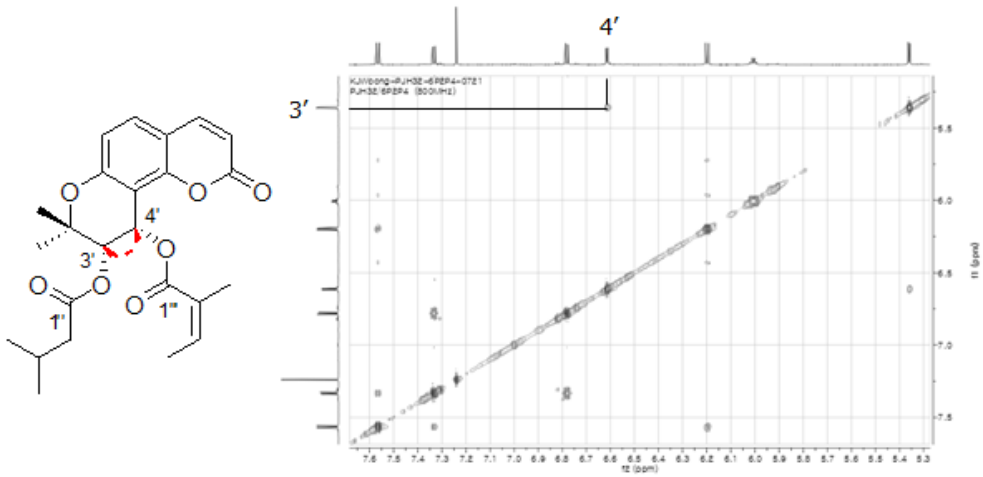

Figure 15. NOESY spectrum of compound **9** (800 MHz, $CDCl_3$)

2.4. Compounds 8, 10, 11, and 15

The molecular formula of **8** was determined to be $C_{23}H_{28}O_7$ using HRESIMS. Similar to **1**, compound **8** was inferred to have khellactone and 2-methylbutyryl moieties from ^{1}H NMR spectrum. Compound **8** possessed *n*-butyryl group, whose ^{1}H signals were observed at δ_H 2.30 (2H, dt, *J* = 7.4, 1.7 Hz, H-2’’), 1.66 (2H, sxt, *J* = 7.4 Hz, H-3’’), and 0.95 (3H, t, *J* = 7.4 Hz, H-4’’), instead of isobutyryl group (Figure 16). The connectivity between khellactone, butyryl, and 2-methylbutyryl moieties were deduced by HMBC correlations. The configurations of (3’*S*,4’*S*) were identified by *J* value (4.9 Hz), NOESY correlation, and similar ECD pattern with **1** (Figure 12). Compound **8** was firstly isolated from nature and named (3’*S*,4’*S*)-3'-*O*-butyryl-4'-*O*-(2-methylbutyryl)khellactone.

Compound **10** had the molecular formula $C_{21}H_{24}O_8$, suggested by HRCIMS. Different to compound **2**, **10** showed 3-hydroxyisovaleryl signals at δ_H 2.59 (1H, d, *J* = 15.4 Hz, H-2’’’a), 2.50 (1H, d, *J* = 15.4 Hz, H-2’’’b), 1.34 (3H, s, H-4’’’), and 1.33 (3H, s, H-5’’’), instead of senecioyl moiety (Figure 17). Based on HMBC spectrum, it was determined that acetyl and 3-hydroxyisovaleryl moieties were located at 3’ and 4’, respectively. The 3’*S*,4’*S* configurations were established by coupling constant (4.8 Hz), NOESY interaction, and similar ECD spectrum with **2** (Figure 12). Compound **10** was named (3’*S*,4’*S*)-3'-*O*-acetyl-4'-*O*-(3-hydroxyisovaleryl)khellactone and it was firstly isolated from nature.

Compound **11** possessed the molecular formula $C_{21}H_{24}O_8$, indicated by HRESIMS. The ^{1}H NMR spectrum suggested that **11** was similar to **2** except for the 3-hydroxy-2-methylbutyryl signals at δ_H 2.49 (1H, qui, *J* = 7.2 Hz, H-2’’’), 3.92 (1H, m, H-3’’’), 1.22 (3H, d, *J* = 6.3 Hz, H-4’’’), 1.16 (3H, d, *J* = 7.2 Hz, H-5’’’), and 3.52 (1H, d, *J* = 5.4 Hz, 3’’’-OH) (Figure 18). In the HMBC spectrum, the interaction between H-4’ and the carbonyl carbon (C-1’’’) of 3-hydroxy-2-methylbutyryl moiety was confirmed. The absolute configuration was identified as (3’*S*,4’*S*) based on the coupling constant (4.9 Hz), a NOESY correlation, and similar ECD pattern with **2** (Figure 12). Compound **11** was named (3’*S*,4’*S*)-3'-*O*-acetyl-4'-*O*-(3-hydroxy-2-methylbutyryl)khellactone and it was newly isolated from nature.

The molecular formula of compound **15** was determined as $C_{20}H_{24}O_6$, suggested

by HRESIMS. The ^{1}H NMR spectrum indicated that **15** had differnce with **1** at the 3'- and 4'- stubstituents (Figure 19). Especially, the upshifted signal at δ_H 4.83 (1H, d, *J* = 4.6 Hz, H-4') and methoxy signal at δ_H 3.70 (3H, s, 4'-OMe) were observed. From the HMBC spectrum, the location of 2-methylbutyryl and methoxy groups was established. The (3'*S*,4'*S*) configuration was suggested by the *J* value (4.9 Hz), a NOESY correlation, and similar ECD pattern with **1** (Figure 12). Compound **15** was obtained for the first time from nature and it was named (3'*S*,4'*S*)-4'-*O*-methyl-3'-*O*-(2-methylbutyryl)khellactone.

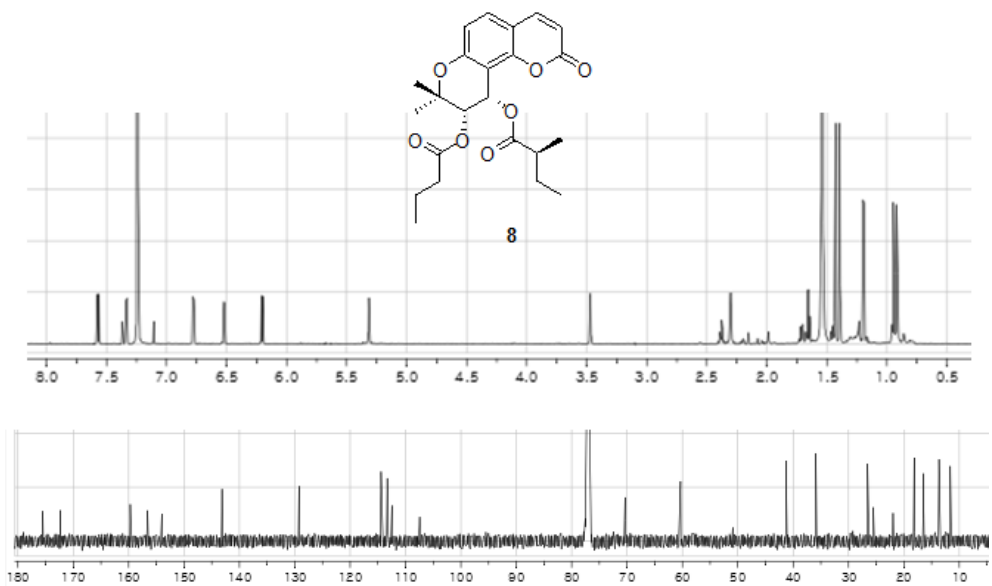

Figure 16. ^{1}H and ^{13}C NMR spectra of compound **8** (800/200 MHz, $CDCl_3$)

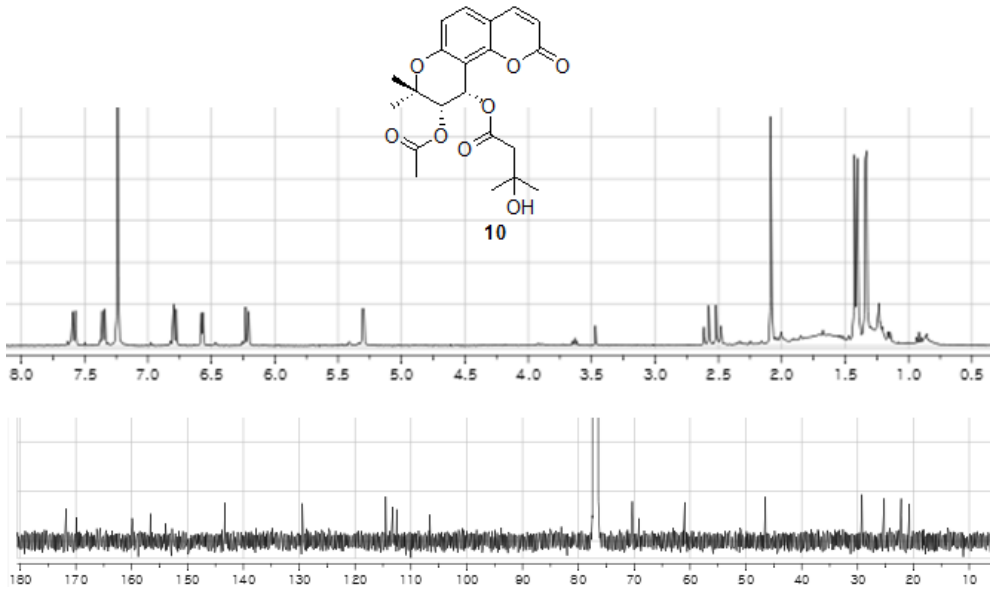

Figure 17. ^{1}H and ^{13}C NMR spectra of compound **10** (400/100 MHz, $CDCl_3$)

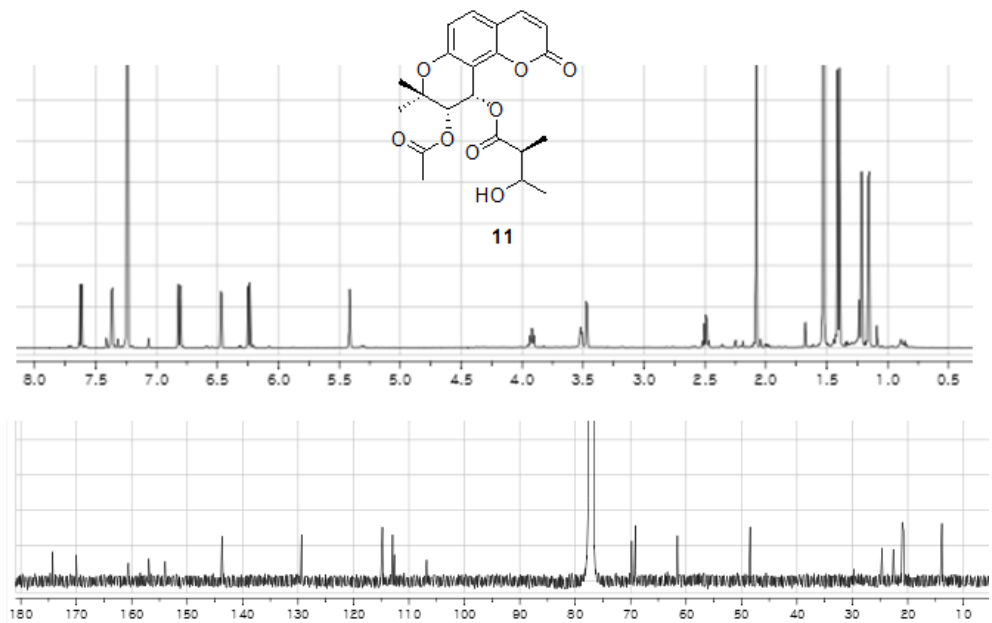

Figure 18. ^{1}H and ^{13}C NMR spectra of compound **11** (600/150 MHz, $CDCl_3$)

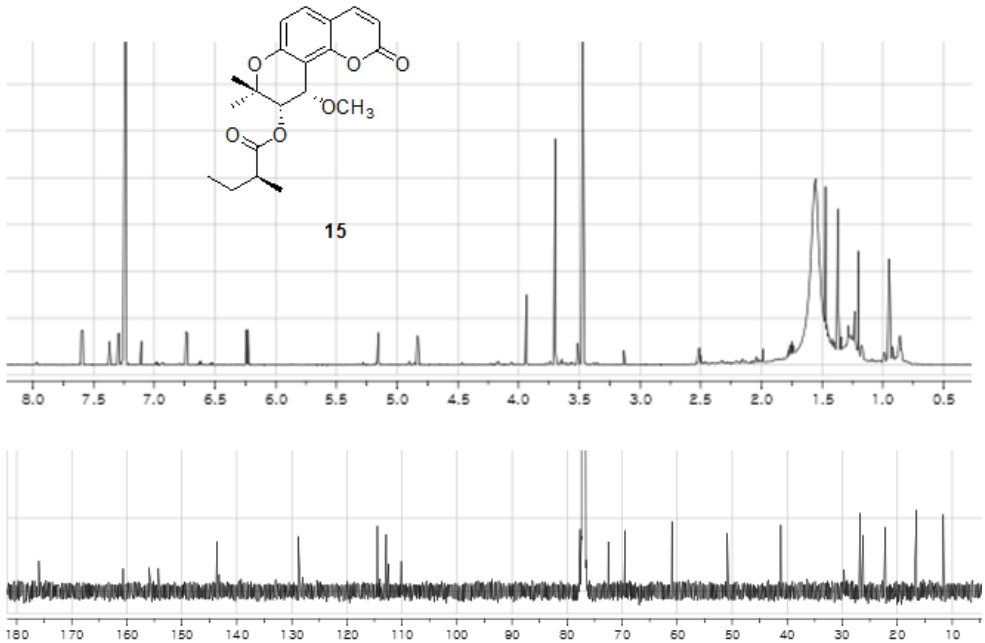

Figure 19. ^{1}H and ^{13}C NMR spectra of compound **15** (800/200 MHz, $CDCl_3$)

2.5. Compounds 6

The molecular formula of **6**, $C_{23}H_{28}O_7$, was indicated by HRCIMS. Different to **1**, compound **6** possessed isovaleryl moiety, whose ^1H signals were obatained at δ_H 2.28 (1H, dd, *J* = 14.4, 6.7 Hz, H-2’’’a), 2.17 (1H, m, H-2’’’b), 2.13 (1H, m, H-3’’’), 0.97 (3H, d, *J* = 6.3 Hz, H-4’’’), and 0.95 (3H, d, *J* = 6.3 Hz, H-5’’’) (Figure 20). HMBC correlations between H-3’/C-1’’ and H-4’/C-1’’’ determined the connectivity of khellactone, isobutyryl, and isovaleryl moieties. The (3’*S*,4’*S*) configurations were established by *J* value (4.9 Hz) and NOESY correlation between H-3’ and H-4’, and similar ECD pattern with **1** (Figure 12). Compound **6** was named (3’*S*,4’*S*)-3'-*O*-isobutyryl-4'-*O*-isovalerylkhellactone, which was isolated for the first time from nature.

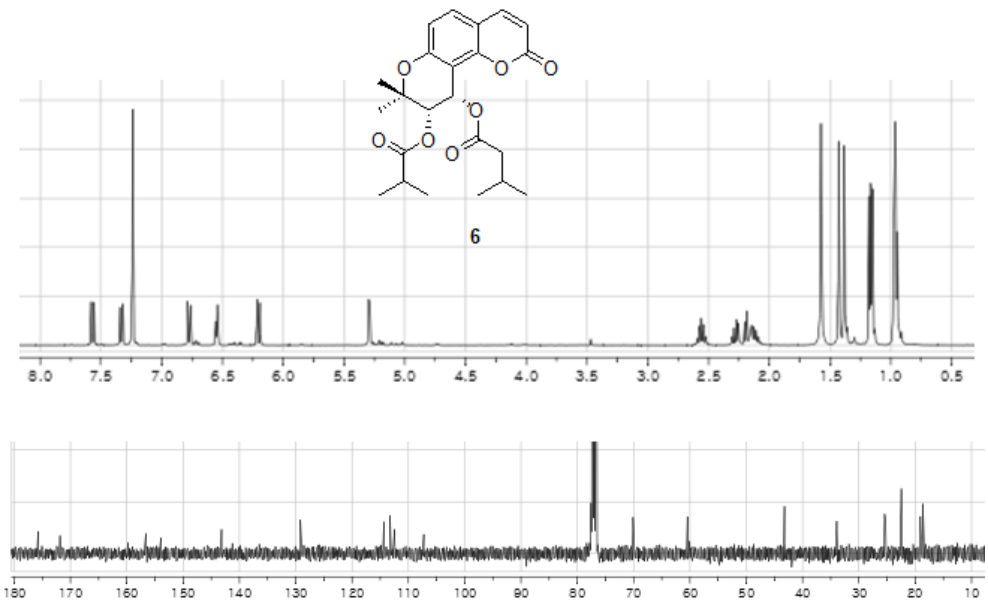

Figure 20. ^1H and ^{13}C NMR spectra of compound **6** (400/100 MHz, $CDCl_3$)

2.6. Compounds 3, 4, 7, and 13

Compound **3** was obtained as colorless needles. It has the molecular formula $C_{23}H_{28}O_7$, suggested by HRCIMS. In the ^1H and ^{13}C NMR spectra, the signals of compound **3** was similar to compound **1** (Figure 21). Based on HMBC spectrum, the attachment of 2-methylbutyryl at C-3' and isobutyryl at C-4' was confirmed. As a result, compound **3** was positional isomer of compound **1**. The J value (4.9 Hz) and NOESY interaction between H-3' and H-4', and similar ECD pattern with **1** revealed the 3'*S*,4'*S* configurations (Figure 12). Compound **3** was determined as (3'*S*,4'*S*)-4'-*O*-isobutyryl-3'-*O*-(2-methylbutyryl)khellactone and it was firstly isolated from nature.

Compound **4** possessed the molecular formula $C_{24}H_{28}O_7$, which was established by HRCIMS. The ^1H NMR spectrum of **4** suggested that it was similar to **3** except for the senecioyl signals (Figure 22). Based on HMBC correlation and MS fragmentation (base peak, M^+ - OSen), the connection of senecioyl group to 4'-position of khellactone was confirmed. Based on the coupling constant (4.9 Hz), a NOESY correlation, and similar ECD pattern with **3**, the absolute configuration was assigned as (3'*S*,4'*S*) (Figure 12). Compound **4** was determined as (3'*S*,4'*S*)-3'-*O*-(2-methylbutyryl)-4'-*O*-senecioylkhellactone, which was newly isolated from nature.

The molecular formula of compound **7**, $C_{24}H_{28}O_7$, was suggested by HRESIMS. The ^1H NMR spectrum of **7** resembled that of **3** except for angeloyl group signals (Figure 23). The HMBC correlation revealed the connectivities between 2-methylbutyryl group (C-1'') and H-3', and angeloyl group (C-1''') and H-4'. The configuration was established as (3'*S*,4'*S*) based on the *J* value (4.9 Hz), a NOESY correlation, and similar negative and positive Cotton effects with **1** (Figure 12). Compound **7** was acquired for the first time from nature and named (3'*S*,4'*S*)-4'-*O*-angeloyl-3'-*O*-(2-methylbutyryl)khellactone.

Compound **13** had the molecular formula $C_{19}H_{22}O_6$, was determined by HRESIMS. Different to **3**, the upshifted signal at δ_H 5.40 (1H, d, *J* = 4.9 Hz, H-4') and hydroxy signal at δ_H 3.12 (1H, br s, 4'-OH) were observed, which means that compound **13** was monoacylkhellactone (Figure 24). HMBC correlations between H-3' and C-1'' revealed the position of 2-methylbutyryl group at C-3'. Based on the *J* value (4.9 Hz)

and NOESY interaction between H-3’ and H-4’, and similar ECD pattern with **3**, the (3’*S*,4’*S*) configurations were assigned (Figure 12). Compound **13** was newly isolated from nature and named (3’*S*,4’*S*)-3'-*O*-(2-methylbutyryl)khellactone.

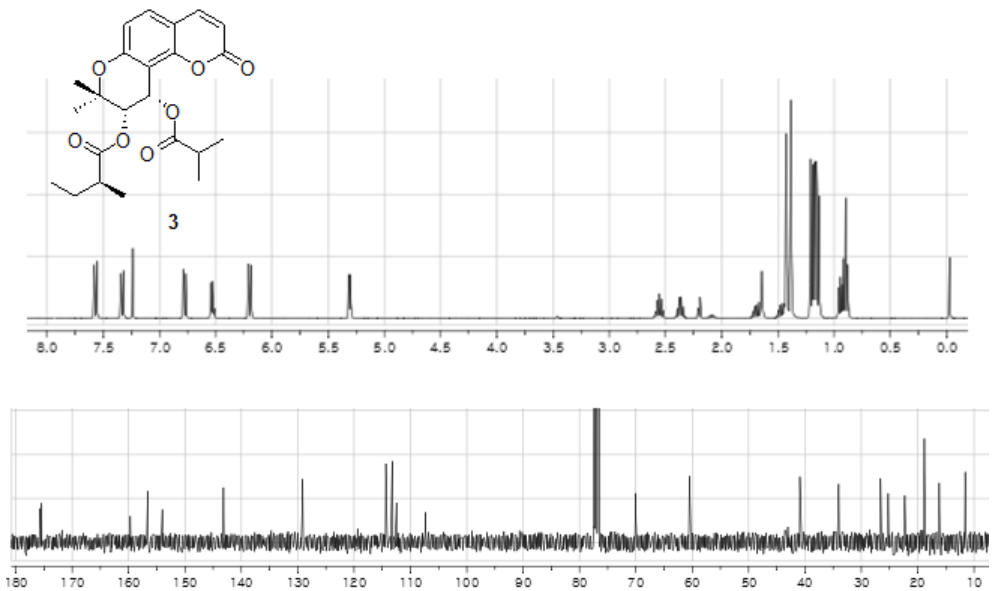

Figure 21. ^{1}H and ^{13}C NMR spectra of compound **3** (400/100 MHz, $CDCl_3$)

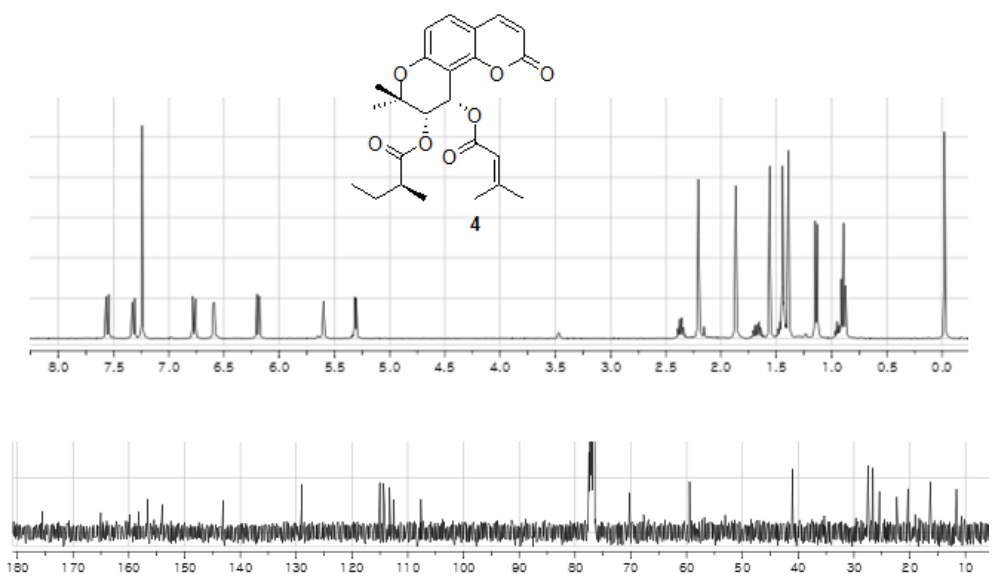

Figure 22. ^{1}H and ^{13}C NMR spectra of compound **4** (400/100 MHz, $CDCl_3$)

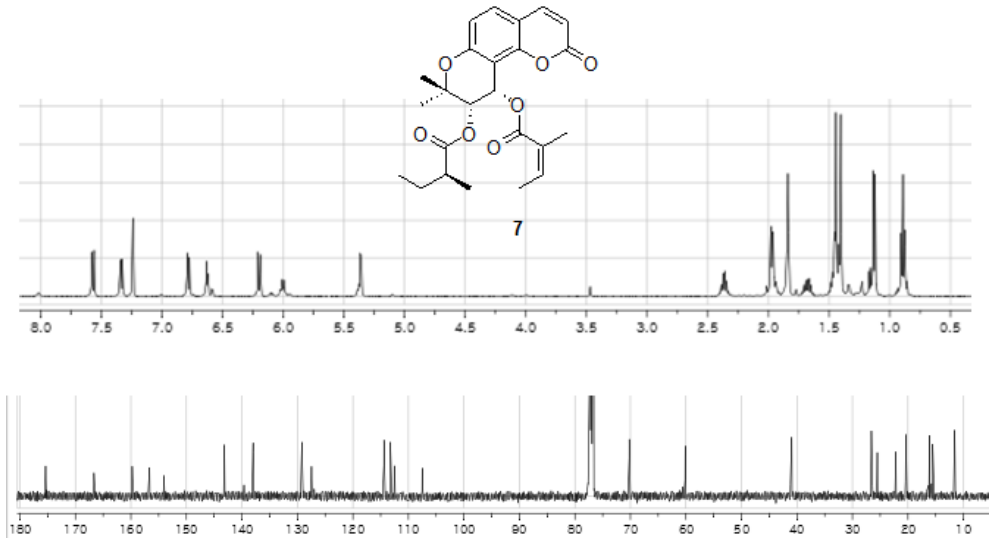

Figure 23. ^{1}H and ^{13}C NMR spectra of compound **7** (500/125 MHz, $CDCl_3$)

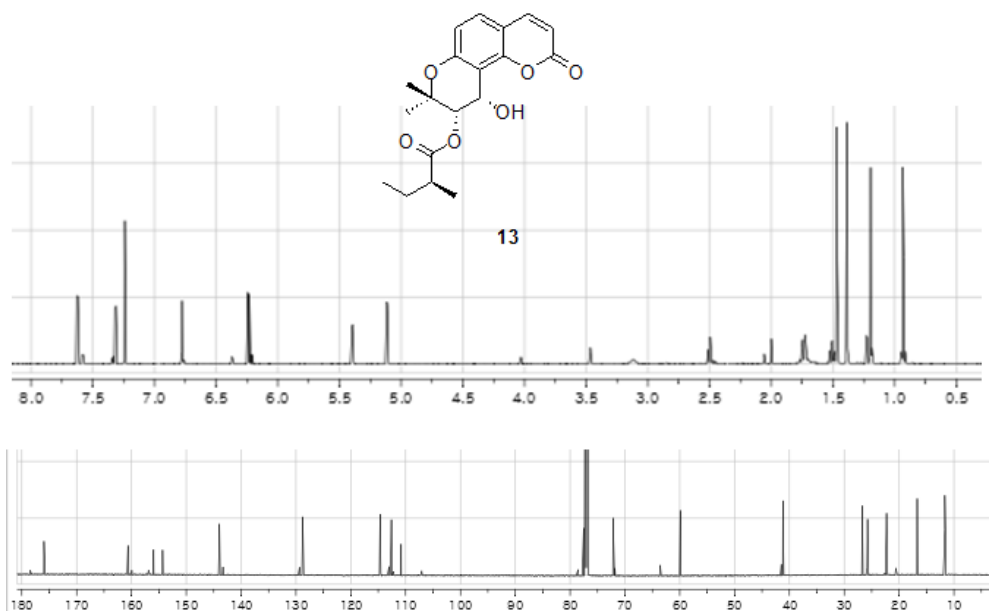

Figure 24. ^{1}H and ^{13}C NMR spectra of compound **13** (800/200 MHz, $CDCl_3$)

2.7. Compounds 5 and 21, 22, and 23

Compound **5** was isolated as white amorphous powder and its molecular formula $C_{23}H_{28}O_7$ was suggested by HRCIMS. In the ^1H and ^{13}C NMR spectra, the signals of compound **5** resembled that of compound **4** (Figure 25). From the HMBC correlations, senecioyl and 2-methylbutyryl moieties were positioned to C-3' and C-4', respectively. Based on above finding, compound **5** was positional isomer of compound **4**. The J value (5.0 Hz) and NOESY correlation of H-3' and H-4', and similar ECD pattern with **4** suggested the 3'*S*,4'*S* configurations (Figure 12). Compound **5** was assigned as (3'*S*,4'*S*)-4'-*O*-(2-methylbutyryl)-3'-*O*-senecioyl khellactone and it was firstly isolated from nature.

The molecular formulas of compounds **21-23** were indicated by ESIMS. The ^1H NMR spectra of **21-23** were similar to **5**, except for the 4'-substituent. (Figures 26-28). The 3'-senecioyl khellactone moiety was confirmed by HMBC correlation between carbonyl carbon (C-1'') of senecioyl group and H-3' or MS fragmentation (*m/z* 327, $M^+ - OR_2$, R_2 = 4'-substituent). The *J* value (4.8-5.0 Hz) between H-3' and H-4' and similar ECD pattern with **5** established the 3'*S*,4'*S* configurations (Figure 12). Compounds **21-23** were identified as (3'*S*,4'*S*)- 4'-*O*-angeloyl-3'-*O*-senecioylkhellactone (Wang et al. 2015), (3'*S*,4'*S*)- 3',4'-di-*O*-senecioylkhellactone (Lee et al. 2014), and (3'*S*,4'*S*)-4'-*O*-isovaleryl-3'-*O*-senecioylkhellactone (peujaponisin) (Ikeshiro et al. 1992).

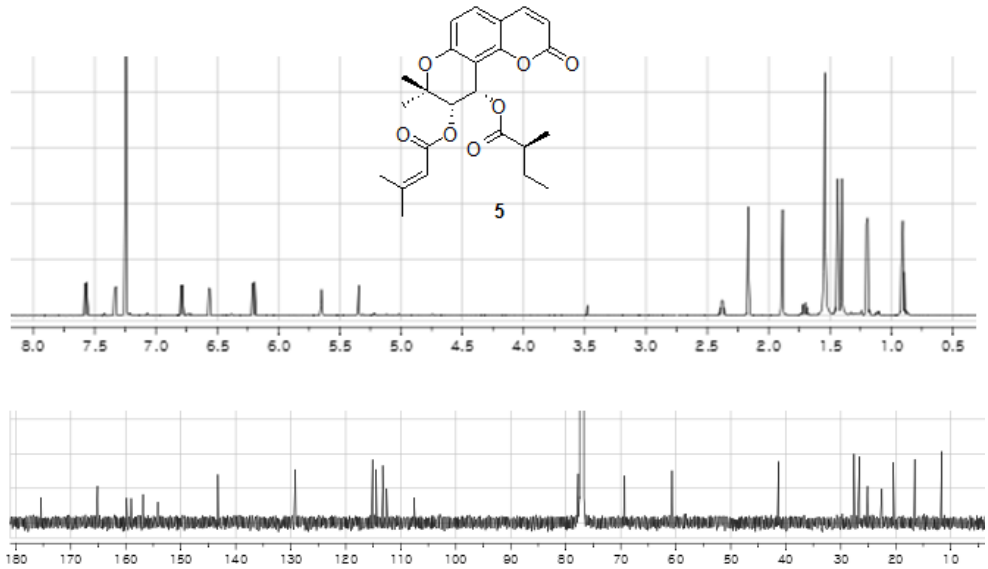

Figure 25. ^{1}H and ^{13}C NMR spectra of compound **5** (600/150 MHz, $CDCl_3$)

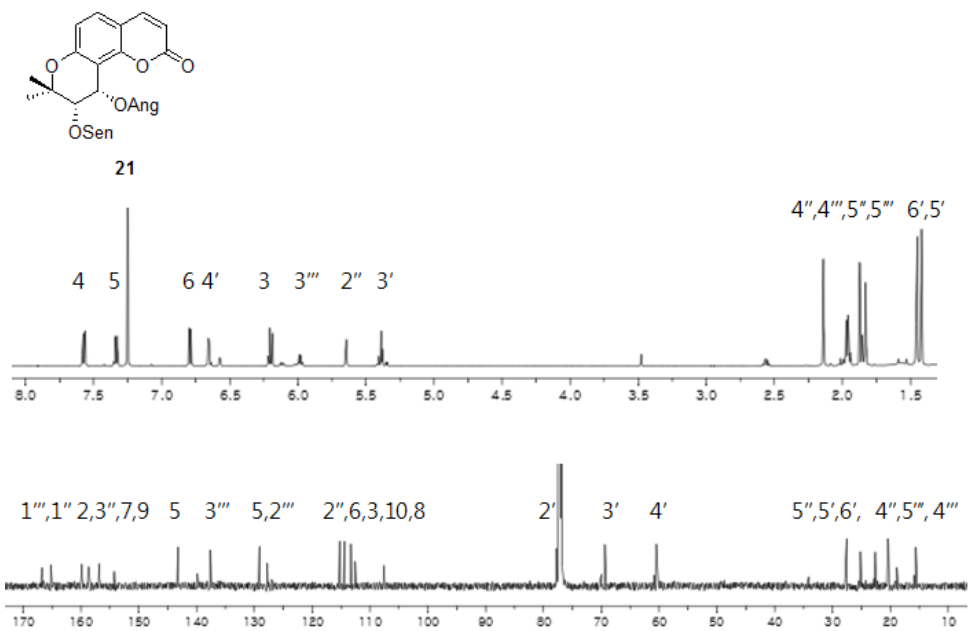

Figure 26. ^{1}H and ^{13}C NMR spectra of compound **21** (600/150 MHz, $CDCl_3$)

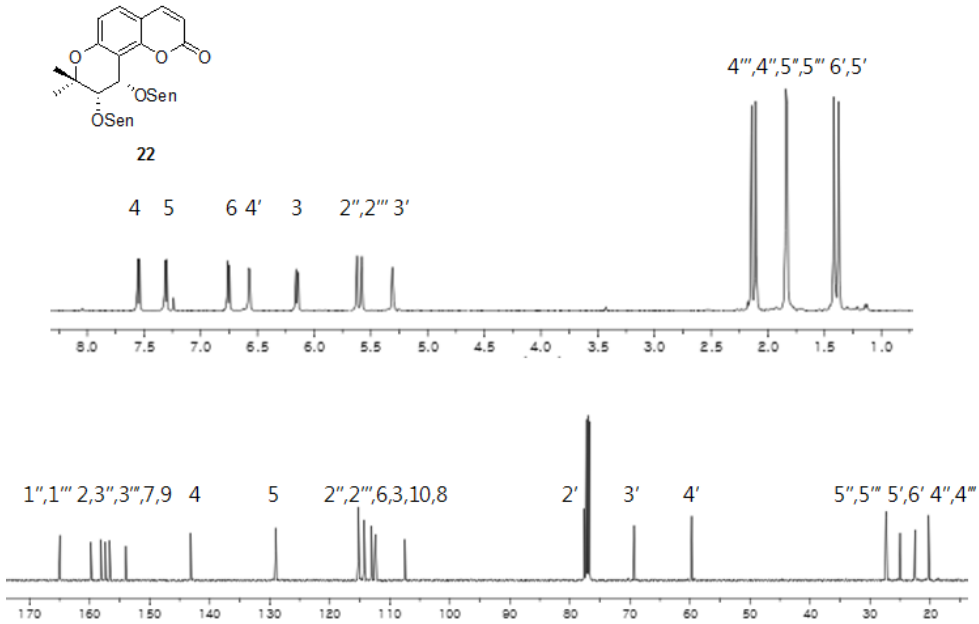

Figure 27. ^{1}H and ^{13}C NMR spectra of compound **22** (500/125 MHz, $CDCl_3$)

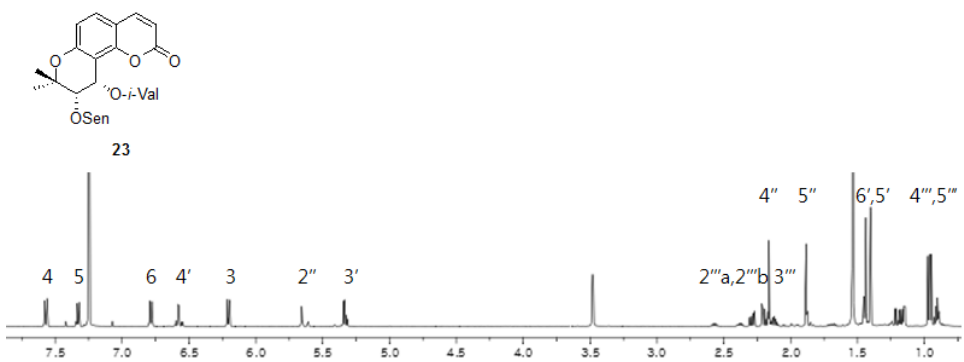

Figure 28. ^{1}H NMR spectrum of compound **23** (600 MHz, $CDCl_3$)

2.8. Compounds 12, 24, 25, 26, 27, and 40

Compound **12** possessed the molecular formula $C_{21}H_{24}O_7$, determined by HRESIMS. In the ^{1}H NMR spectrum, **12** displayed 2-methylbutyryl signals at δ_H 2.35 (1H, sxt, *J* = 7.0 Hz, H-2’’’), 1.66 (1H, m, H-3’’’a), 1.41 (1H, m, H-3’’’b), 0.88 (3H, t, *J* = 7.4 Hz, H-4’’’), and 1.15 (3H, d, *J* = 7.0 Hz, H-5’’’), dinstinct from compound **2** (Figure 29). By the HMBC experiment, it was suggested that acetyl and 2-methylbutyryl groups were positioned at 3’ and 4’, respectively. The 3’*S*,4’*S* configurations were confirmed by coupling constant (4.9 Hz), NOESY correlation, and similar ECD pattern with **2** (Figure 12). Compound **12** was isolated for the first time from nature and named (3’*S*,4’*S*)-3'-*O*-acetyl-4'-*O*-(2-methylbutyryl) khellactone.

The molecular formulas of compounds **24-27**, and **40** were determined using ESIMS. Similar to **12**, the signals of khellactone and 3’-substituent were detected in the ^{1}H NMR spectra of **24-27**, and **40** (Figures 30-34). In the case of **24**, it was indicated as monoacylkhellactone based on the upshifted signals at δ_H 5.40 (1H, d, *J* = 5.0 Hz, H-4’). The HMBC correlation between acetyl group (C-1’’) and H-3’ revealed the presence of 3’-acetylkhellactone ester moieties of **25-27**, and **40**. The relative configuration was established as *cis*-orientation based on the coupling constant (4.8-5.0 Hz) between H-3’ and H-4’. In comparison with the ECD spectrum of **12**, the absolute configurations of **24-27** and **40** were determined as 3’*S*,4’*S* and 3’*R*,4’*R*, respectively (Figures 12 and 35). The structures of **24-27**, and **40** were assigned to be (3’*S*,4’*S*)-3'-*O*-acetylkhellactone (qianhucoumarin B) (Kong et al. 1996; Kong et al. 1993), (3’*S*,4’*S*)- 3’-*O*-acetyl-4’-*O*-angeloylkhellactone (pteryxin) (Song et al. 2014), (3’*S*,4’*S*)-3'-*O*-acetyl-4'-*O*-isobutyrylkhellactone (hyuganin D) (Wang et al. 2015), (3’*S*,4’*S*)-3'-*O*-acetyl-3'-*O*-isovalerylkhellactone (suksdorfin, corymbocoumarin) (Tosun et al. 2005), and (3’*R*,4’*R*)-3’,4’-di-*O*-acetylkhellactone (qianhucoumarin D) (Valencia-Islas et al. 2002).

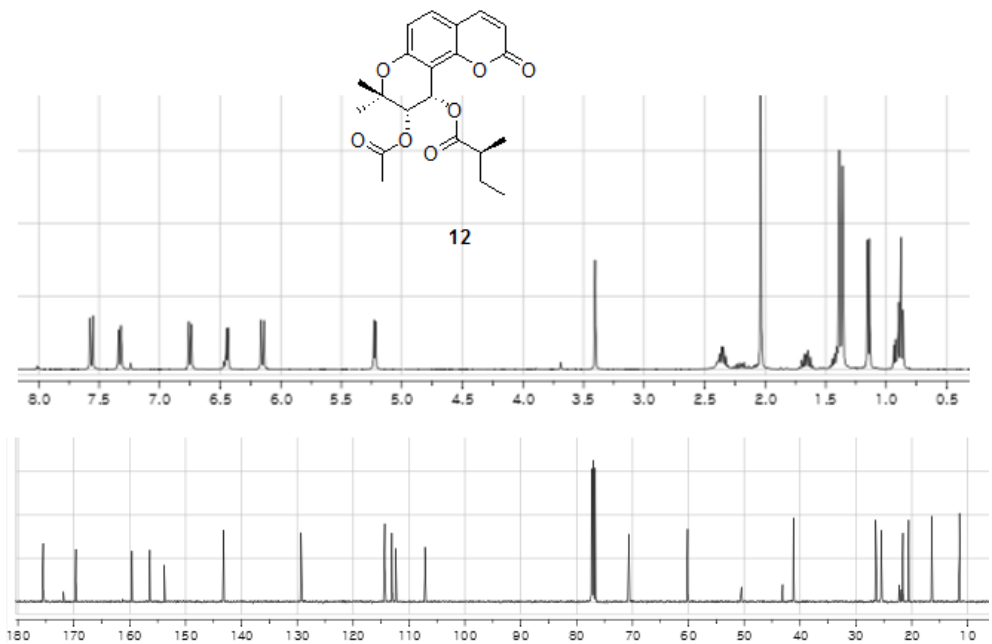

Figure 29. ^{1}H and ^{13}C NMR spectra of compound **12** (400/100 MHz, $CDCl_3$)

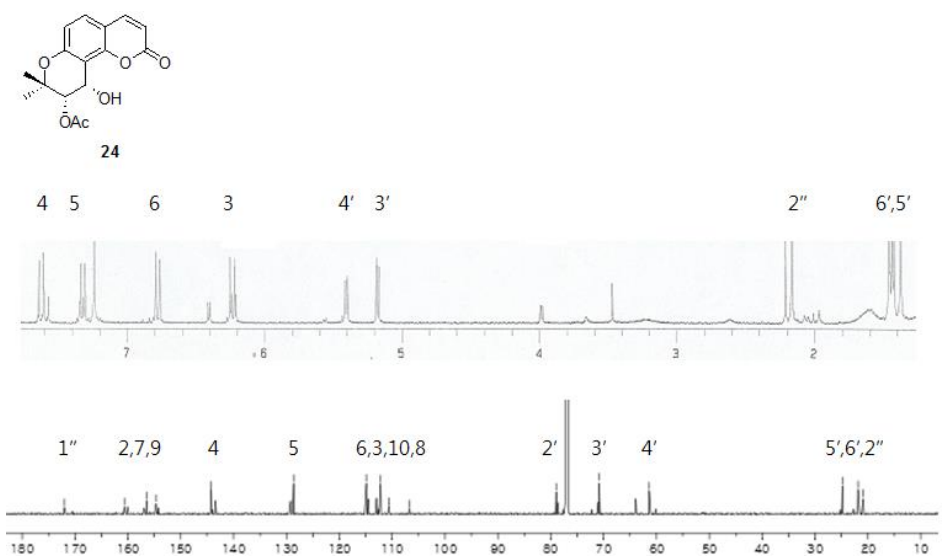

Figure 30. ^{1}H and ^{13}C NMR spectra of compound **24** (300/200 MHz, $CDCl_3$)

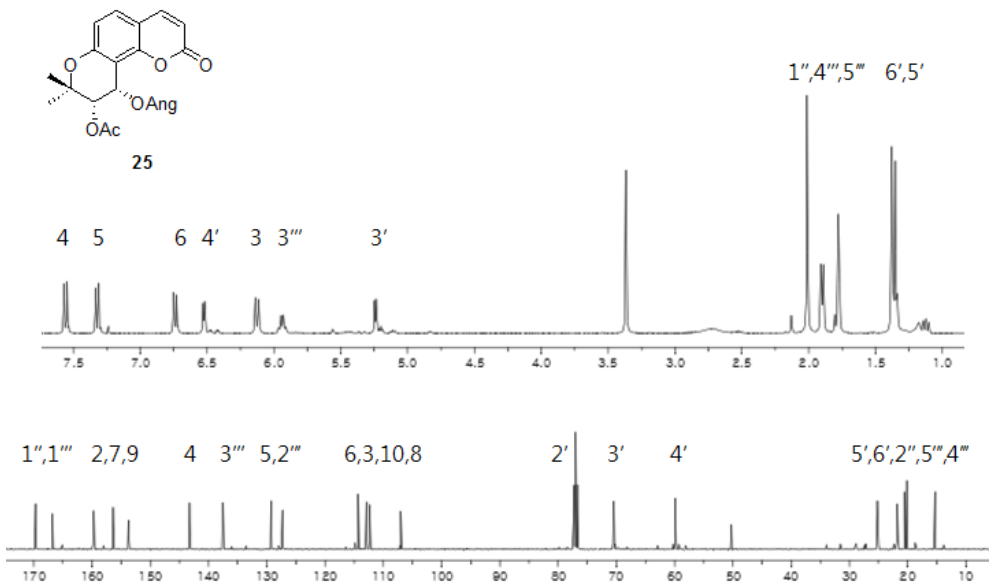

Figure 31. ^{1}H and ^{13}C NMR spectra of compound **25** (400/100 MHz, $CDCl_3$)

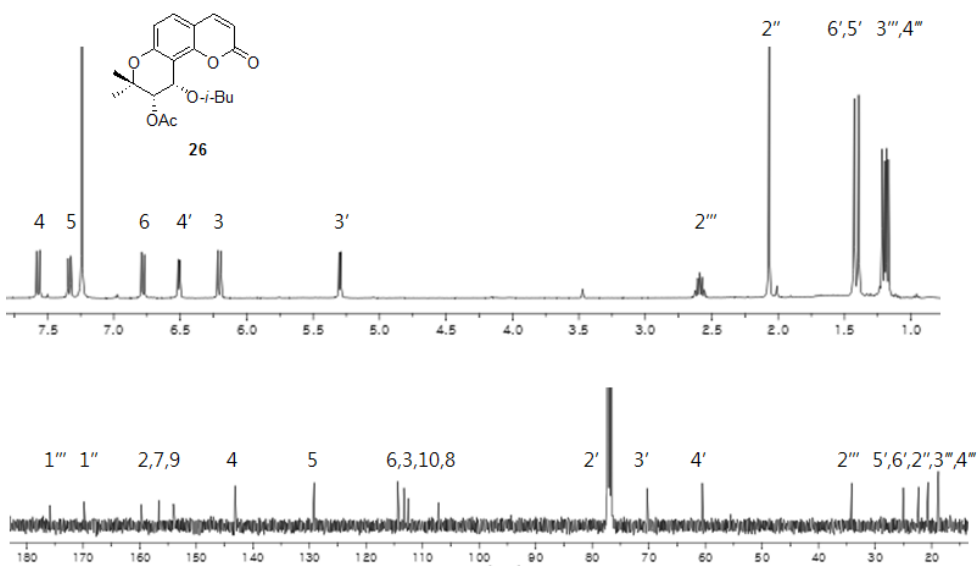

Figure 32. ^{1}H and ^{13}C NMR spectra of compound **26** (400/100 MHz, $CDCl_3$)

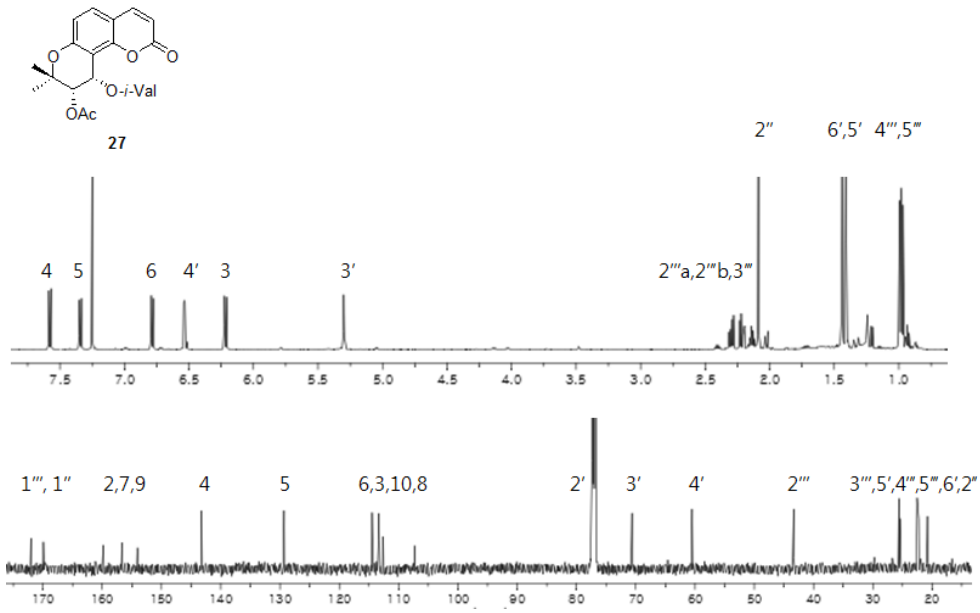

Figure 33. ^{1}H and ^{13}C NMR spectra of compound **27** (600/150 MHz, $CDCl_3$)

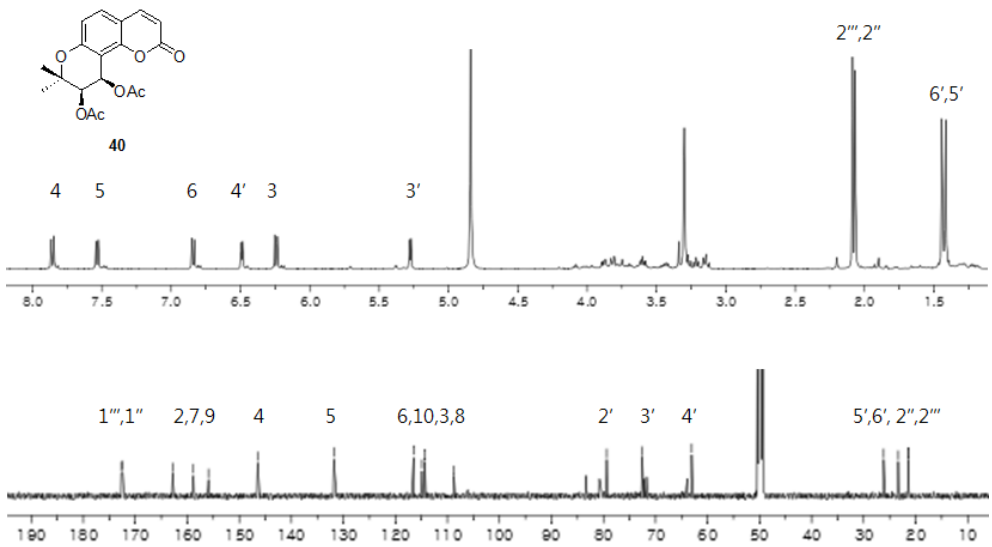

Figure 34. ^{1}H and ^{13}C NMR spectra of compound **40** (500/125 MHz, CD_3OD)

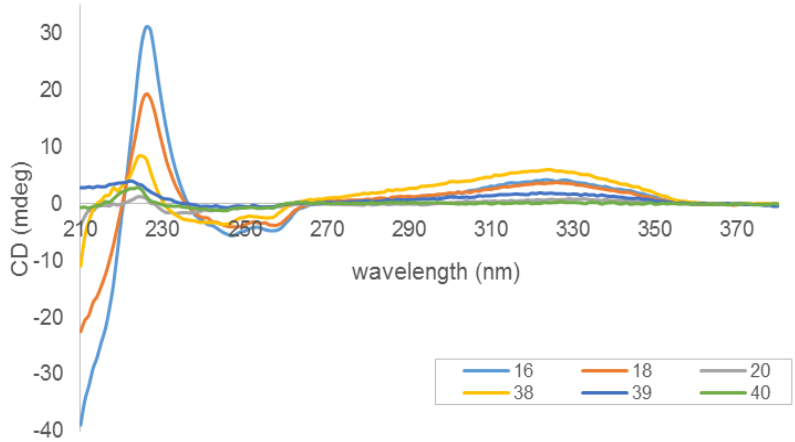

Figure 35. ECD curves of **16**, **18**, **20**, and **38-40**

2.9. Compounds 14 and 28, 29, and 30

Compound **14** was isolated as white amorphous powder and its molecular formula $C_{19}H_{22}O_6$ was determined by HRESIMS. The ^{1}H NMR spectrum of **14** was similar to **13** except for the upshifted signal at δ_H 4.01 (1H, d, *J* = 4.7 Hz, H-3'), downshifted signal at δ_H 6.36 (1H, d, *J* = 4.7 Hz, H-4'), and hydroxy signal at δ_H 2.96 (1H, br s, 3'-OH) (Figure 36). In the HMBC spectrum, H-3' displayed correlations with carbonyl carbon (C-1'') of 2-methylbutyryl group. The 3'*S*,4'*S* configuration was assigned by the coupling constant (4.7 Hz), NOESY correlation, and a Cotton effect at 318 nm (Figure 12). Compound **14** was newly isolated from nature and named (3'*S*,4'*S*)-4'-*O*-(2-methylbutyryl)khellactone.

Using ESIMS, the molecular formulas of compounds **28-30** were indicated. The ^{1}H NMR spectra of **28-30** resembled that of **14**, whose signals revealed the presence of khellactone and 4'-substituent except for **28** (Figures 37-39). The *J* value (4.6-4.7 Hz) between H-3' and H-4' and a Cotton effect at 326-328 nm in the ECD spectra suggested the absolute configurations of **28-30** as 3'*S*,4'*S* (Figure 12). Compounds **28-30** were assigned as (-)-*cis*-khellactone (Wang et al. 2015), (3'*S*,4'*S*)-4'-*O*-acetylkhellactone (qianhucoumarin C) (Kong et al. 1993), and (3'*S*,4'*S*)-3'-hydroxy-4'-*O*-angeloyloxy-3',4'-dihydroseselin (Tosun et al. 2005).

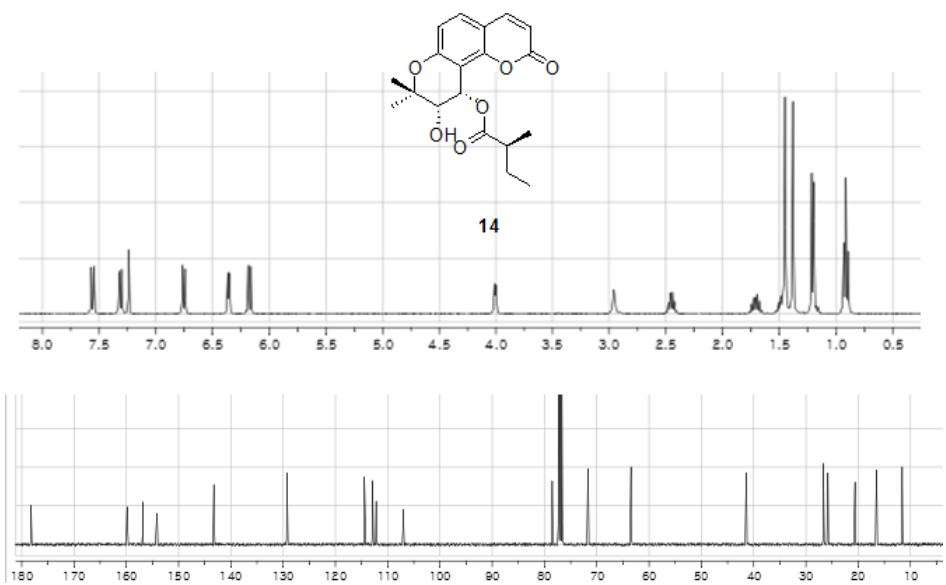

Figure 36. ^{1}H and ^{13}C NMR spectra of compound **14** (400/100 MHz, $CDCl_3$)

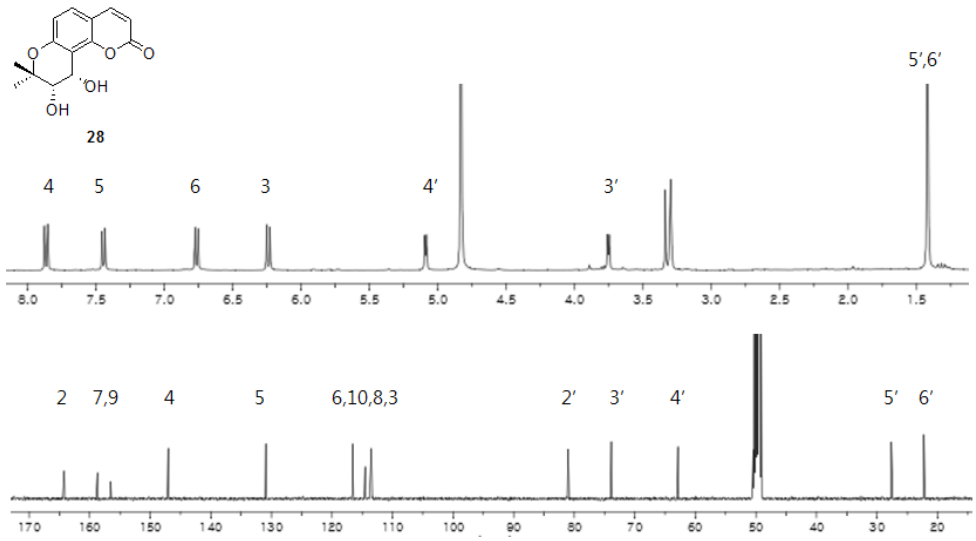

Figure 37. ^{1}H and ^{13}C NMR spectra of compound **28** (400/100 MHz, CD_3OD)

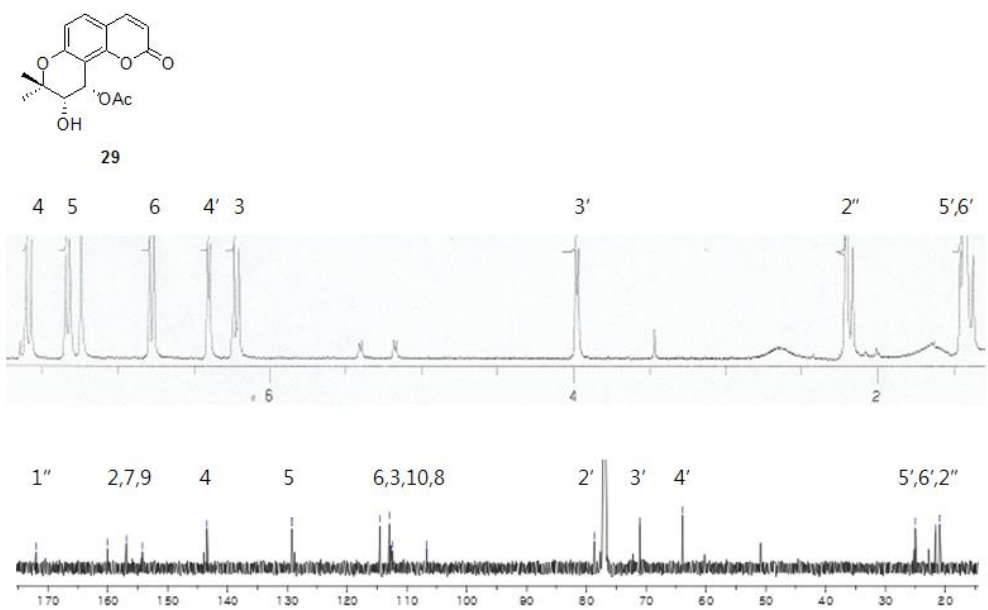

Figure 38. ^{1}H and ^{13}C NMR spectra of compound **29** (300/200 MHz, $CDCl_3$)

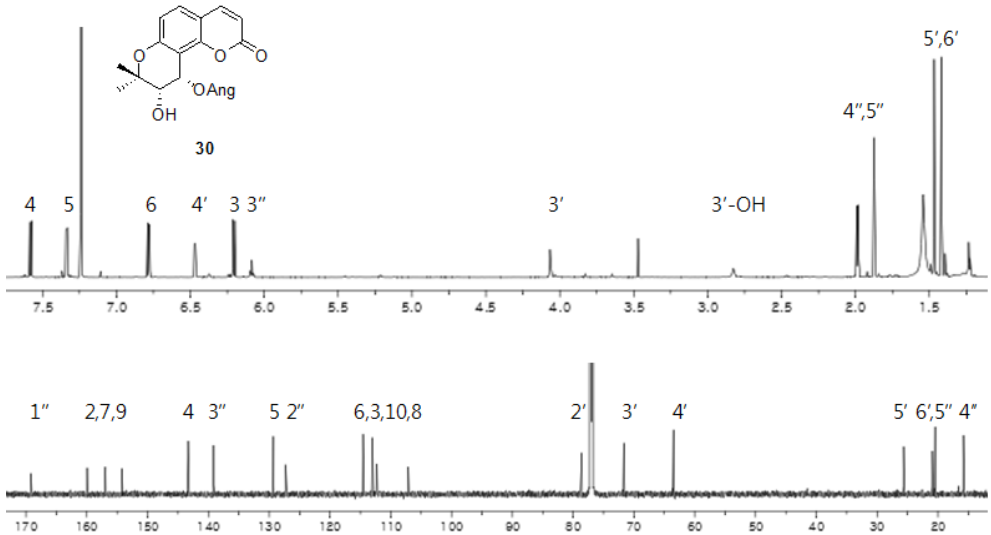

Figure 39. ^{1}H and ^{13}C NMR spectra of compound **30** (800/200 MHz, $CDCl_3$)

2.10. Compounds 31, 32, 33, and 34

Based on ESIMS, the molecular formulas of compounds **31-34** were established. Similar to **1**, the ^{1}H NMR spectra of **31-34** revealed the presence of khellactone and angeloyl group, instead of isobutyryl group at 3'-position (Figures 40-43). The presence of 3'-angeloylkhellactone moieties of **31** and **33-34** was confirmed by HMBC interactions. The *J* value (4.8-4.9 Hz) and NOESY interaction between H-3' and H-4' and a negative Cotton effect at 324-328 nm suggested the 3'*S*,4'*S* configurations of **31-34** (Figures 12). Therefore, the structures of compounds **31-34** were assigned to be (3'*S*,4'*S*)-3'-*O*-angeloyl-4'-*O*-(2-methylbutyryl)khellactone (praeruptorin F) (Lv et al. 2013), (3'*S*,4'*S*)-3',4'-di-*O*-angeloylkhellactone (anomalin, praeruptorin B) (Song et al. 2012), (3'*S*,4'*S*)-3'-*O*-angeloyloxy-4'-hydroxy-3',4'-dihydroseselin (Tosun et al. 2005), and (3'*S*,4'*S*)-3'-*O*-angeloyl-4'-*O*-senecioylkhellactone (calipteryxin) (Song et al. 2012).

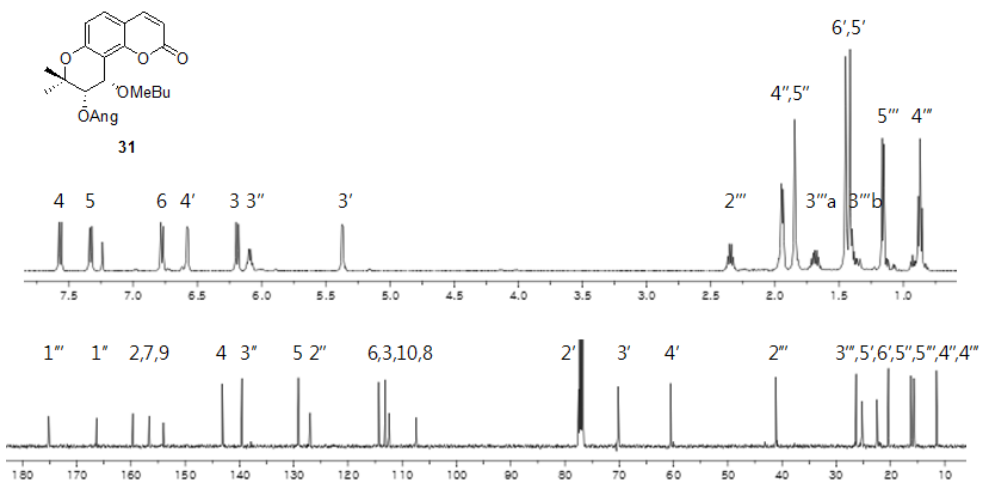

Figure 40. ^{1}H and ^{13}C NMR spectra of compound **31** (600/150 MHz, $CDCl_3$)

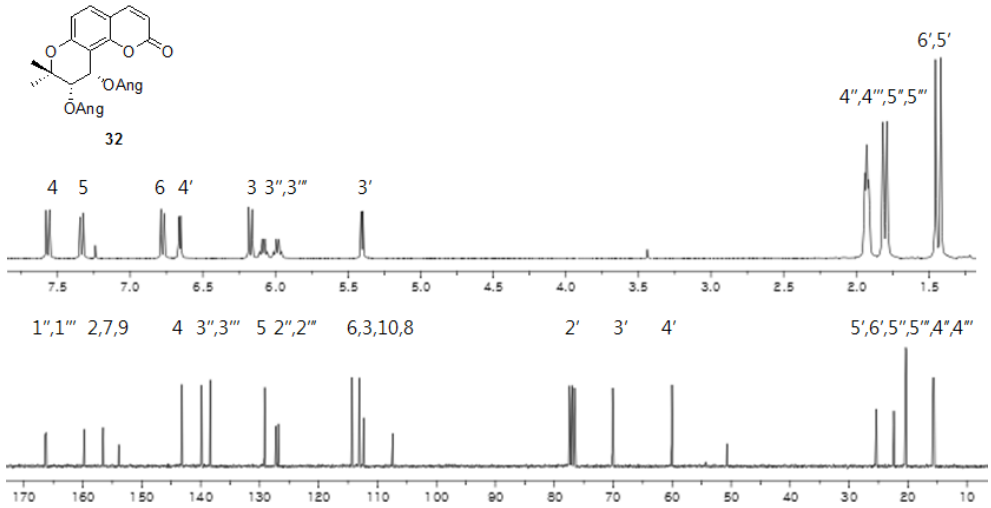

Figure 41. ^{1}H and ^{13}C NMR spectra of compound **32** (400/75 MHz, $CDCl_3$)

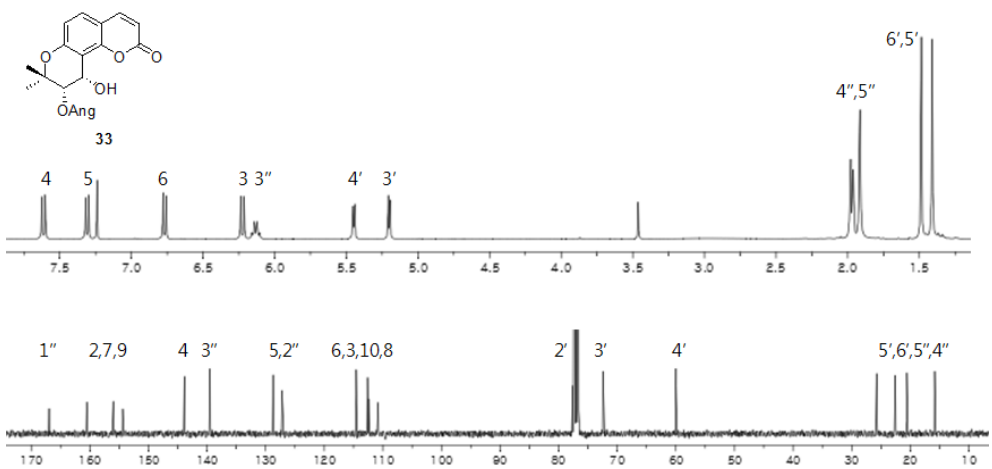

Figure 42. ^{1}H and ^{13}C NMR spectra of compound **33** (400/100 MHz, $CDCl_3$)

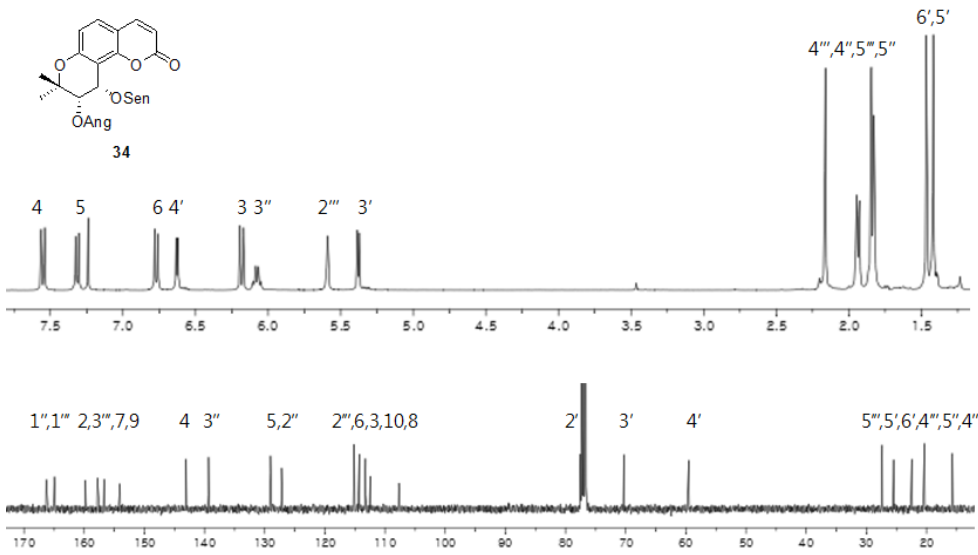

Figure 43. ^{1}H and ^{13}C NMR spectra of compound **34** (400/100 MHz, $CDCl_3$)

2.11. Compounds 35, 36, and 37

Compounds **35-37** were obtained as white amorphous powders, whose molecular formulas were indicated based on ESIMS. The ^{1}H NMR spectra of **35-37** displayed the signals of khellactone and isovaleryl moiety, which resembles that of **9** (Figures 44-46). The HMBC interaction or MS fragmentation (*m/z* 329, M^{+} - OR_2, R_2 = 4'-substituent) revealed that **35-37** are possessing 3'-isovalerylkhellactone moiety. The coupling constant (4.6-5.1 Hz) between H-3' and H-4' and a negative Cotton effect at 323-326 nm indicated that the configurations of **31-34** were 3'*S*,4'*S* (Figure 12). Compounds **35-37** were assigned as (3'*S*,4'*S*)-3'-*O*-isovaleryl-4'-*O*-senecioylkhellactone (Lee et al. 2014), (3'*S*,4'*S*)-3',4'-di-*O*-isovalerylkhellactone (Song et al. 2012), and (3'*S*,4'*S*)-3'-*O*-isovaleryl-4'-*O*-(2-methylbutyryl) khellactone (praeruptorin H) (Lv et al. 2013).

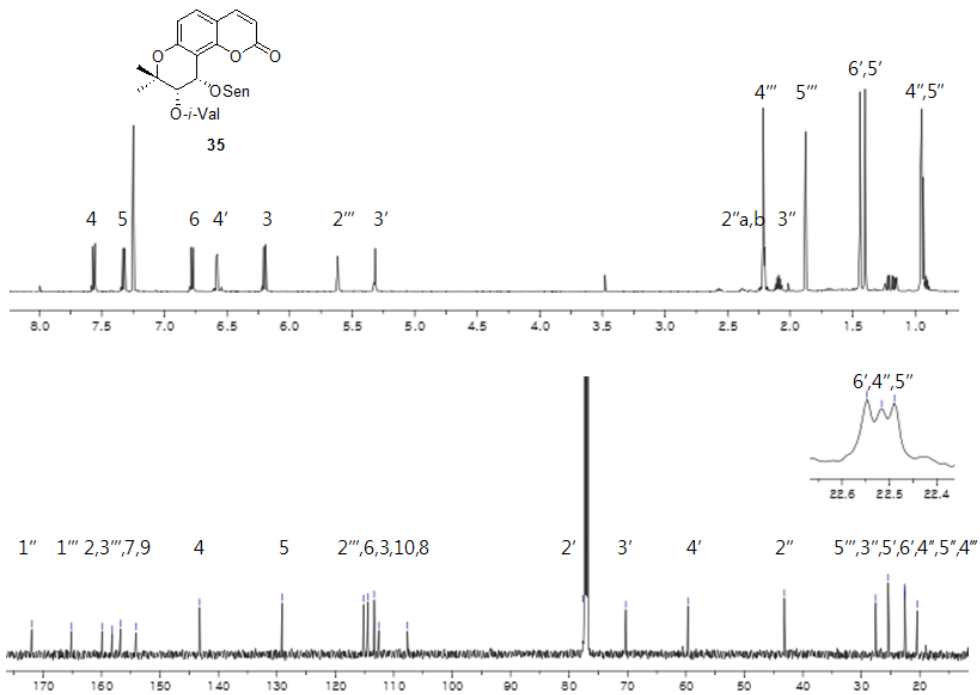

Figure 44. ^{1}H and ^{13}C NMR spectra of compound **35** (600/150 MHz, $CDCl_3$)

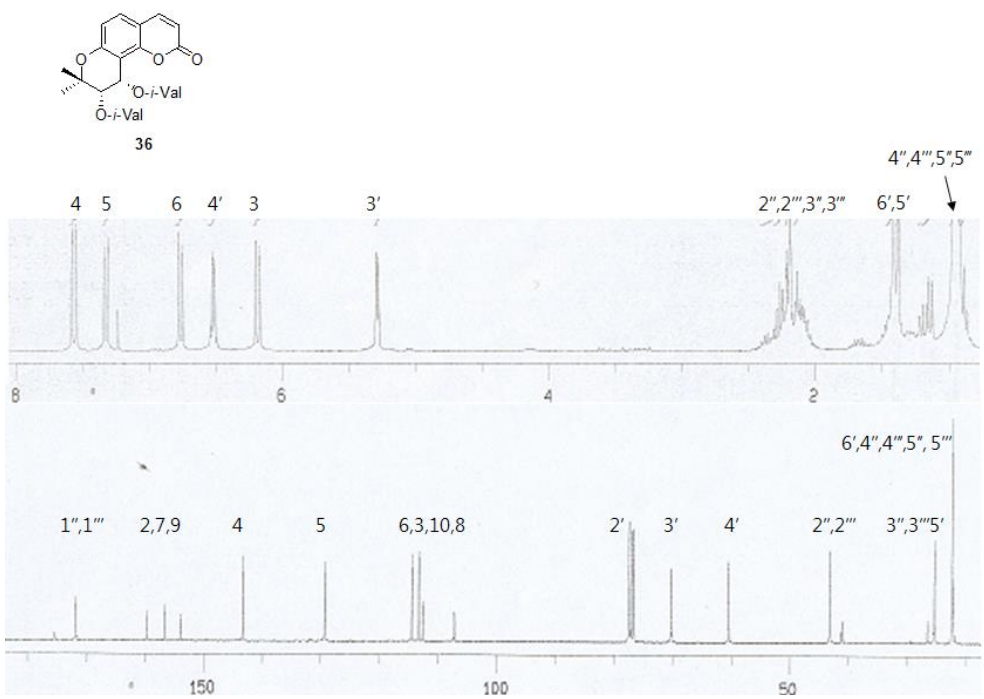

Figure 45. ^{1}H and ^{13}C NMR spectra of compound **36** (300/75 MHz, $CDCl_3$)

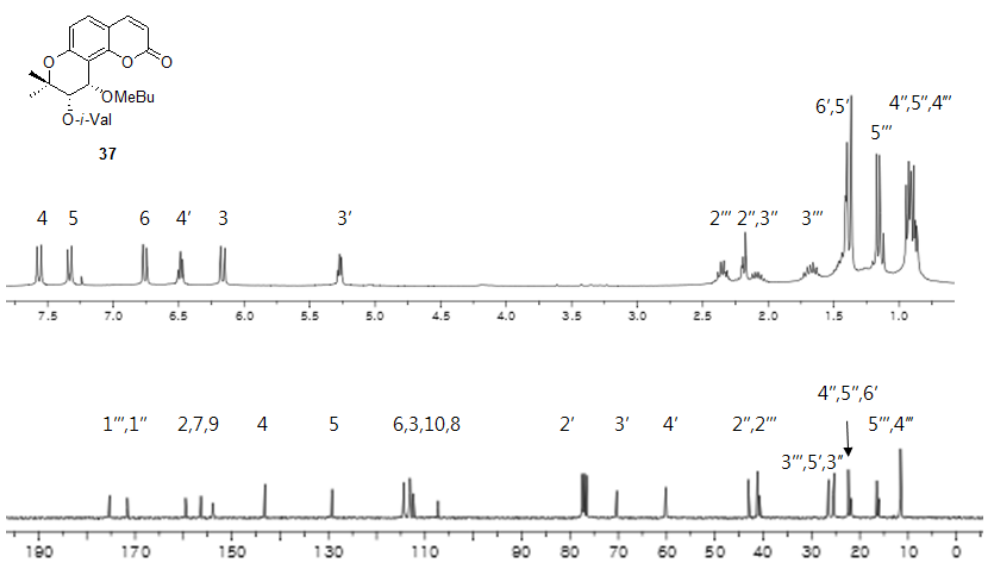

Figure 46. ^{1}H and ^{13}C NMR spectra of compound **37** (600/150 MHz, $CDCl_3$)

2.12. Compounds 38 and 39

Compounds **38-39** were isolated as white amorphous powder, whose molecular formulas $C_{19}H_{20}O_5$ and $C_{19}H_{22}O_5$ were suggested by ESIMS. The proton signals of methine and methylene in pyran were observed [**38**: δ_H 5.13 (1H, t, *J* = 4.9 Hz, H-3'), 3.18 (1H, dd, *J* = 18.0, 4.9 Hz, H-4'a), and 2.98 (1H, dd, *J* = 18.0, 4.9 Hz, H-4'b); **39**: δ_H 5.12 (1H, t, *J* = 5.2 Hz, H-3'), 3.18 (1H, dd, *J* = 17.8, 5.2 Hz, H-4'a), and 2.94 (1H, dd, *J* = 17.8, 5.2 Hz, H-4'b)], which indicated the presence of angular 3'-acyloxypyranocoumarin moiety (Figures 47-48). The ECD spectra of **38-39** showed similar pattern with that of **40**, so the inferred absolute configurations of **38-39** were 3'*S* (Figure 35). In comparison with the optical rotation and spectral data in the literature, compounds **38-39** were determined as (3'*R*)-*O*-senecioyllomatin and (3'*R*)-*O*-isovaleroyllomatin (Buendia-Trujillo et al. 2014; Bohlmann and Rode 1968).

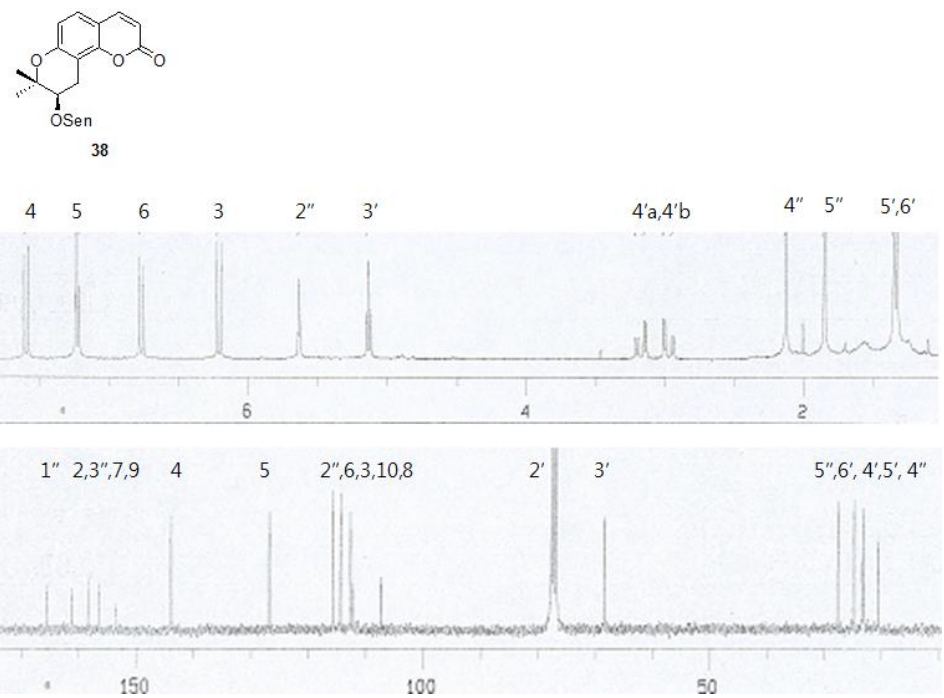

Figure 47. ^{1}H and ^{13}C NMR spectra of compound **38** (300/75 MHz, $CDCl_3$)

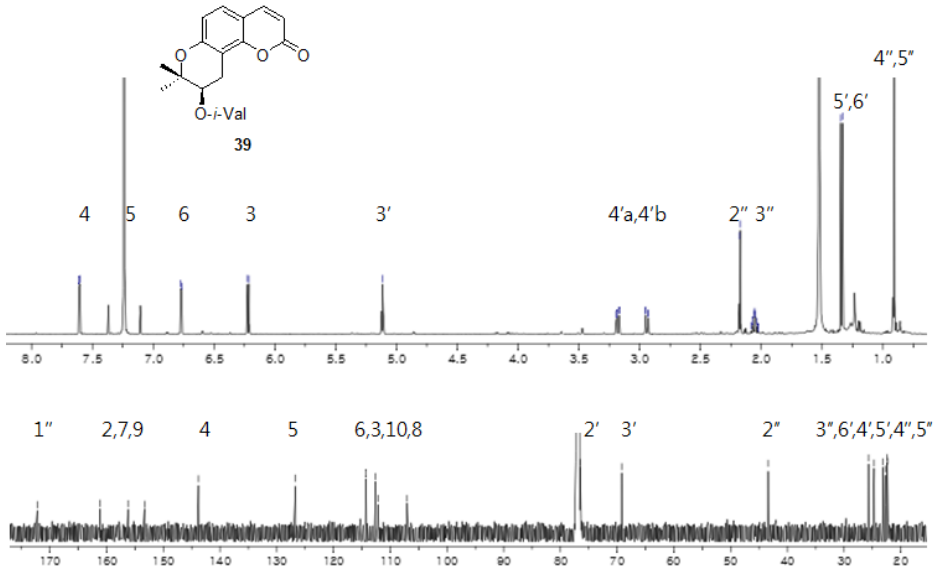

Figure 48. ^{1}H and ^{13}C NMR spectra of compound **39** (800/200 MHz, $CDCl_3$)

2.13. Compounds 16, 17, 18, 19, and 20

Compound **16**, **E1** (enantiomeric mixture of **17** and **18**), and **E2** (enantiomeric mixture of **19** and **20**) were isolated from same fraction, H39. Compound **16** possessed the molecular composition $C_{19}H_{20}O_6$, indicated by HRCIMS (*m/z* 345.1335 $[M+H]^+$). In the ^1H and ^{13}C NMR spectra, **16** showed resemblance with its diastereomer **17**, except for the proton and carbon signals at δ_H 6.08 (1H, d, *J* = 3.4 Hz, H-4'), δ_C 67.8 (C-4'), whereas that of **17** was displayed at δ_H 6.43 (1H, d, *J* = 4.8 Hz, H-4'), δ_C 63.0 (C-4') (Figure 49). Because of the coupling constant (3.4 Hz) and the absence of a NOESY interaction, the relative configuration at the 3' and 4'-positions was suggested as *trans*. The absolute configuration of **16** at 3'-position was established as *S* based on the Mosher method (Figure 50). Due to the *trans* orientation between the 3' and 4' positions, the configuration at the 4' position was assigned as *R*. The experimental ECD spectrum of **16** was in good agreement with the calculated ECD spectrum of that (Figure 51). Based on the above findings, Compound **16** was determined to be (3'*S*,4'*R*)-4'-*O*-senecioylkhellactone and it was isolated for the first time from nature.

To determine the absolute configuration, **E1** (enantiomeric mixture of compounds **17** and **18**) was derivatized by the Mosher reagents. After MTPA reaction of **E1**, the (*S*)-MTPA esters **17a** and **18a**, and (*R*)-MTPA esters **17b** and **18b** were isolated by HPLC. The absolute configurations of **17** and **18** were suggested as 3'*S*,4'*S* and 3'*R*,4'*R* based on the Mosher method (Figure 52).

Based on the ^1H and ^{13}C NMR spectra, it was revealed that compounds **19** and **20** were positional isomer of compounds **17** and **18** (Figures 54-57). In the same manner with **17** and **18**, the configurations of **19** and **20** were determined as 3'*S*,4'*S* and 3'*R*,4'*R* (Figure 53).

After discovering enantiomeric mixtures (**E1** and **E2**), enantioseparation was carried out on a chiral-selective column. From **E1** and **E2**, compounds **17** and **18**, and **19** and **20** were isolated, respectively. Based on the opposite optical rotations, mirror symmetric ECD patterns, and similar NMR spectra, the structures of the enantiomers were confirmed. In addition, the calculated ECD spectra of **17-20** displayed similar positive and negative Cotton effects with the experimental ECD

spectra of them (Figures 58-61). Because of similar ratios of the MTPA reaction products and enantioseparation products, RP-HPLC analysis of MTPA esters could be an alternative way to confirm the enantiomer existence. Taken together, the structure of compounds **17-20** were assigned to be (3'*S*,4'*S*)-4'-*O*-senecioylkhellactone, (3'*R*,4'*R*)-4'-*O*-senecioyl khellactone, (3'*S*,4'*S*)-3'-*O*-senecioylkhellactone, and (3'*R*,4'*R*)-3'-*O*-senecioyl khellactone (Ikeshiro et al. 1993; M. Swager and H. Cardellina Ii 1985; Gonzalez et al. 1979).

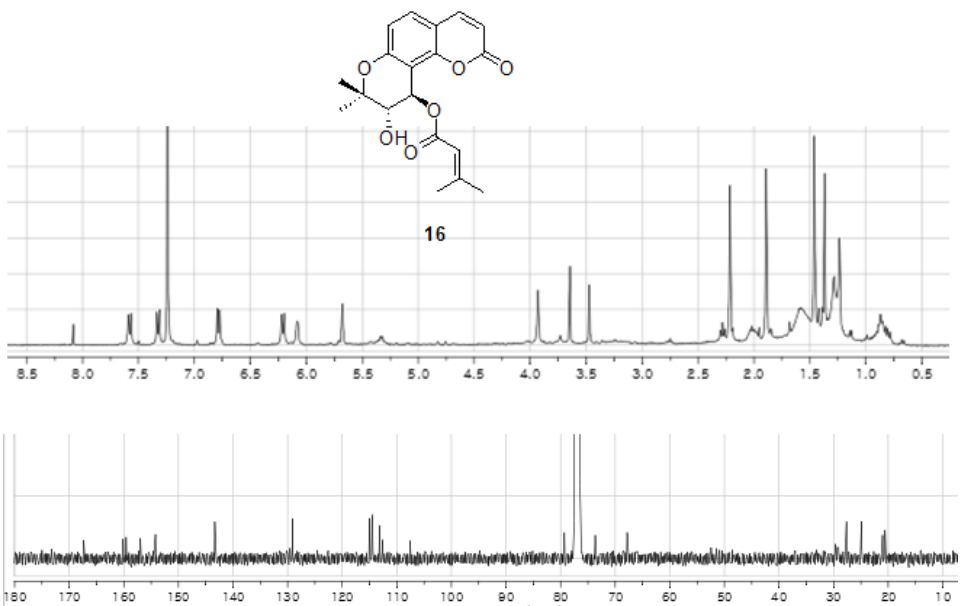

Figure 49 ^{1}H and ^{13}C NMR spectra of compound **16** (400/100 MHz, $CDCl_3$)

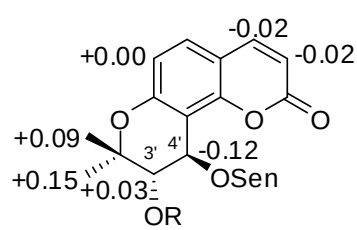

16a R=(*S*)-MTPA ester
16b R=(*R*)-MTPA ester

Figure 50. $\Delta\delta$ (δ_S-δ_R) values obtained from MTPA esters for compound **16**

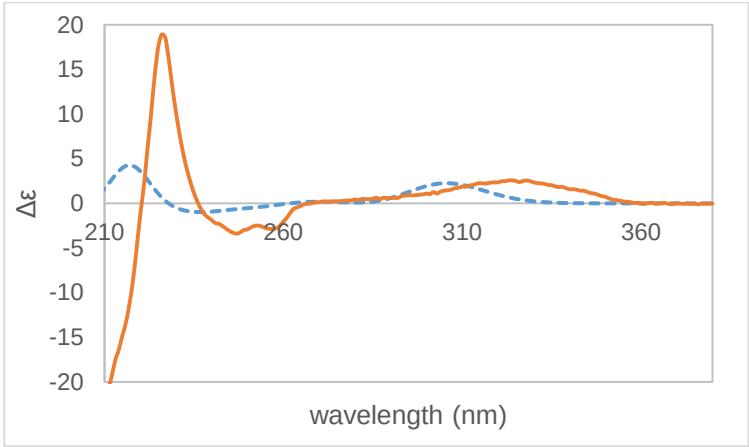

Figure 51. Calculated (dashed) and experimental (solid) ECD spectra of **16**

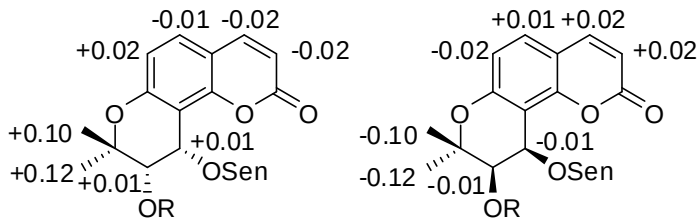

17a R=(*S*)-MTPA ester
17b R=(*R*)-MTPA ester

18a R=(*S*)-MTPA ester
18b R=(*R*)-MTPA ester

Figure 52. $\Delta\delta$ (δ_S-δ_R) values obtained from MTPA esters for compounds **17** and **18**

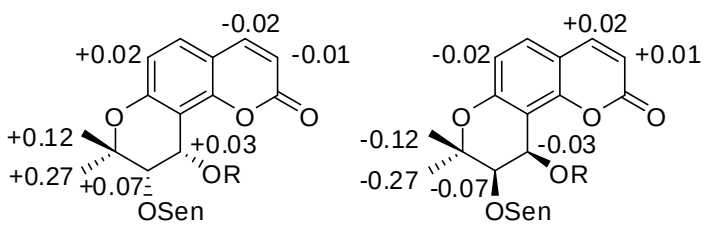

19a R=(*S*)-MTPA ester
19b R=(*R*)-MTPA ester

20a R=(*S*)-MTPA ester
20b R=(*R*)-MTPA ester

Figure 53. $\Delta\delta$ (δ_S-δ_R) values obtained from MTPA esters for compounds **19** and **20**

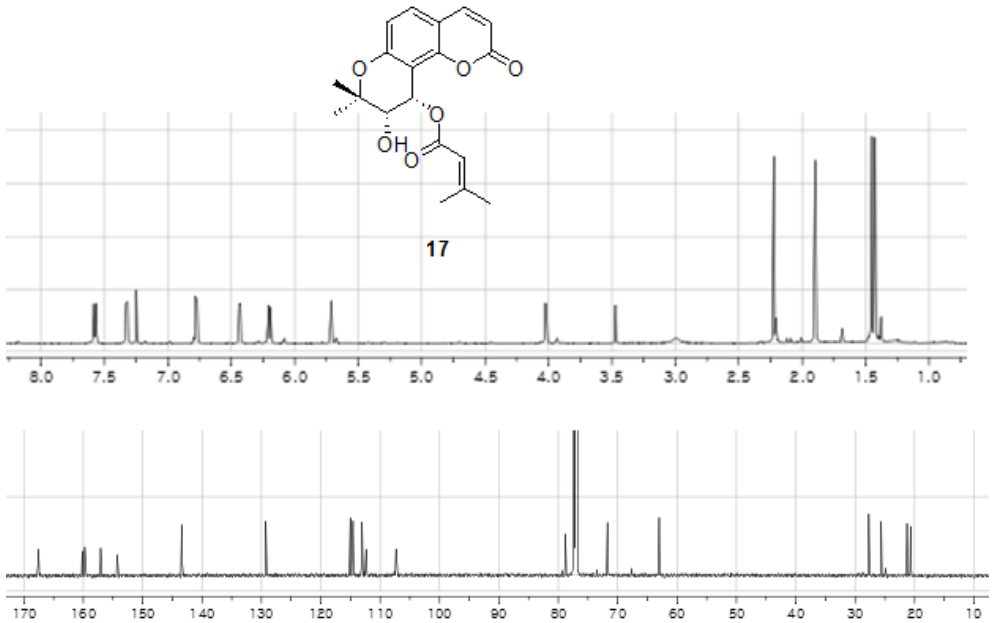

Figure 54. ^{1}H and ^{13}C NMR spectra of compound **17** (600/150 MHz, $CDCl_3$)

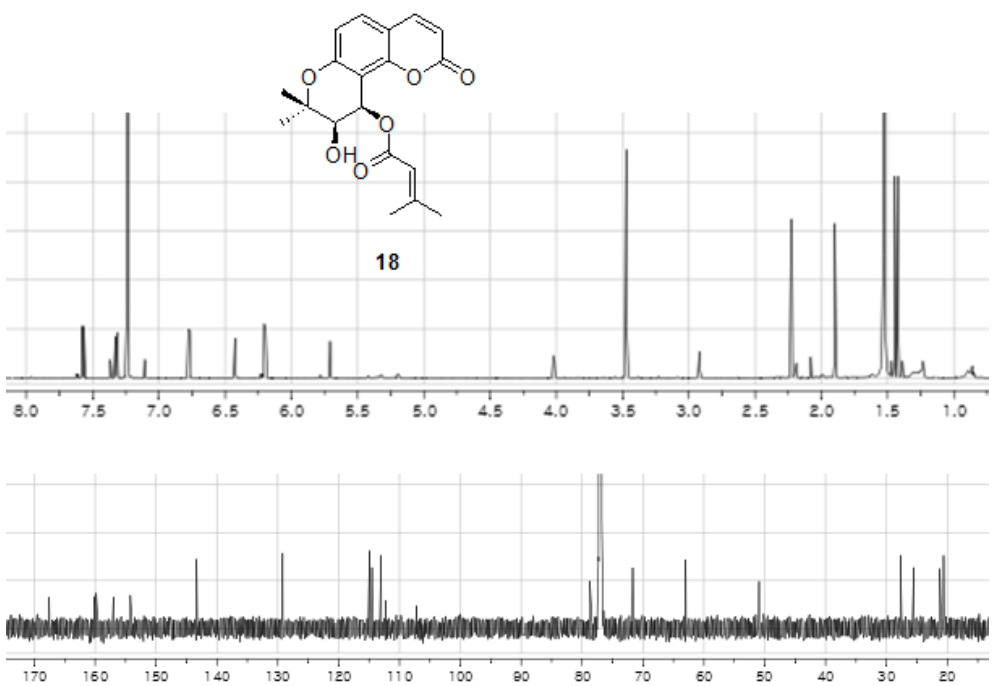

Figure 55. ^{1}H and ^{13}C NMR spectra of compound **18** (800/200 MHz, $CDCl_3$)

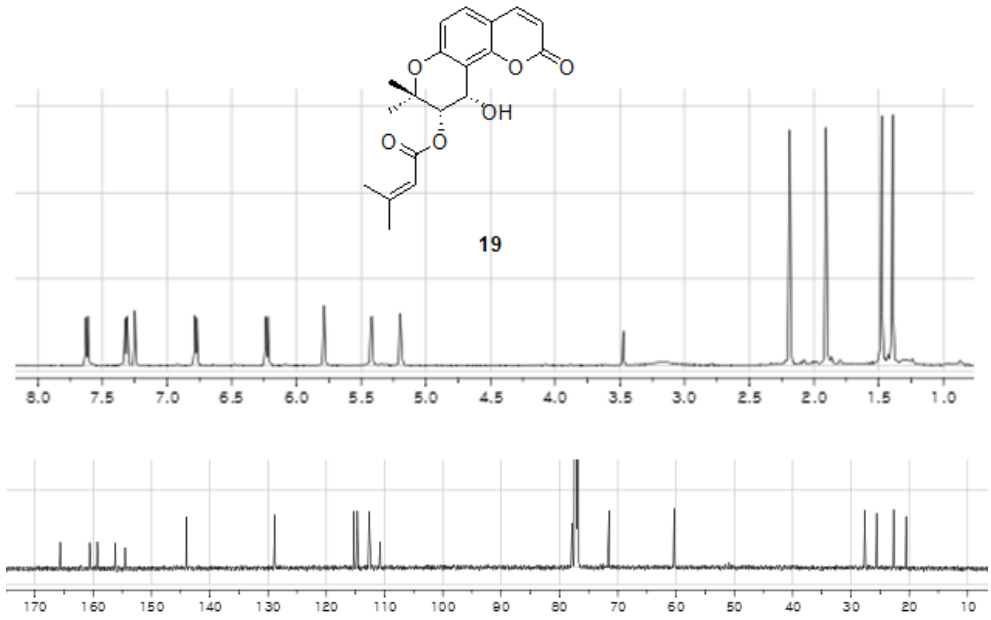

Figure 56. ^{1}H and ^{13}C NMR spectra of compound **19** (600/150 MHz, $CDCl_3$)

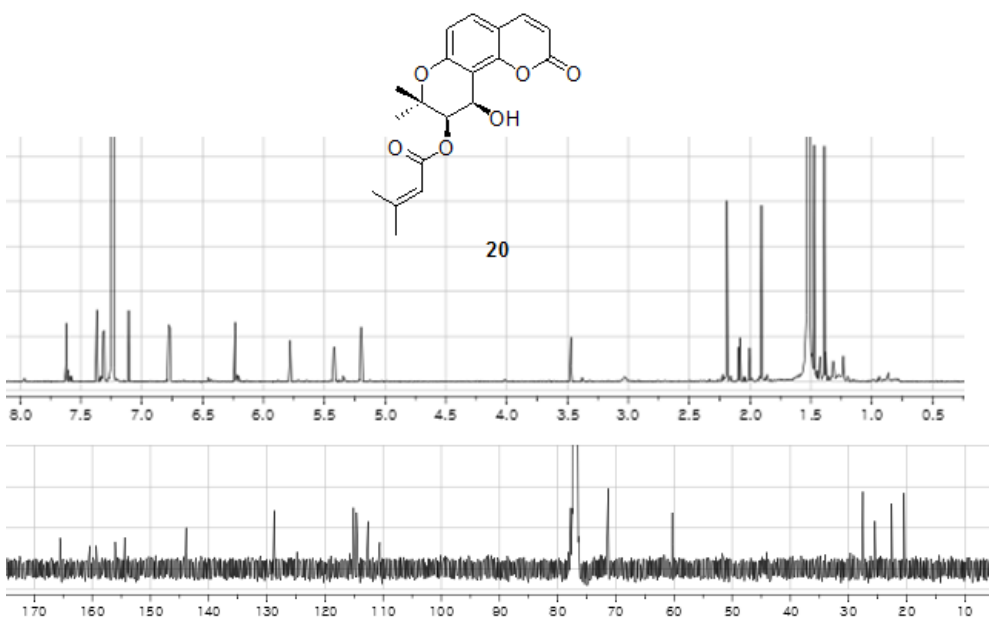

Figure 57. ^{1}H and ^{13}C NMR spectra of compound **20** (800/200 MHz, $CDCl_3$)

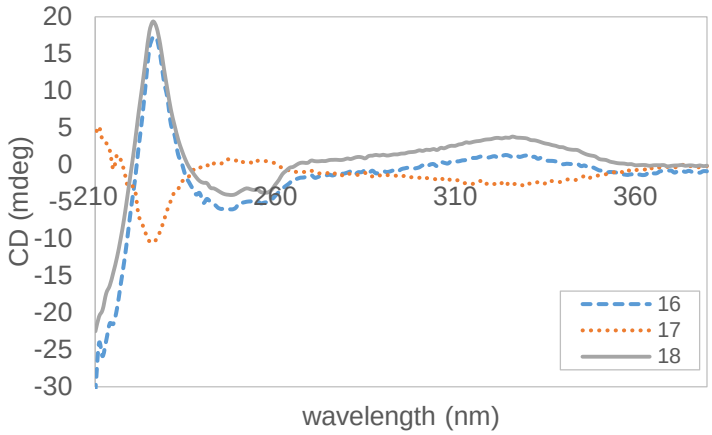

Figure 58. Experimental ECD spectra of **16-18**

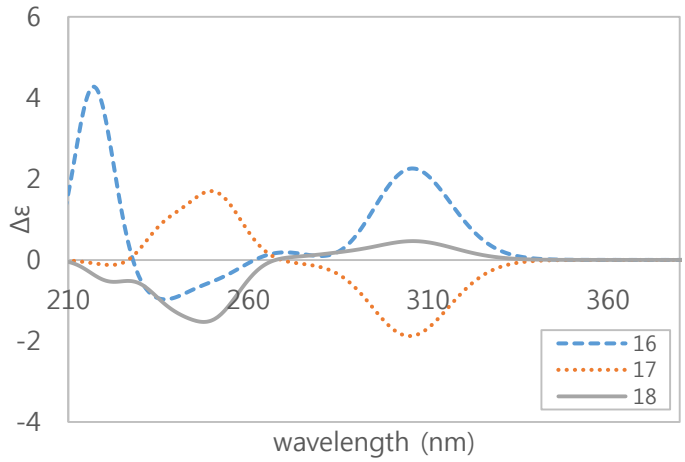

Figure 59. Calculated ECD spectra of **16-18**

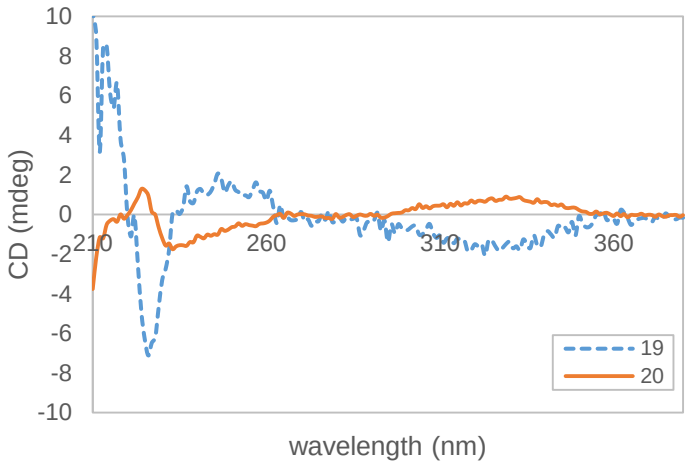

Figure 60. Experimental ECD spectra of **19-20**

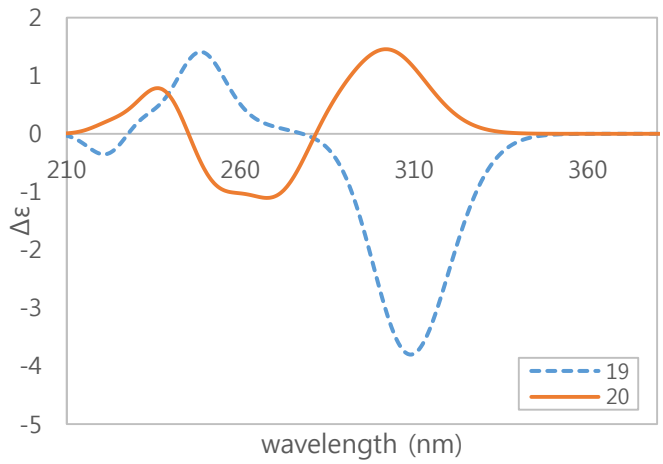

Figure 61. Calculated ECD spectra of **19-20**

Chapter 3. Structure Elucidation of Angular Furanocoumarins

3.1. Compounds 41-43

In HRCIMS, molecular ion peak of **41** was observed at *m/z* 361.1284 $[M+H]^+$ and its molecular composition was established as $C_{19}H_{20}O_7$. In comparison with the ^1H and ^{13}C NMR spectra of pyranocoumarin **17**, the signals at δ_H 6.74 (1H, s, H-3') and 4.20 (1H, br s, 2'-OH), and δ_C 112.8 (C-2') exhibited significant differences, which revealed the presence of angular monohydro-monohydroxy-furanocoumarin skeleton (Figure 62). The attachment of isopropyl group, angular furan, coumarin, and senecioyl group was confirmed by HMBC correlations of H-5' and H-6' with C-2' and C-4', and of 2'-OH with C-2', C-3', and C-4', and of H-3' with C-2', C-4', C-7, C-8, C-9, and C-1'' (Figures 63-64). Due to the intramolecular seven-membered ring hydrogen bonding between 2'-OH and 1''-carbonyl group, the proton signal of 2'-OH was displayed at δ_H 4.20 (br s), which indicated *trans*-orientation at 2' and 3'-positions. The experimental ECD spectrum of **41** showed the similar pattern with the calculated ECD spectrum of 2'*R*,3'*R* isomer (Figure 65). Therefore, the structure of **41** was determined as (2'*R*,3'*R*)-2'-hydroxy-3'-*O*-senecioylvaginol and it was isolated first time from nature.

In the same manner, angular monohydro-monohydroxy-furanocoumarin moiety of **42** and **43** was suggested based on 1D and 2D NMR spectra (Figures 66 and 68). The *trans* configuration at 2' and 3'-position was confirmed by intramolecular hydrogen bonding between 2'-OH and carbonyl oxygen at C-1''. Comparing the calculated ECD spectra of **42-43** to the experimental ECD spectra, the absolute configuration was indicated as 2'*R*,3'*R* (Figures 67 and 69). Compounds **42** and **43** were assinged to be (2'*R*,3'*R*)-2'-hydroxy-3'-*O*-(2-methylbutyryl)vaginol and (2'*R*,3'*R*)-2'-hydroxy-3'-*O*-isovaleryl vaginol and they were firstly obtained from nature.

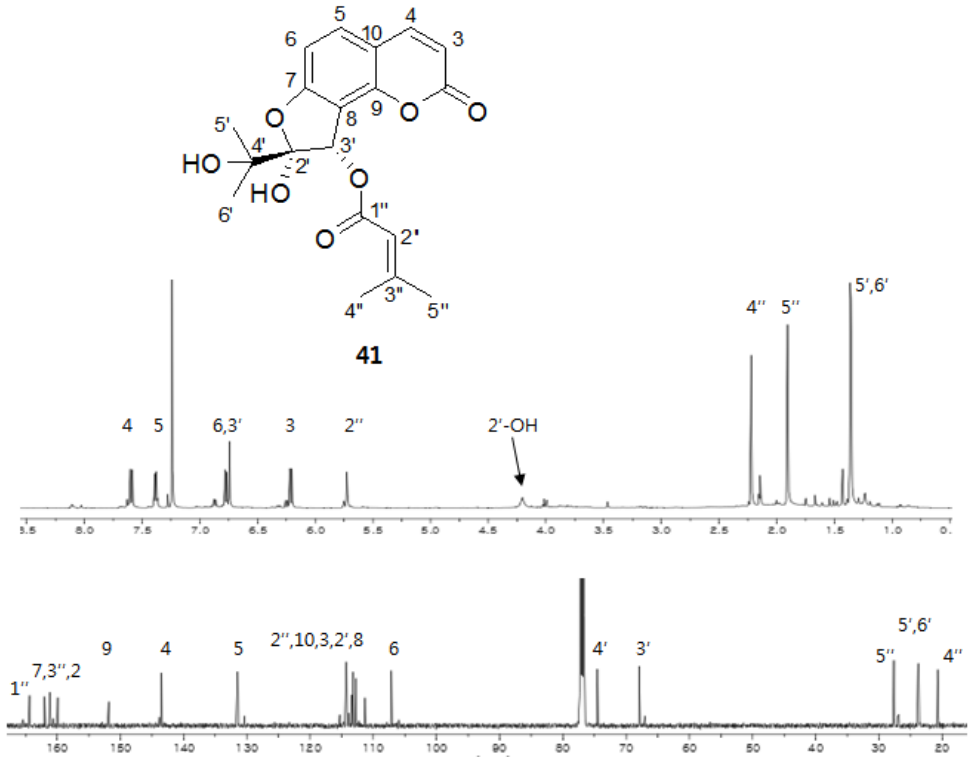

Figure 62. ^{1}H and ^{13}C NMR spectra of compound **41** (500/125 MHz, $CDCl_3$)

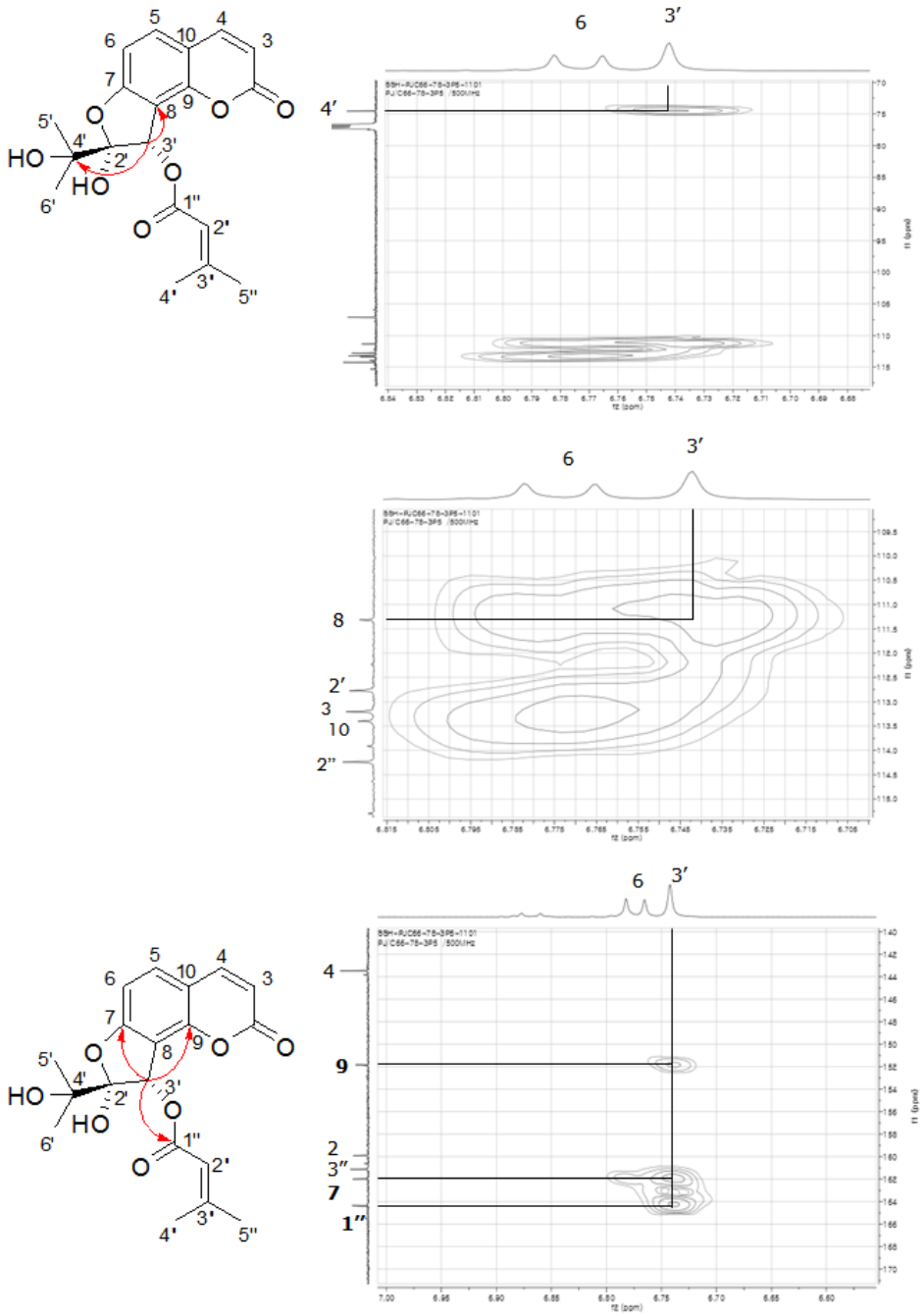

Figure 63. HMBC spectrum of compound **41** (500 MHz, $CDCl_3$)

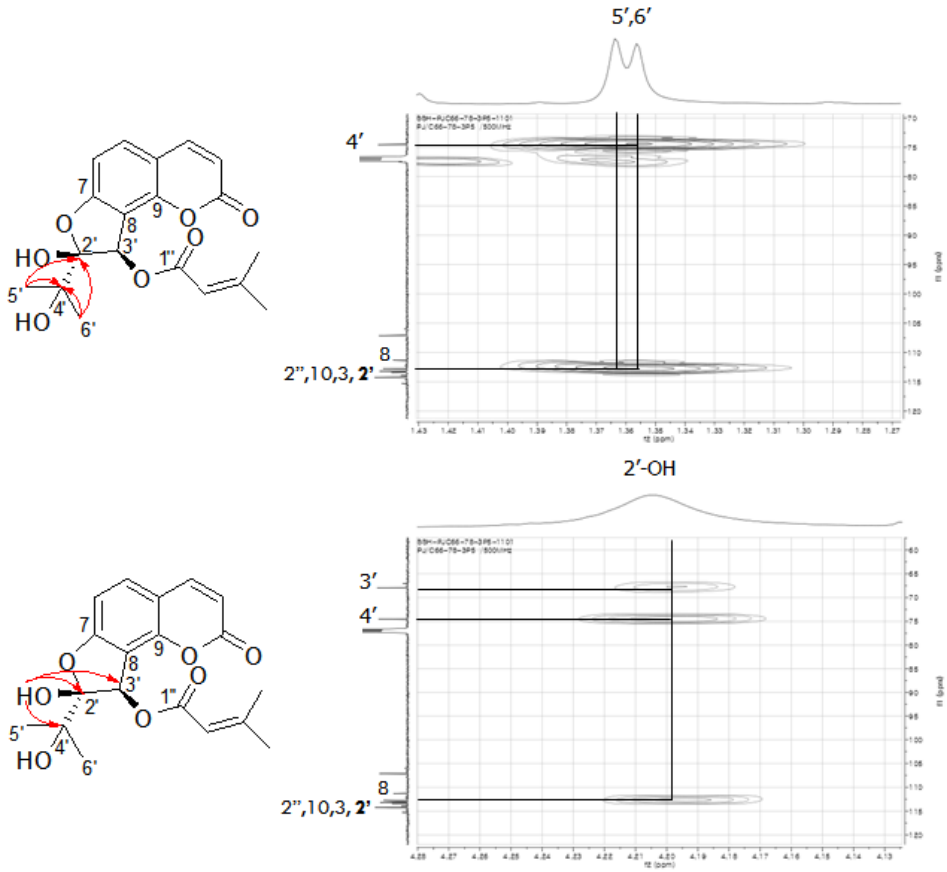

Figure 64. HMBC spectrum of compound **41** (500 MHz, $CDCl_3$)

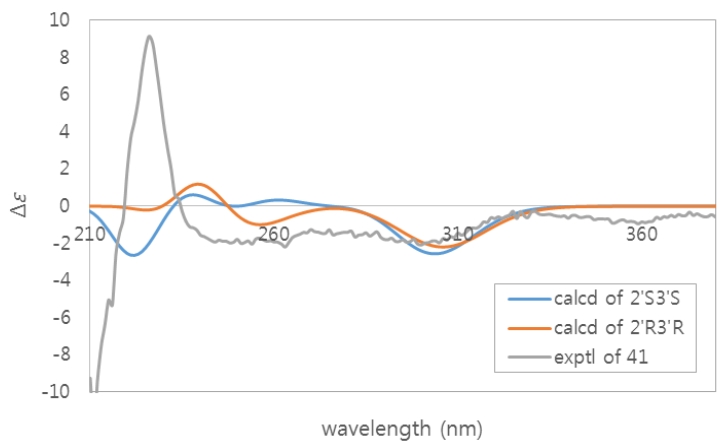

Figure 65. Calculated and experimental ECD curves of **41**

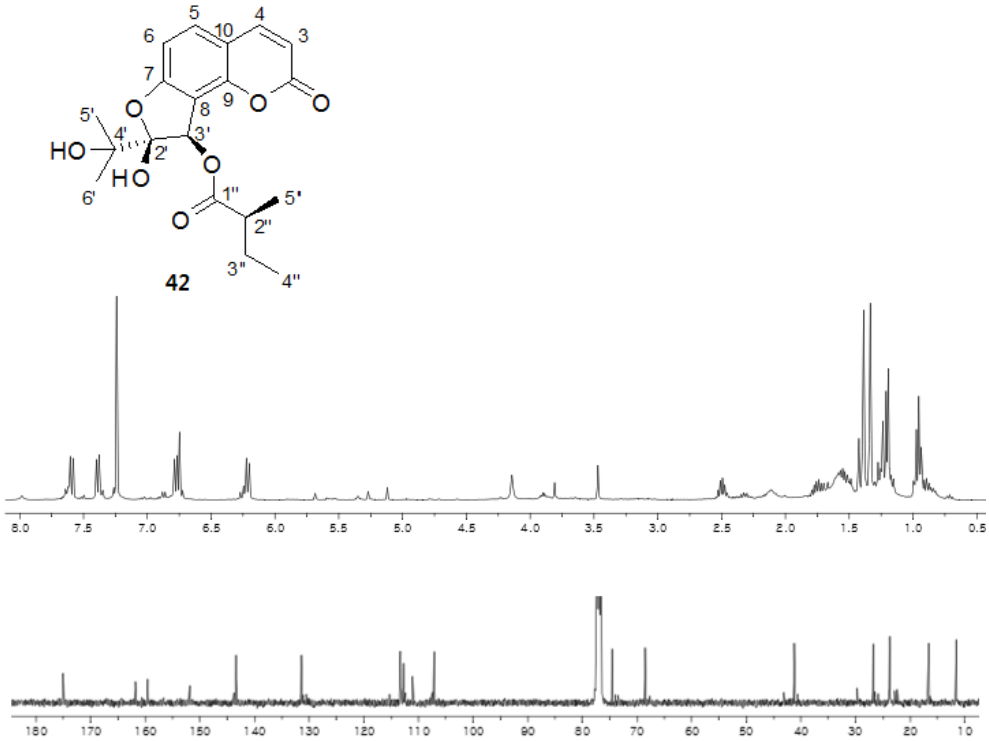

Figure 66. ^{1}H and ^{13}C NMR spectra of compound **42** (400/100 MHz, $CDCl_3$)

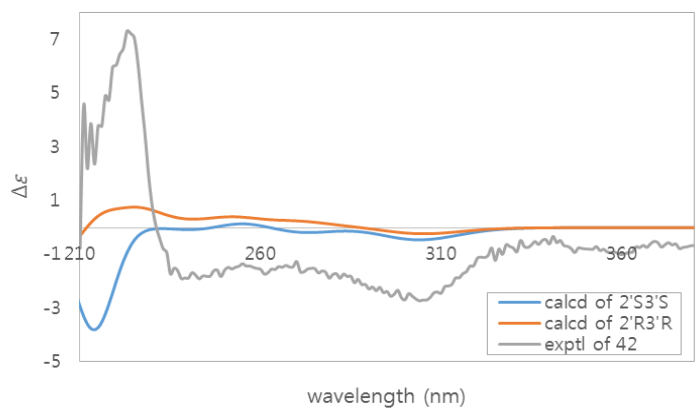

Figure 67. Calculated and experimental ECD curves of **42**

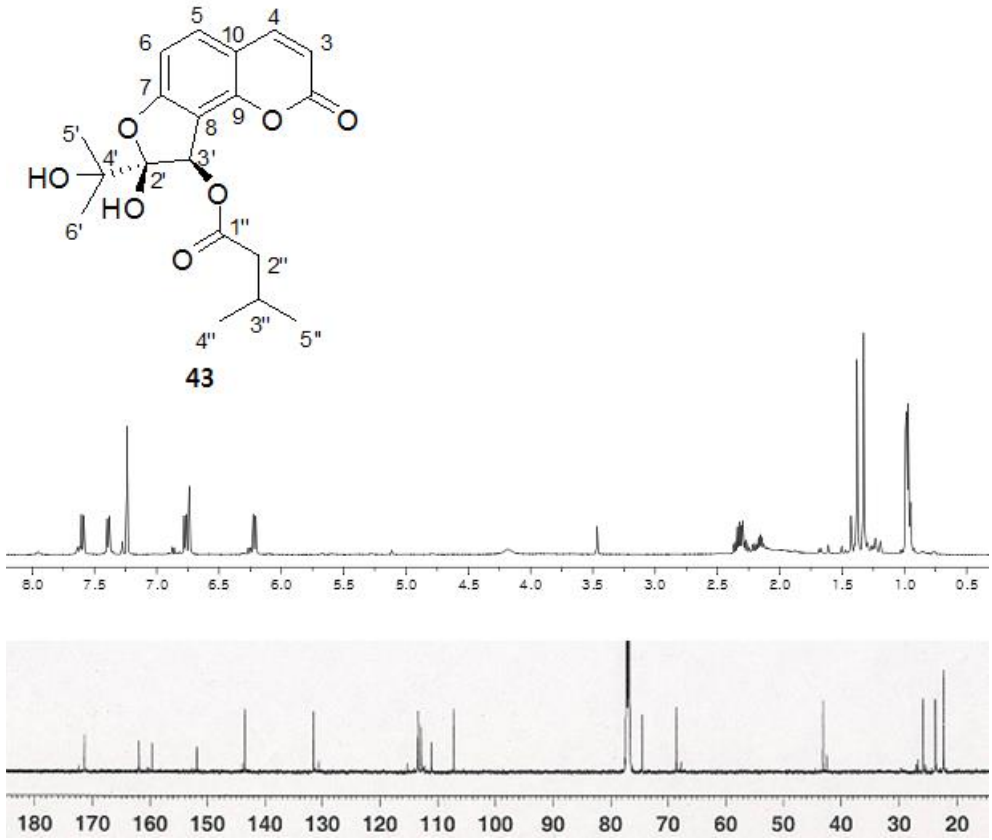

Figure 68. ^{1}H and ^{13}C NMR spectra of compound **43** (500/125 MHz, $CDCl_3$)

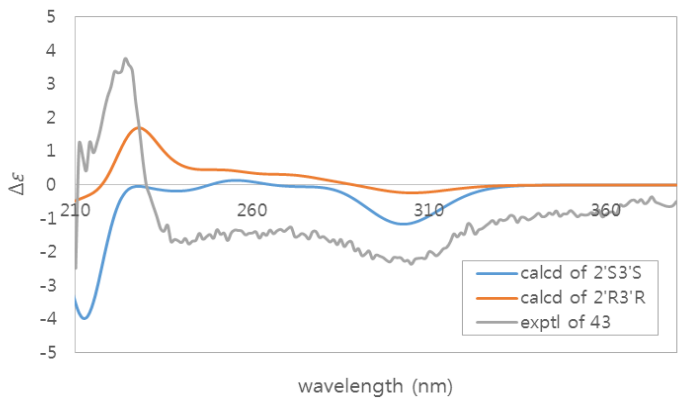

Figure 69. Calculated and experimental ECD curves of **43**

3.2. Compound 48

Compound **48** was acquired as white amorphous powder and its molecular composition $C_{19}H_{20}O_6$ was indicated by ESIMS. Different to **41**, the ^{1}H and ^{13}C NMR spectra of **48** revealed the presence of angular dihydrofuran moiety, whose signals were observed at δ_H 6.98 (1H, d, *J* = 6.6 Hz, H-3') and 6.98 (1H, d, *J* = 6.6 Hz, H-2'), and δ_C 94.4 (C-2') (Figure 70). The relative configuration at 2' and 3'-position was defined as *cis* based on the *J* value (6.6 Hz). Therefore, the structure of **48** was identified as 3'-*O*-senecioylvaginidiol (Mohammadi et al. 2010).

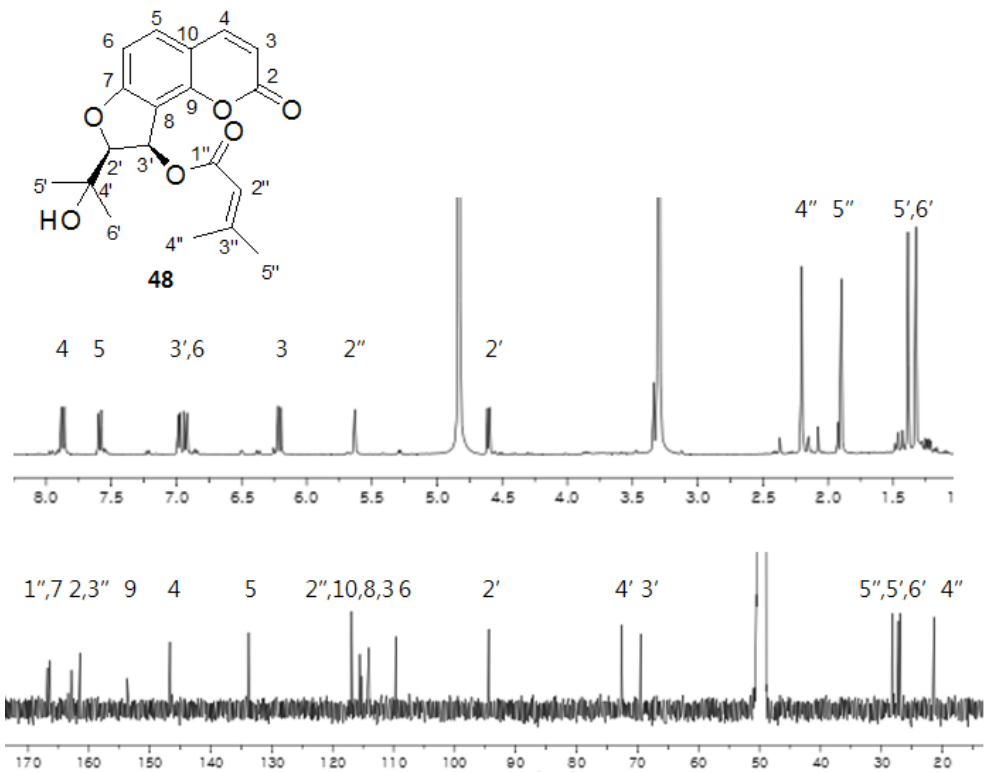

Figure 70. ^{1}H and ^{13}C NMR spectra of compound **48** (400/100 MHz, CD_3OD)

Chapter 4. Structure Elucidation of Other Compounds

4.1. Compound 44

Compound **44** was obtained as white amorphous powder. Its molecular composition $C_{14}H_{14}O_4$ was determined by ESIMS. In the ^{1}H NMR spectrum of **44**, the presence of linear-type dihydrofuranocoumarin moiety was revealed based on the signals of two singlet methines at δ_H 7.39 (1H, s, H-5) and 6.71 (1H, s, H-8) and the signals of isopentyl moiety at δ_H 4.74 (1H, dd, J = 9.0, 8.4 Hz, H-2'), 3.24 (2H, m, H-3'), 1.28 (3H, s, H-5'), and 1.22 (3H, s, H-6') (Figure 71). In comparison with the optical rotation in the literature, compound **44** was defined as (+)-marmesin (nodakenetin) (Znati et al. 2014; Jiang et al. 2011).

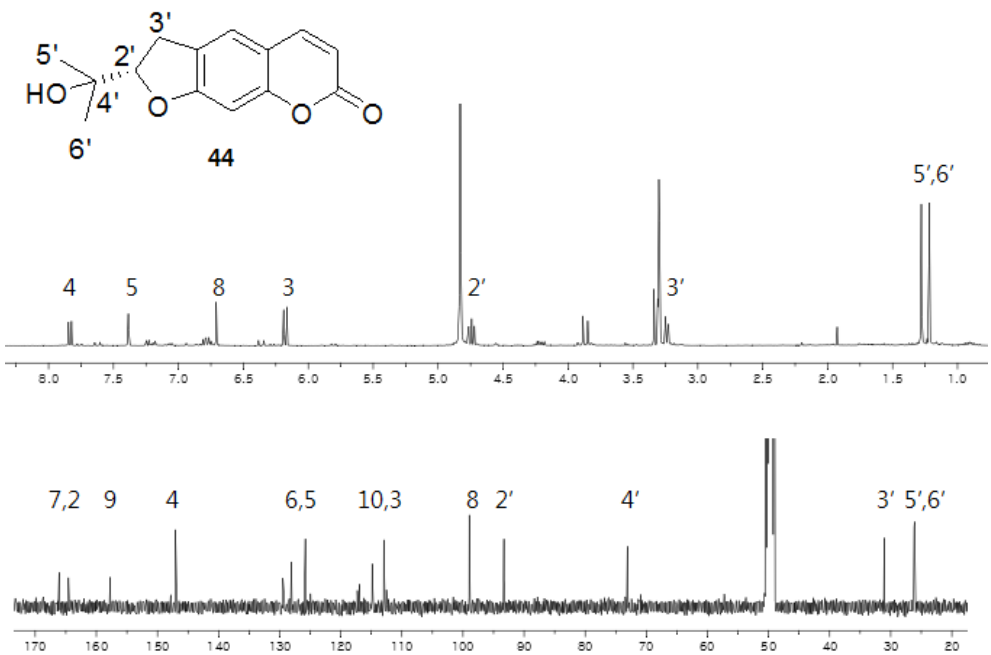

Figure 71. ^{1}H and ^{13}C NMR spectra of compound **44** (400/100 MHz, CD_3OD)

4.2. Compounds 45-47

The molecular composition of compound **45** was established as $C_{18}H_{20}O_7$ based on ESIMS. The proton signals of two doublet methines at δ_H 7.83 (1H, d, *J* = 2.3 Hz, H-2'), 7.23 (1H, d, *J* = 2.3 Hz, H-3') revealed the furanocoumarin moiety in this structure (Figure 72). In the proton NMR, the signals of 5-OMe and isopentyl group at C-8 were also observed. The 5-OMe was located at C-5 based on the NOESY correlation of 5-OMe with H-3' and H-4. The structure of **45** was identified as 9-(2-hydroxy-3-methoxy-3-methylbutoxy)bergapten (Bergendorff et al. 1997).

The molecular formulas of compounds **46** and **47** were determined by ESIMS. Based on the proton signals of two methines [**46**: δ_H 7.57 (1H, d, *J* = 2.4 Hz, H-2'), 6.93 (1H, dd, *J* = 2.4, 0.9 Hz, H-3'); **47**: δ_H 7.58 (1H, d, *J* = 2.4 Hz, H-2'), 6.98 (1H, dd, *J* = 2.4, 0.8 Hz, H-3')], furanocoumarin moieties were suggested (Figures 73 and 74). The structure of linear-type furanocoumarin without substituent at C-8 position was confirmed by the carbon signals at [**46**: δ_C 94.2 (C-8); **47**: δ_C 94.5 (C-8)]. The substituents at C-8 were indicated by ^{1}H and ^{13}C NMR spectra. Therefore, the structures of **46** and **47** were assigned as isoimperatorin and 5-(2-hydroxy-3-methoxy-3-methylbutoxy) psoralen (Bergendorff et al. 1997).

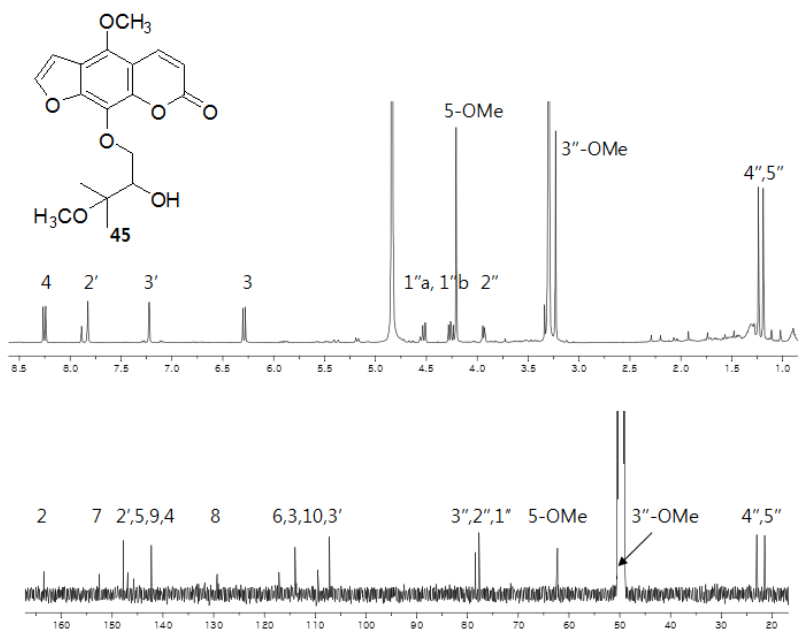

Figure 72. ^{1}H and ^{13}C NMR spectra of compound **45** (400/100 MHz, CD_3OD)

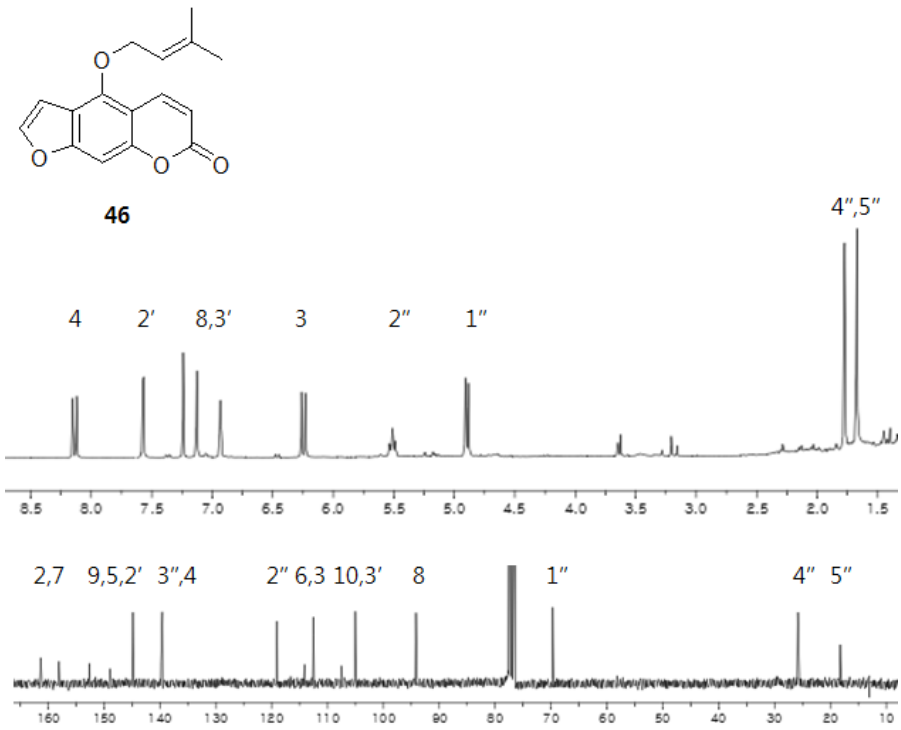

Figure 73. ^{1}H and ^{13}C NMR spectra of compound **46** (300/75 MHz, $CDCl_3$)

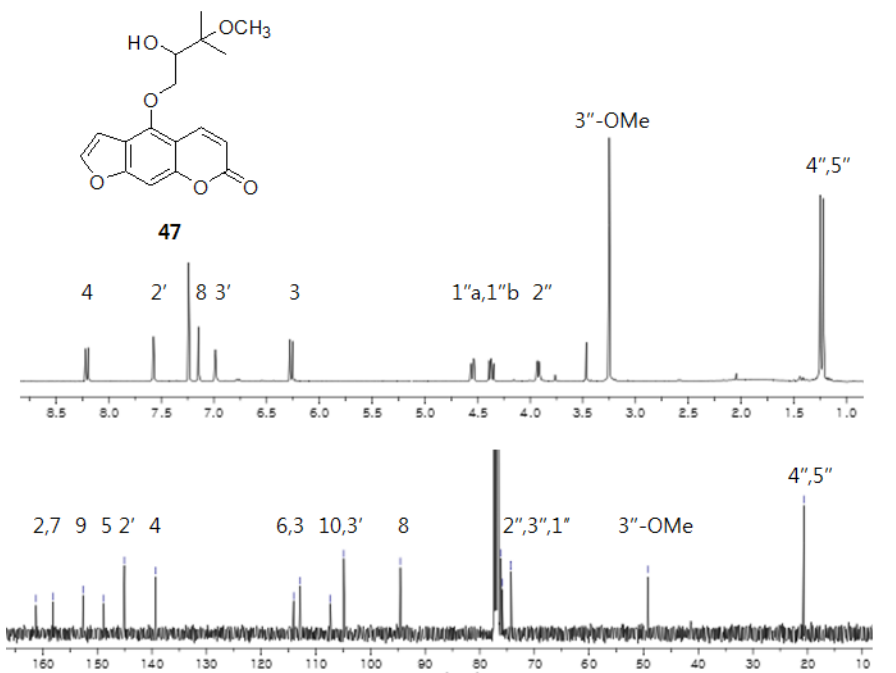

Figure 74. ^{1}H and ^{13}C NMR spectra of compound **47** (400/100 MHz, $CDCl_3$)

4.3. Compound 49

The molecular formula of compound **49**, $C_{19}H_{20}O_5$, was established by ESIMS. The presence of linear-type pyranocoumarin moiety was indicated based on the proton signals of two singlet methines at δ_H 7.12 (1H, s, H-5) and 6.77 (1H, s, H-8) and isopentyl moiety at δ_H 5.06 (1H, t, *J* = 4.8 Hz, H-3'), 3.17 (1H, dd, *J* = 17.0, 4.8 Hz, H-4'a), 2.84 (1H, dd, *J* = 17.0, 4.8 Hz, H-4'b), 1.36 (3H, s, H-5'), and 1.34 (3H, s, H-6') (Figure 75). The signals of senecioyl moieties were also observed in ^{1}H NMR δ_H at 5.64 (1H, br s, H-2''), 2.12 (3H, br s, H-4''), and 1.85 (3H, br s, H-5''). In comparison with the optical rotation in the literature, the structure of **49** was identified as (*S*)-(+)-decursin (Lee et al. 2010; Kim et al. 2016).

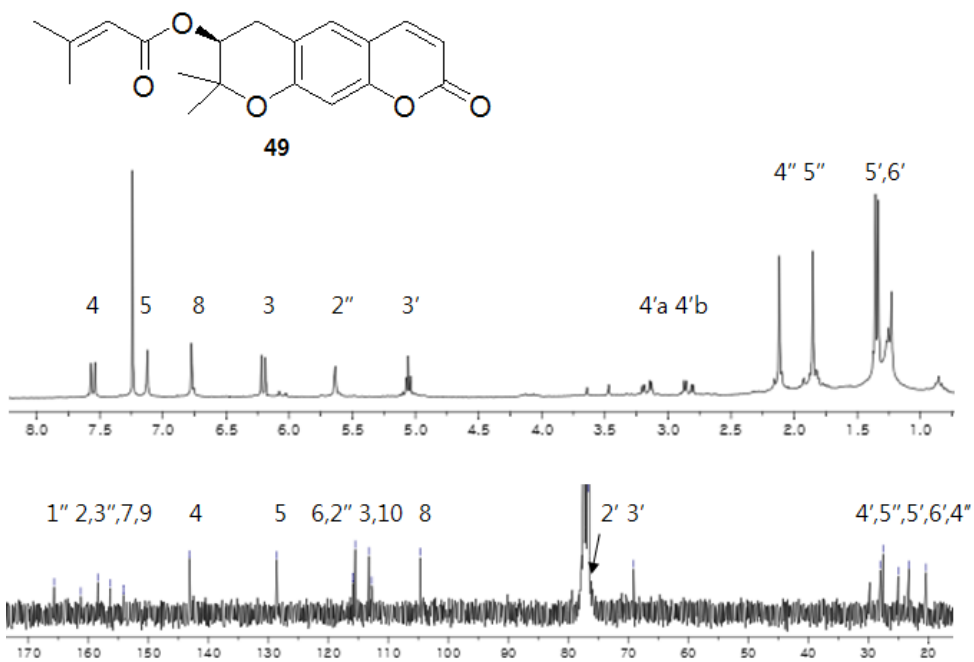

Figure 75. ^{1}H and ^{13}C NMR spectra of compound **49** (300/75 MHz, $CDCl_3$)

4.4. Compounds 50-51

The molecular formula of compound **50** was determined to be $C_{14}H_{14}O_4$ by ESIMS. In the ^{1}H NMR spectrum, 7,8-disubstituted coumarin moiety was established, whose signals were observed at δ_H 7.81 (1H, d, *J* = 9.4 Hz, H-4), 7.29 (1H, d, *J* = 8.5 Hz, H-5), 6.80 (1H, d, *J* = 8.5 Hz, H-6), 6.16 (1H, d, *J* = 9.4 Hz, H-3) (Figure 76). In addition, the isopentyl group was indicated based on the signals at δ_H 5.53 (1H, t, *J* = 7.3 Hz, H-2'), 3.89 (2H, s, H-4'), 3.56 (2H, d, *J* = 7.3 Hz, H-1'), and 1.87 (3H, s, H-5'). Therefore, the structure of **50** was determined as isoarnottinin (Elgamal et al. 1993).

Compound **51** was isolated as white amorphous powder and its molecular formula $C_9H_6O_3$ was established by ESIMS. Based on the ^{1}H NMR, 7-hydroxycoumarin moiety was confirmed [δ_H 9.74 (1H, s, 7-O*H*), 7.84 (1H, d, *J* = 9.4 Hz, H-4), 7.44 (1H, d, *J* = 8.5 Hz, H-5), 6.78 (1H, dd, *J* = 8.5, 2.2 Hz, H-6), 6.70 (1H, d, *J* = 2.2 Hz, H-8), 6.17 (1H, d, *J* = 9.4 Hz, H-3)] (Figure 77). The structure of **51** was identified as umbelliferone (Li et al. 2014).

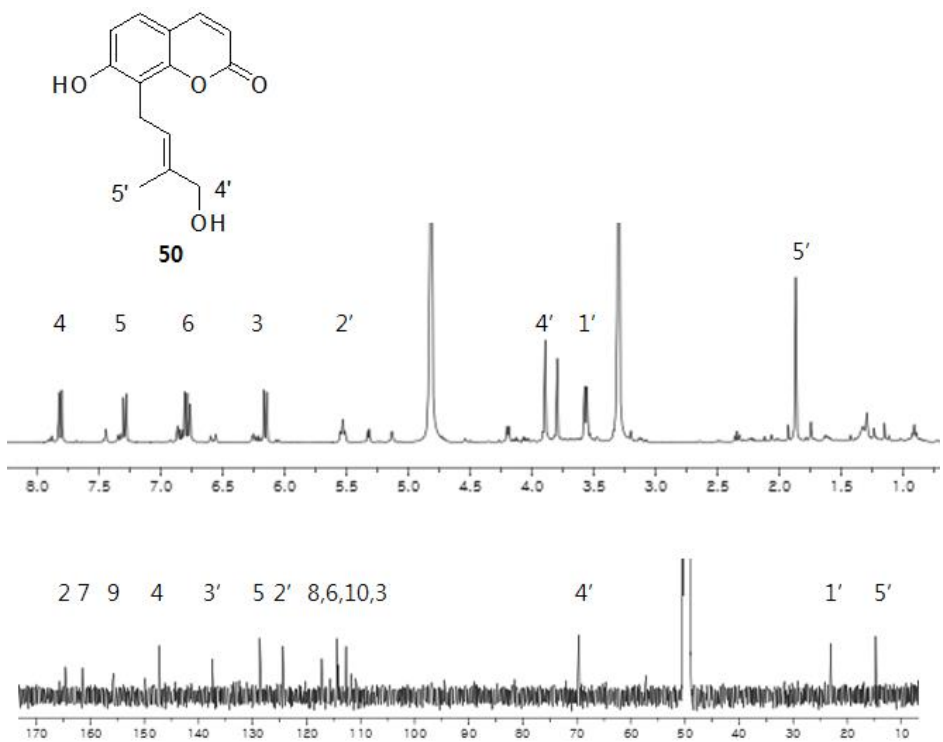

Figure 76. ^{1}H and ^{13}C NMR spectra of compound **50** (400/100 MHz, CD_3OD)

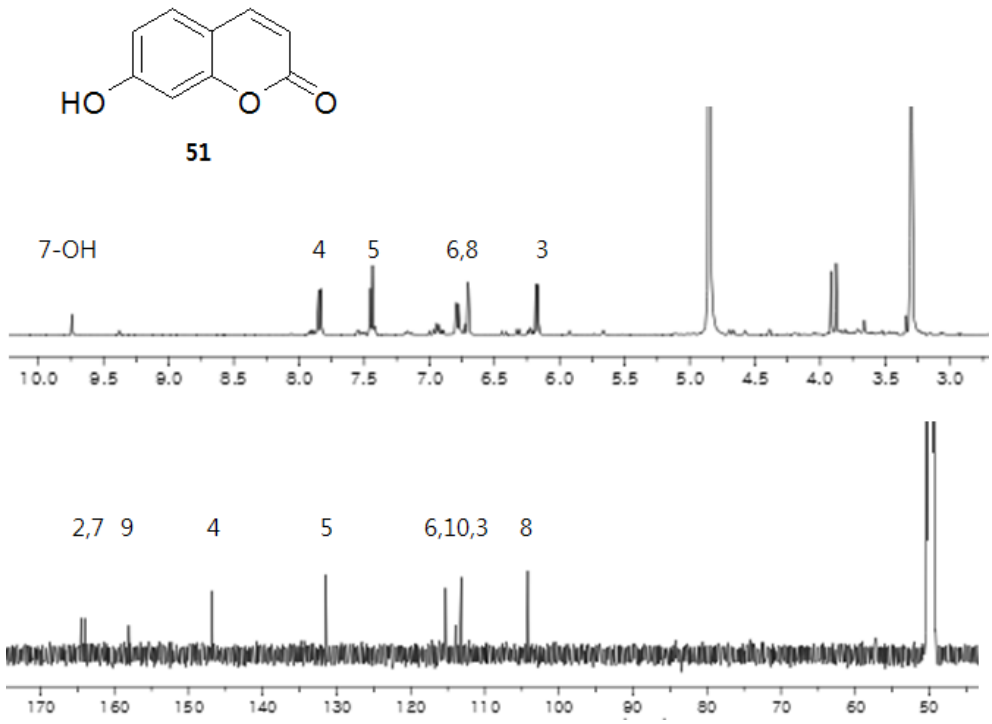

Figure 77. ^{1}H and ^{13}C NMR spectra of compound **51** (500/125 MHz, CD_3OD)

4.5. Compounds 52-55

The molecular composition of compound **52**, $C_{11}H_{10}O_4$ was established by ESIMS. The 6,7-dimethoxycoumarin moiety was indicated based on the proton signals at δ_H 7.86 (1H, d, *J* = 9.4 Hz, H-4), 7.12 (1H, s, H-5), 6.96 (1H, s, H-8), 6.24 (1H, d, *J* = 9.4 Hz, H-3), 3.90 (3H, s, 7-OMe), 3.86 (3H, s, 6-OMe) (Figure 78). The structure of **52** was determined to be scoparone (Vila-Nova et al. 2013).

Based on ESIMS, the molecular formulas of compounds **53-55** were indicated. The presence of 6,7-disubstituted coumarin moiety was suggested based on the proton signals of two singlet methines (H-5 and H-8) (Figures 79-81). The signals of isopentyl groups were observed in ^{1}H NMR [**53**: δ_H 4.76 (1H, br s, H-4'a), 4.72 (1H, br s, H-4'b), 4.27 (1H, dd, *J* = 7.9, 5.7 Hz, H-2'), 2.93 (1H, dd, *J* = 13.6, 5.7 Hz, H-1'a), 2.74 (1H, dd, *J* = 13.6, 7.9 Hz, H-1'b), and 1.77 (3H, s, H-5'); **54**: δ_H 6.29 (1H, dd, J = 12.7, 0.6 Hz, H-1'), 5.81 (1H, d, J = 12.7 Hz, H-2'), and 1.26 (6H, s, H-4', H-5'); **55**: δ_H 5.21 (1H, t, *J* = 7.4 Hz, H-2'), 3.23 (2H, d, *J* = 7.4 Hz, H-1'), 1.70 (3H, s, H-4'), and 1.64 (3H, s, H-5')]. In addition, 7-OMe groups were also confirmed by ^{1}H NMR spectra. Therefore, the structures of **53-55** were assigned as tamarin (isosuberenol) (Gonzalez et al. 1977), (*Z*)-suberenol (Juichi et al. 1988), and suberosin (Marumoto and Miyazawa 2012).

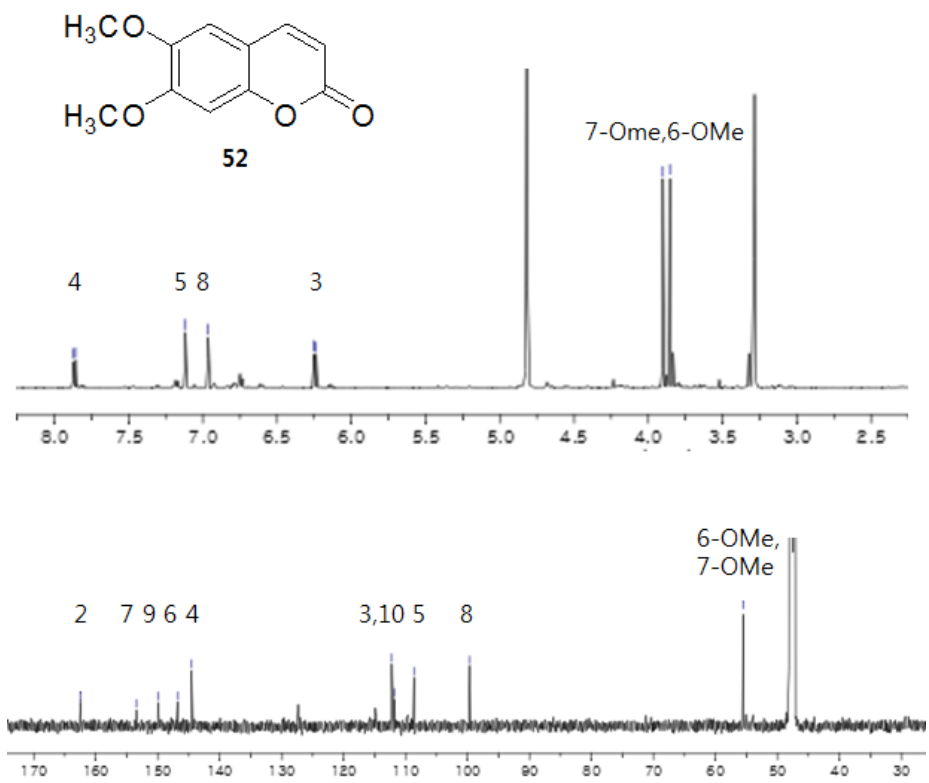

Figure 78. ^{1}H and ^{13}C NMR spectra of compound **52** (600/150 MHz, CD_3OD)

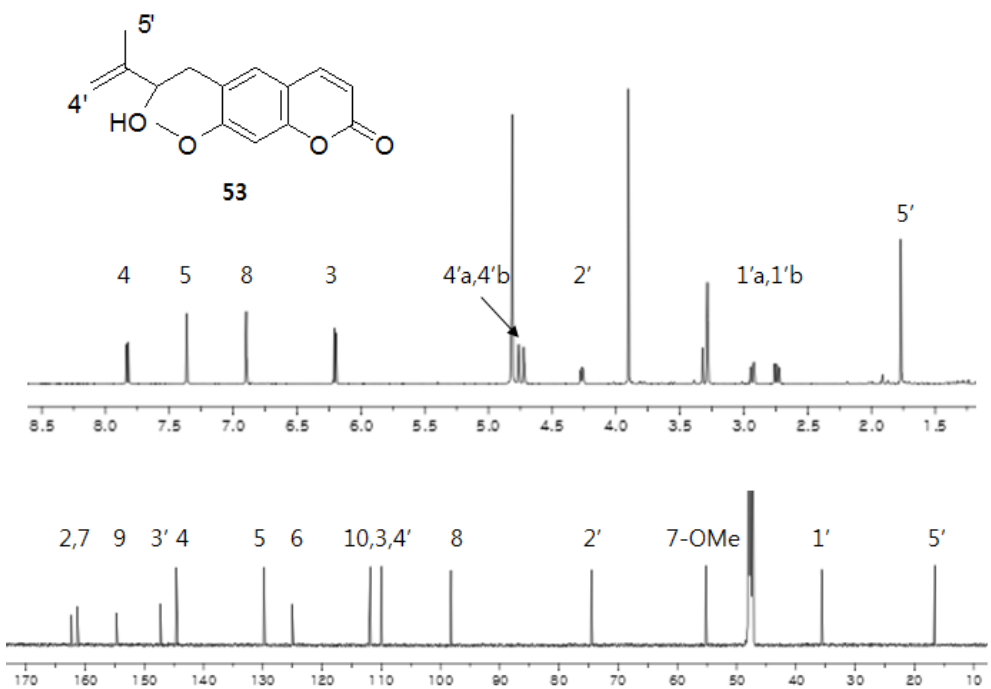

Figure 79. ^{1}H and ^{13}C NMR spectra of compound **53** (600/150 MHz, CD_3OD)

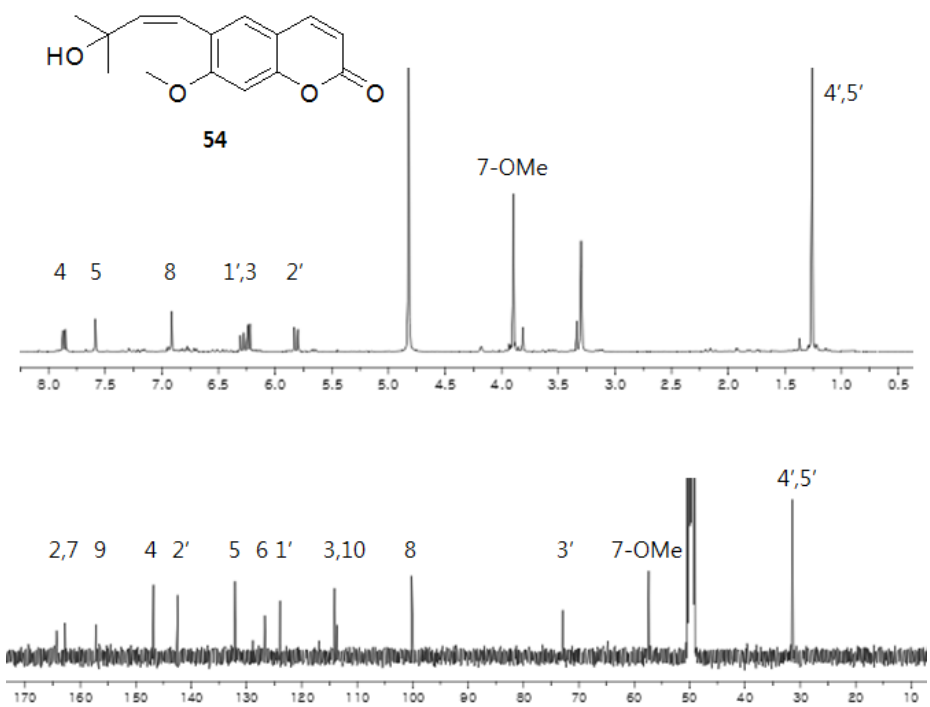

Figure 80. ^{1}H and ^{13}C NMR spectra of compound **54** (400/100 MHz, CD_3OD)

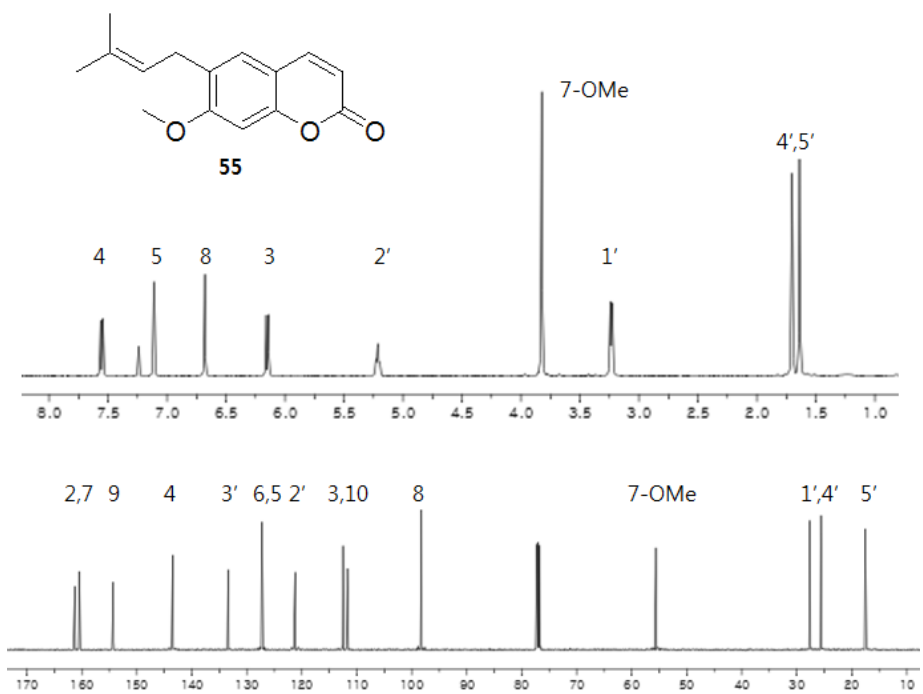

Figure 81. ^{1}H and ^{13}C NMR spectra of compound **55** (500/125 MHz, $CDCl_3$)

4.6. Compounds 56-58

Compound **56** possessed the molecular formula $C_{14}H_{16}O_5$, which was indicated by ESIMS. The presence of 6,7-disubstituted coumarin moiety was established based on the proton signals of two singlet methines at δ_H 7.38 (1H, s, H-5) and 6.71 (1H, s, H-8) and the signals of isopentyl moiety were also observed at δ_H 3.60 (1H, d, *J* = 10.4 Hz, H-2'), 3.07 (1H, d, *J* = 14.0 Hz, H-1'a), and 2.53 (1H, dd, *J* = 14.0, 10.4 Hz, H-1'b), 1.24 (6H, s, H-4', H-5') (Figure 82). The structure of **56** was identified as peucedanol (Ikeshiro et al. 1994).

The molecular compositions of **57** and **58** were suggested by ESIMS. The ^{1}H NMR spectra of **57** and **58** were similar to that of **56**, except for the signals of glucosyl and apiosyl moieties of **57** and **58** (Figures 83-84) The anomeric proton signals of glucosyl and apiosyl groups were observed [**57**: δ_H 4.96 (1H, d, *J* = 7.2 Hz, H-1'''); **58**: 4.97 (1H, d, *J* = 2.6 Hz, H-1'''), 4.90 (1H, d, *J* = 7.3 Hz, H-1'')]. The connectivities between sugar moiety and coumarin were confirmed by the HMBC correlations [**57**: H-1'''/C-7; **58**: H-1'''/C-6'' and H-1'''/C-7]. Therefore, the structures of **57-58** were determined as peucedanol 7-*O*-*β*-D-glucopyranoside and peujaponiside (Ikeshiro et al. 1994).

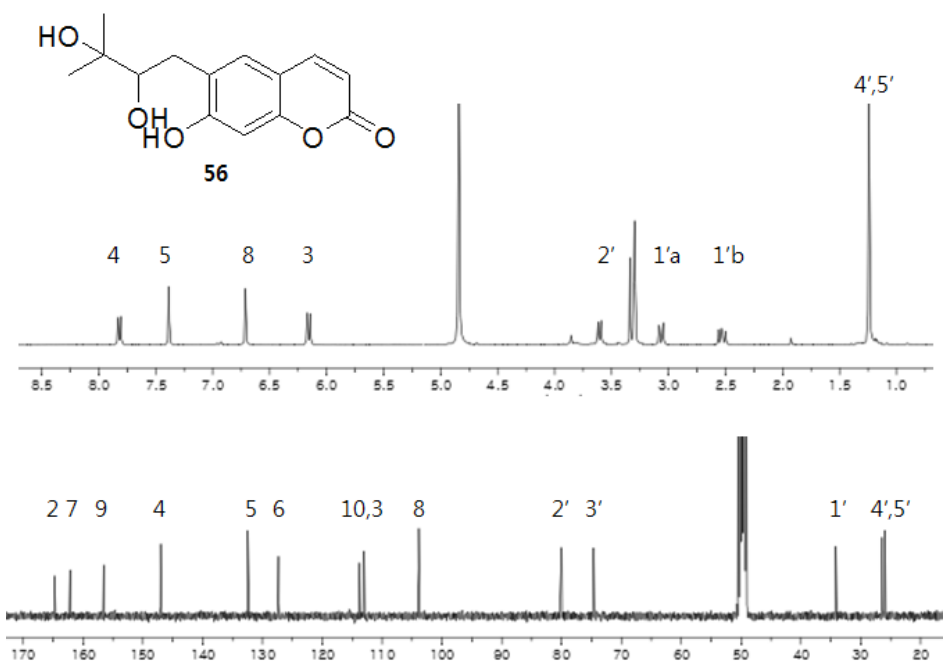

Figure 82. ^{1}H and ^{13}C NMR spectra of compound **56** (400/100 MHz, CD_3OD)

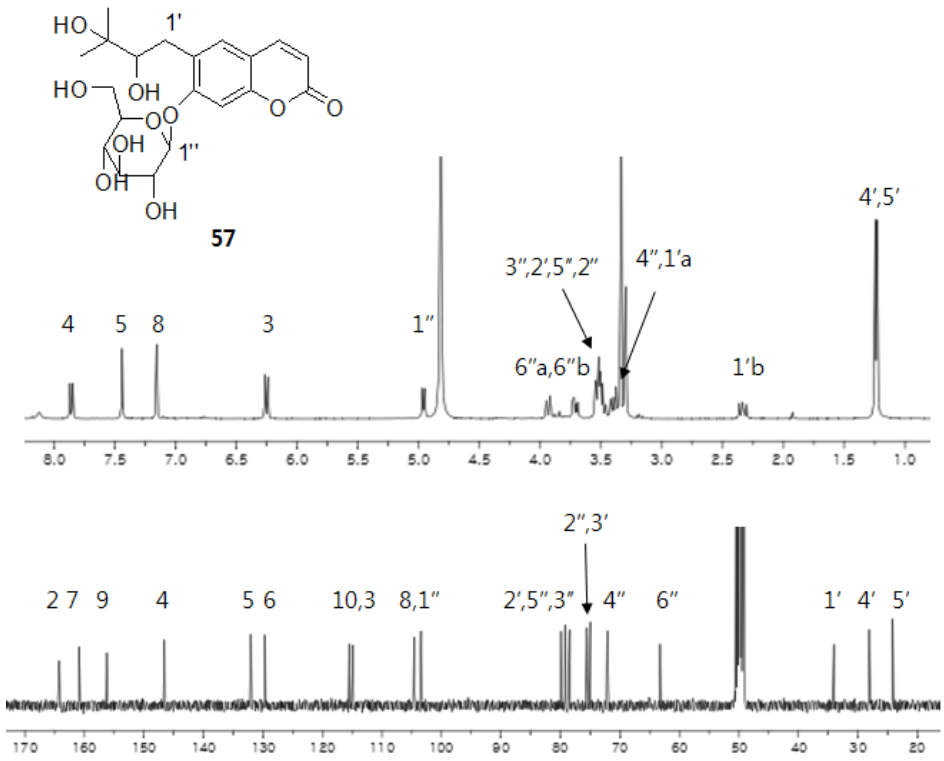

Figure 83. ^{1}H and ^{13}C NMR spectra of compound **57** (400/100 MHz, CD_3OD)

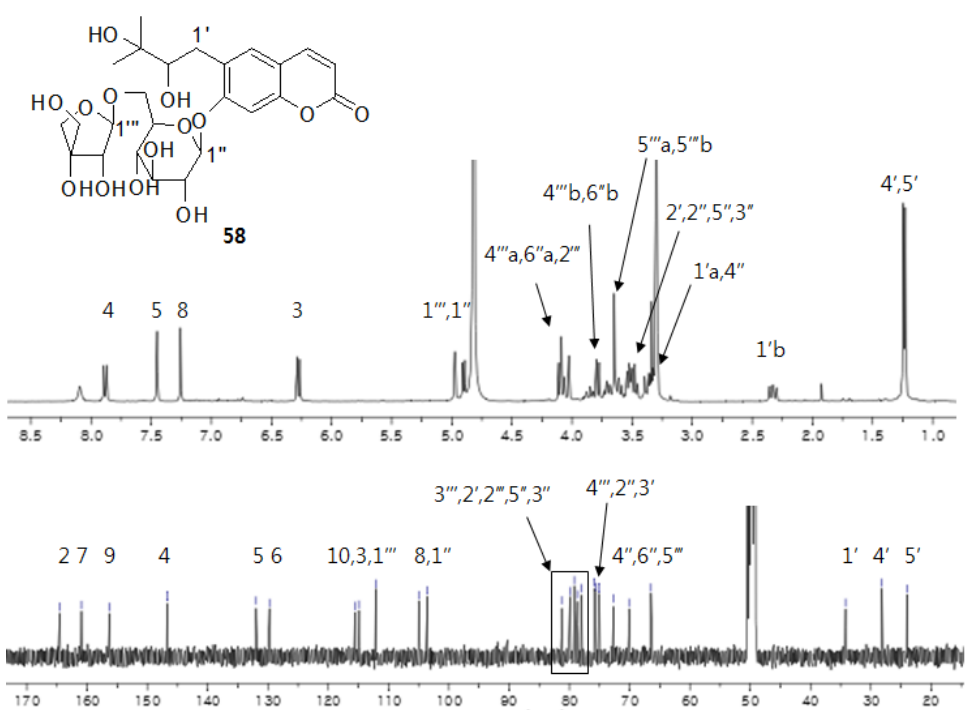

Figure 84. ^{1}H and ^{13}C NMR spectra of compound **58** (400/100 MHz, CD_3OD)

4.7. Compound 59

Based on ESIMS, the molecular composition of compound **59** was established as $C_{11}H_{10}O_4$. In the proton NMR spectrum, the presence of chromone moiety was revealed, whose signals were observed as two doublet methines with meta-coupling [δ_H 6.34 (1H, d, *J* = 2.2 Hz, H-8) and 6.32 (1H, d, *J* = 2.2 Hz, H-6)], one singlet methine [δ_H 6.01 (1H, s, H-3)], and one singlet methyl [δ_H 2.33 (3H, s, 2-Me)] (Figure 85). In comparison with the literature, the structure of **59** was defined as eugenin (Shul'ts et al. 2012).

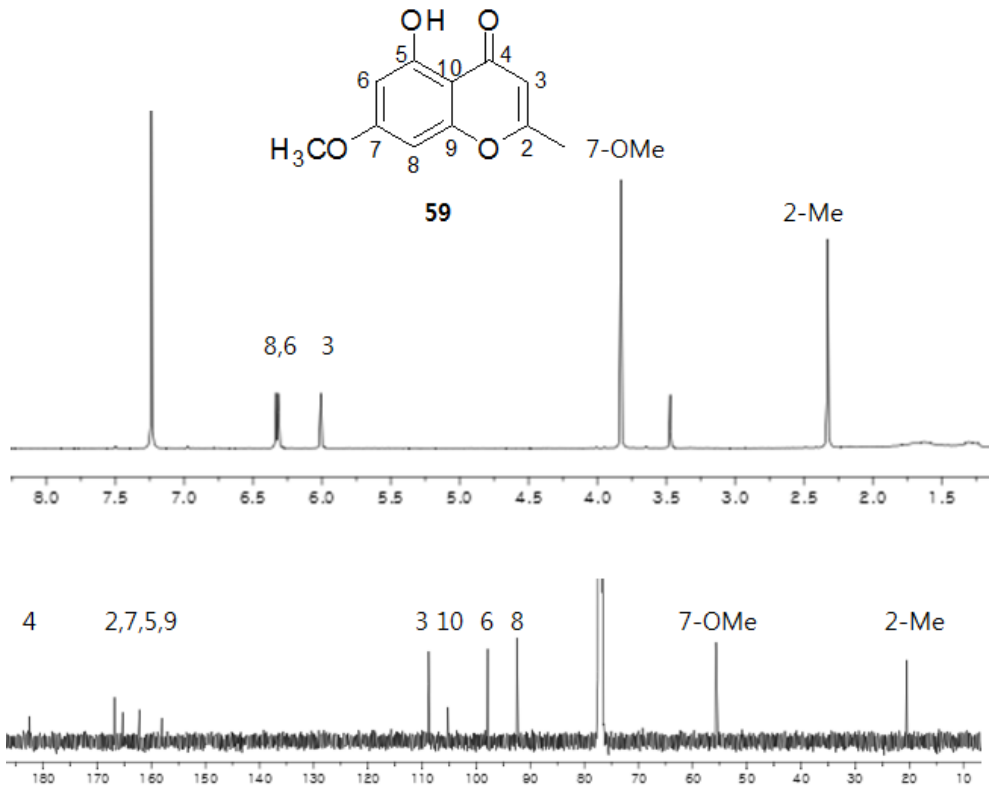

Figure 85. ^{1}H and ^{13}C NMR spectra of compound **59** (400/100 MHz, $CDCl_3$)

4.8. Compounds 60-61

Compound **60** had the molecular formula $C_{18}H_{18}O_6$, which was determined by ESIMS. The proton NMR spectrum of **60** revealed the presence of partial structures, whose signals were observed as 1,2,4-trisubstituted benzene [δ_H 7.09 (1H, d, *J* = 1.6 Hz, H-2), 7.00 (1H, dd, *J* = 8.5, 1.6 Hz, H-6), and 6.79 (1H, d, *J* = 8.5, H-5)], para-disubstituted benzene [δ_H 7.24 (2H, d, *J* = 8.5 Hz, H-2', H-6') and 6.79 (2H, d, *J* = 8.5, H-3', H-5')], double bond with *trans*-orientation [δ_H 7.59 (1H, d, *J* = 15.9 Hz, H-7) and 6.33 (1H, d, *J* = 15.9 Hz, H-8)], and –CH(OH)CH_2O- subunit [δ_H 4.87 (1H, m, H-7'), 4.23 (2H, m, H-8')] (Figure 86). The connectivities of partial structures were confirmed by the HMBC interactions between H-7 and C-1, 2, 6, 8, and 9 and H-8' and C-1', 7', and 9. Therefore, the structure of **60** was elucidated as 6,*β*-dihydroxyphenethyl *trans*-ferulate (decursidate) (Yakabe et al. 2012).

The molecular formula of compound **61**, $C_{18}H_{18}O_5$, was indicated by ESIMS. Different to **60**, the proton NMR spectrum of **61** showed the signals of *cis*-oriented olefinic group at δ_H 6.86 (1H, d, *J* = 12.8 Hz, H-7) and 5.78 (1H, d, *J* = 12.8 Hz, H-8) and –OCH_2-CH_2- subunit at δ_H 4.29 (2H, t, *J* = 7.1 Hz, H-8') and 2.86 (2H, t, *J* = 7.1 Hz, H-7'), instead of trans-oriented double bond and –CH(OH)CH_2O- subunit (Figure 87). The HMBC correlations from H-7 to C-2, 6, and 9 and from H-8' to C-1', 7', and 9 suggested the connections of partial structures. Taken together, the structure of **61** was determined as 6-hydroxyphenethyl *cis*-ferulate (Yakabe et al. 2012).

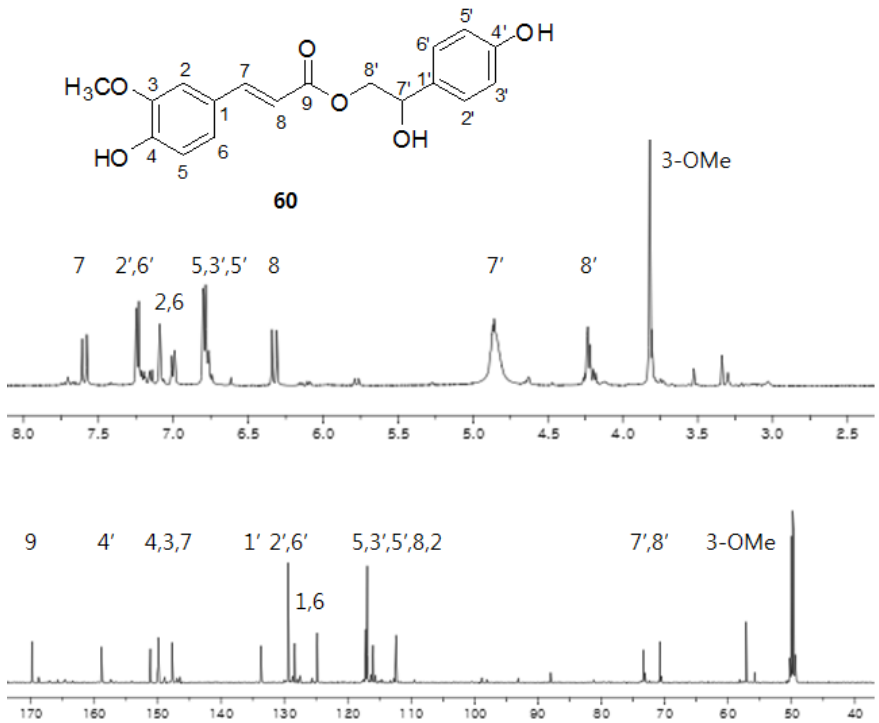

Figure 86. ^{1}H and ^{13}C NMR spectra of compound **60** (500/125 MHz, CD_3OD)

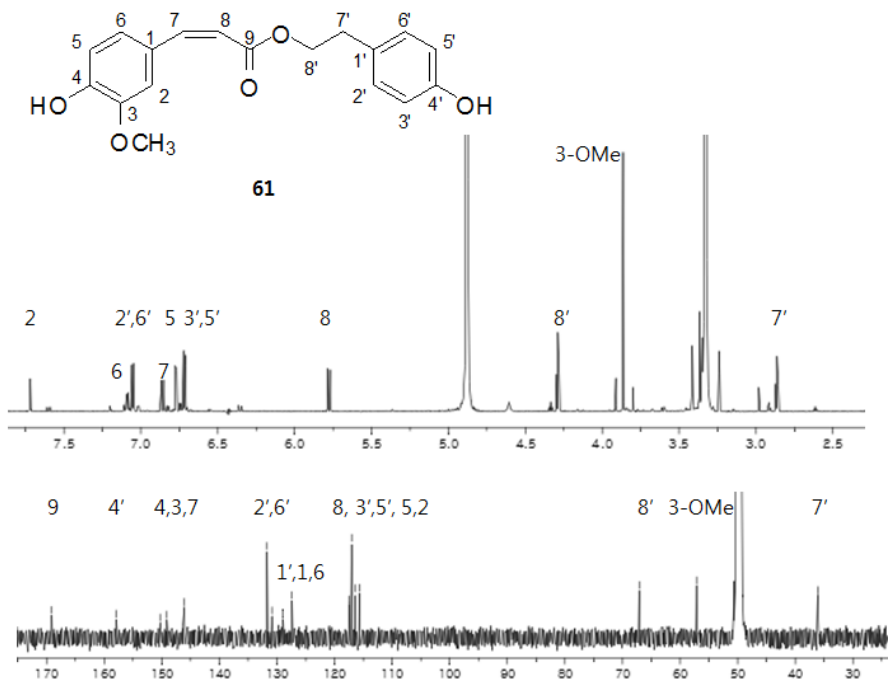

Figure 87. ^{1}H and ^{13}C NMR spectra of compound **61** (800/200 MHz, CD_3OD)

4.9. Compound 62

Compound **62** had molecular formula, $C_{20}H_{22}O_6$, which was established by ESIMS (*m/z* 381 $[M+Na]^+$). In the ^1H and ^{13}C NMR, only 10 proton and 10 carbon signals were detected. In consideration of the lack of the number of protons and carbons, perfectly symmetric structure could be inferred. In ^1H NMR spectrum, the partial structures signals were observed, which were suggested as 1,2,4-trisubstituted aromatic rings [δ_H 6.92 (2H, d, *J* = 1.8 Hz, H-2, H-2'), 6.79 (2H, dd, *J* = 8.1, 1.8 Hz, H-6, H-6'), 6.74 (2H, d, *J* = 8.1 Hz, H-5, H-5')] and –OCH-CH-CH_2O- bridges [δ_H 4.68 (2H, d, *J* = 4.4 Hz, H-7, H-7'), 4.21 (2H, dd, *J* = 9.2, 7.0 Hz, H-9a, H-9'a), 3.82 (2H, dd, *J* = 9.2, 3.7 Hz, H-9b, H-9'b), 3.12 (2H, m, H-8, H-8')] (Figure 88). In comparison with the ECD pattern and optical rotation in the literature, the structure of **62** was assigned as (-)-pinoresinol (Ren et al. 2015).

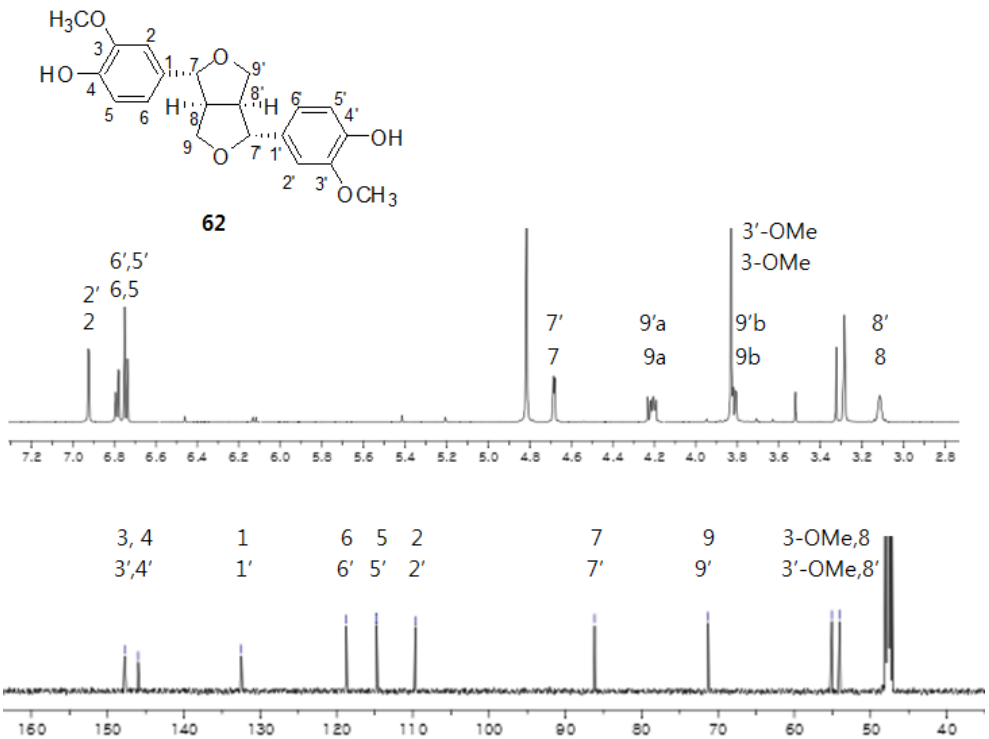

Figure 88. ^1H and ^{13}C NMR spectra of compound **62** (600/150 MHz, CD_3OD)

4.10. Compound 63

The molecular composition of compound **63** was indicated as $C_{10}H_{10}O_4$ by ESIMS. Based on the ^{1}H and ^{13}C NMR spectra, the presence of *trans*-oriented olefinic group, 1,2,4-trisubstituted aromatic ring, and carboxylic acid moiety was suggested, whose signals were observed at δ_H 7.58 (1H, d, *J* = 15.8 Hz, H-7), 6.30 (1H, d, *J* = 15.8 Hz, H-8), 7.17 (1H, s, H-2), 7.05 (1H, d, *J* = 8.1 Hz, H-6), 6.80 (1H, d, *J* = 8.1 Hz, H-5), and δ_C 171.9 (C-9) (Figure 89). The structure of **63** was identified as *trans*-ferulic acid (Nishanbaev et al. 2015).

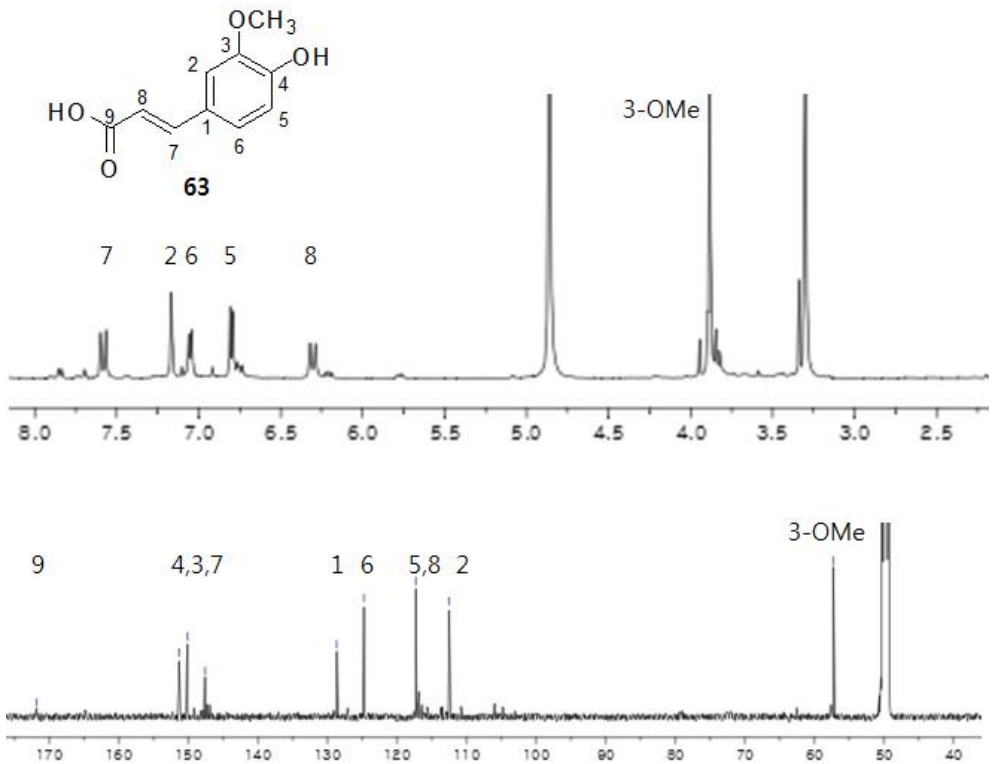

Figure 89. ^{1}H and ^{13}C NMR spectra of compound **63** (500/125 MHz, CD_3OD)

4.11. Compound 64

Compound **64** had the molecular formula of C_9H_7NO, which was determined by ESIMS (*m/z* 146 $[M+H]^+$). In the ^1H NMR spectrum, the signals of aldehyde group and disubstituted aromatic ring were detected at δ_H 9.86 (1H, s, 3-C*H*O), 8.13 (1H, d, *J* = 7.9 Hz, H-4), 7.45 (1H, d, *J* = 7.9 Hz, H-7), 7.25 (1H, t, *J* = 7.9 Hz, H-6), and 7.21 (1H, t, *J* = 7.9 Hz, H-5) (Figure 90). The olefinic signals were also observed at δ_H 8.07 (1H, s, H-2), δ_c 138.3 (C-2), and 118.8 (C-3). The subunits were assembled base on the HMBC correlations of H-7 with C-5 and C-9, H-4 with C-3, C-6, and C-8, and H-2 with C-3, C-8, C-9, and 3-CHO. In consideration of the ESIMS peak (*m/z* 146 $[M+H]^+$) and chemical shift of C-2 (δ_c 138.3) and C-8 (δ_c 137.6), the existence of heteroatom N was inferred and it was located between C-2 and C-8. Taken together, the structure of **64** was assigned as 3-formylindole (Martinez-Luis et al. 2012).

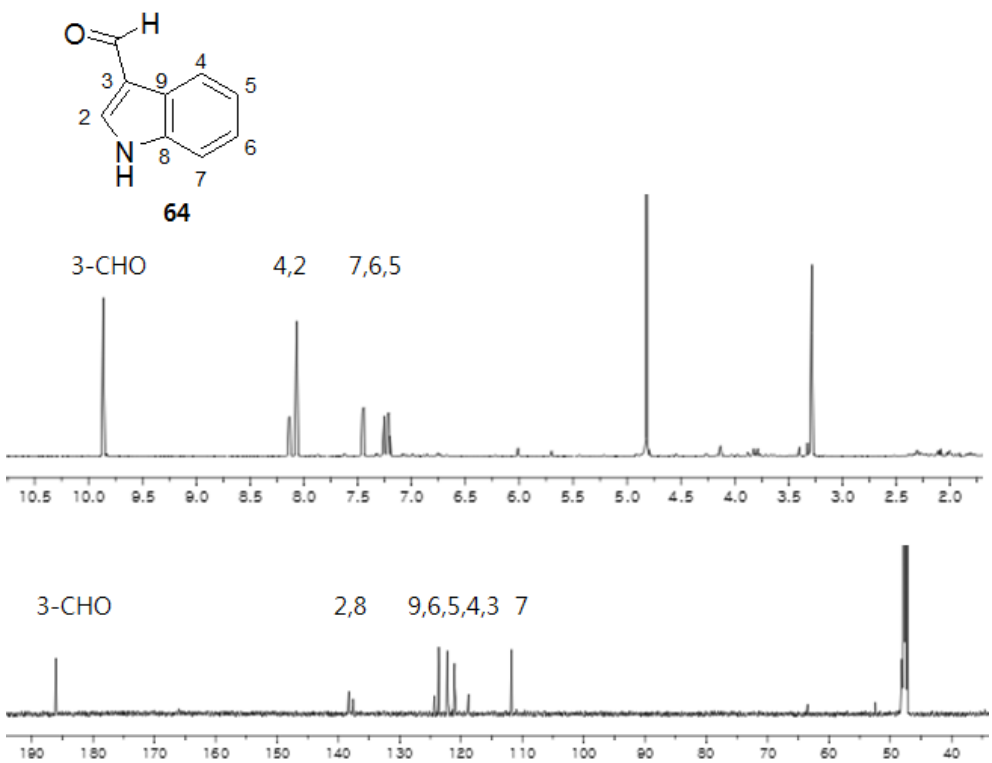

Figure 90. ^1H and ^{13}C NMR spectra of compound **64** (600/150 MHz, CD_3OD)

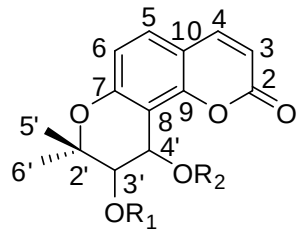

	R_1	R_2	3'	4'
1*	*i*-Bu	MeBu	*S*	*S*
2*	Ac	Sen	*S*	*S*
3*	MeBu	*i*-Bu	*S*	*S*
4*	MeBu	Sen	*S*	*S*
5*	Sen	MeBu	*S*	*S*
6*	*i*-Bu	*i*-Val	*S*	*S*
7*	MeBu	Ang	*S*	*S*
8*	Bu	MeBu	*S*	*S*
9*	*i*-Val	Ang	*S*	*S*
10*	Ac	3-hydroxy-*i*-Val	*S*	*S*
11*	Ac	3-hydroxy-MeBu	*S*	*S*
12*	Ac	MeBu	*S*	*S*
13*	MeBu	H	*S*	*S*
14*	H	MeBu	*S*	*S*
15*	MeBu	Me	*S*	*S*
16*	H	Sen	*S*	*R*
17	H	Sen	*S*	*S*
18	H	Sen	*R*	
19	Sen	H	*S*	*S*
20	Sen	H	*R*	*R*

	R_1	R_2	3'	4'
21	Sen	Ang	*S*	*S*
22	Sen	Sen	*S*	*S*
23	Sen	*i*-Val	*S*	*S*
24	Ac	H	*S*	*S*
25	Ac	Ang	*S*	*S*
26	Ac	*i*-Bu	*S*	*S*
27	Ac	*i*-Val	*S*	*S*
28	H	H	*S*	*S*
29	H	Ac	*S*	*S*
30	H	Ang	*S*	*S*
31	Ang	MeBu	*S*	*S*
32	Ang	Ang	*S*	*S*
33	Ang	H	*S*	*S*
34	Ang	Sen	*S*	*S*
35	*i*-Val	Sen	*S*	*S*
36	*i*-Val	*i*-Val	*S*	*S*
37	*i*-Val	MeBu	*S*	*S*

* New compound

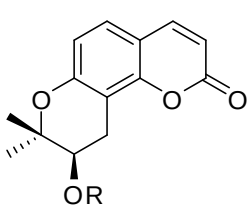

38 R = Sen
39 R = *i*-Val

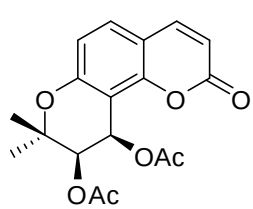

40

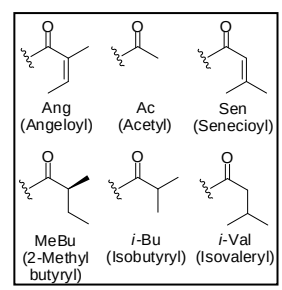

Figure 91. Structures of isolated khellactone esters **1-4**

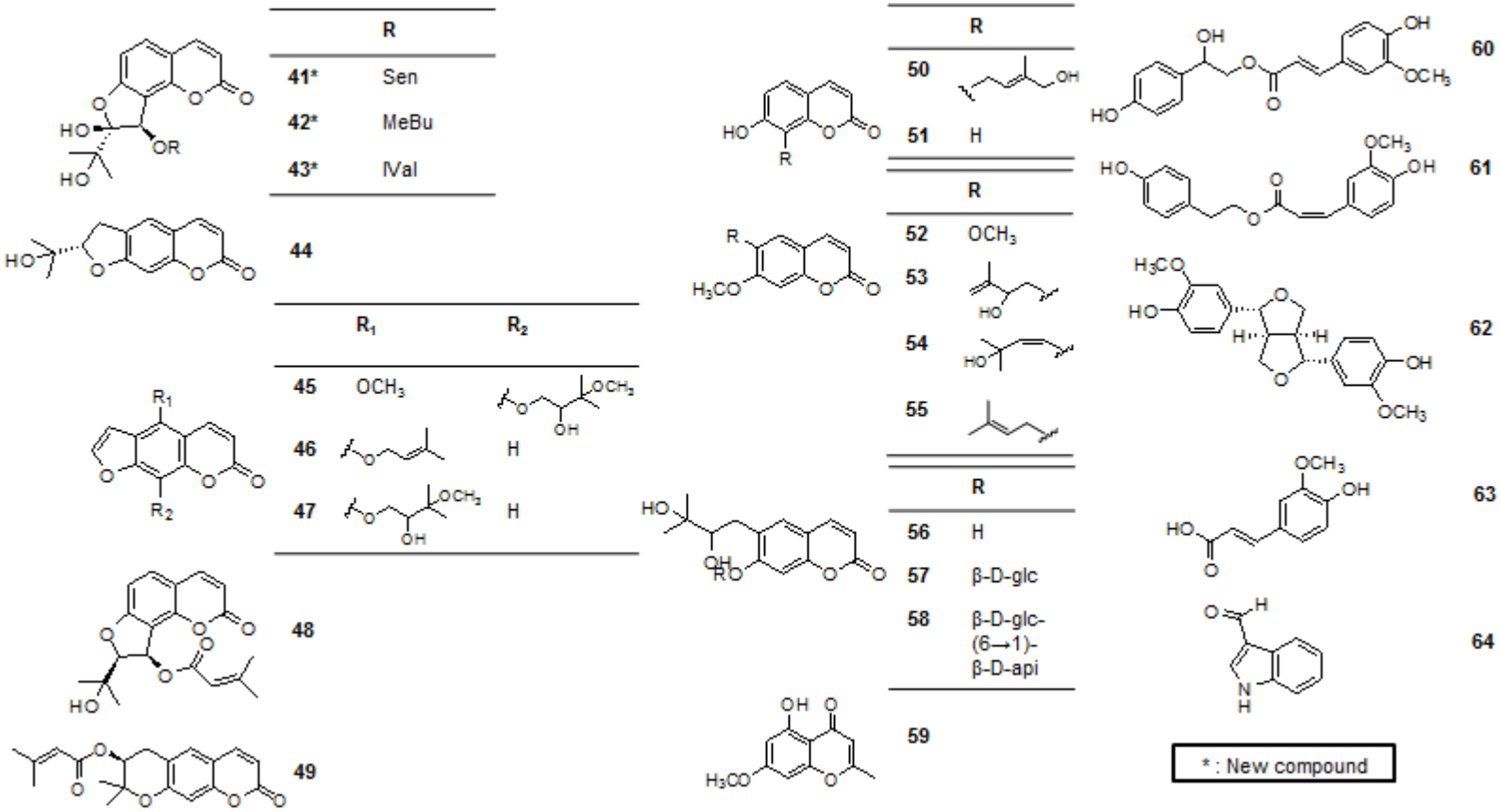

Figure 92. Structures of isolated compounds **41-64**

Chapter 5. Remark

5.1. Acyl migration

The monoacylkhellactones **17**-**20** were isolated from same fraction, H39. Because of the migration between the hydroxyl and senecioyl groups at 3'- and 4'-positions, interconversion between **17** and **19** and between **18** and **20** was observed (Figures 93 and 94). The suggested mechanism of acyl migration was shown in Scheme 1. Seven-membered ring hydrogen bonding between hydroxyl proton and carbonyl oxygen might help the migration of substituent without inversion at 3'- or 4'-position. About 4 days after isolation, the acyl migration reached equilibrium. The migration of the 3'-substituent to the 4'- position was more dominant than vice versa. In this study, a few monoacylkhellactones were isolated along with their positional isomers, such as **13** and **14**, **17** and **19**, **18** and **20**, **24** and **29**, and **30** and **33**.

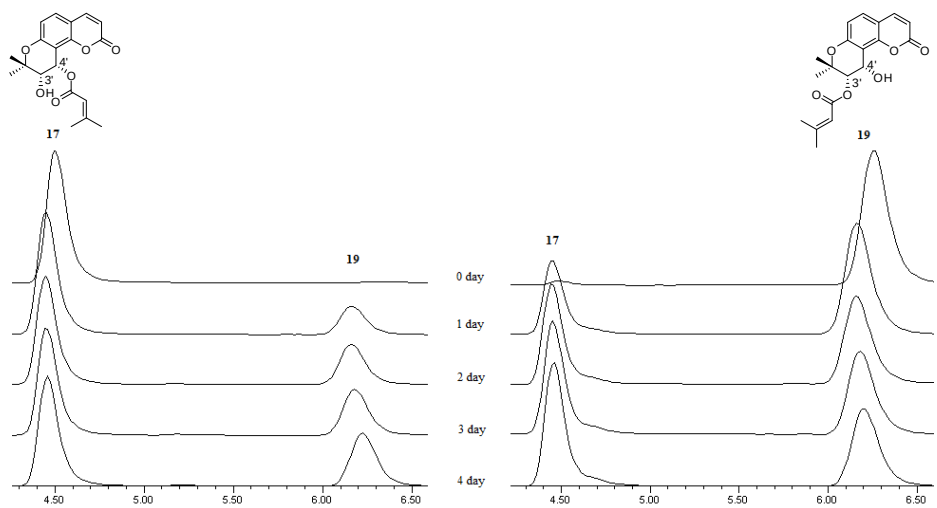

Figure 93. Acyl migration of **17** and **19** over time
(Column: CHIRALPAK IC (4.6 mm x 250 mm, 5 μm); Mobile phase: 100% methanol; Flow rate: 1.0 ml/min; UV detection: 327 nm)

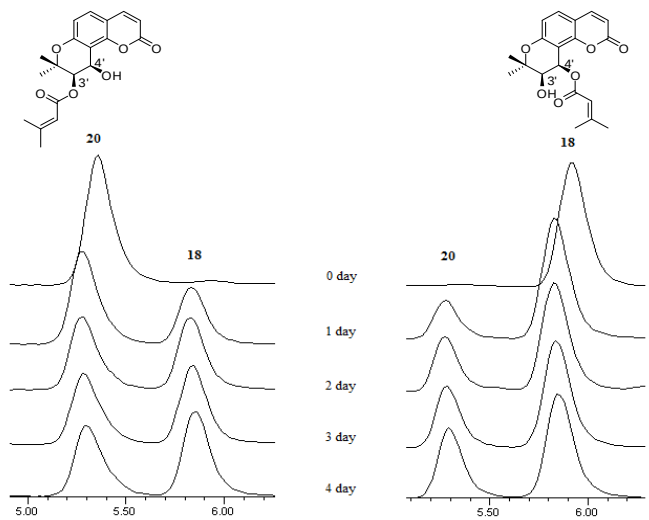

Figure 94. Acyl migration of **18** and **20** over time
(Column: CHIRALPAK IC (4.6 mm x 250 mm, 5 µm); Mobile phase: 100% methanol; Flow rate: 1.0 ml/min; UV detection: 327 nm)

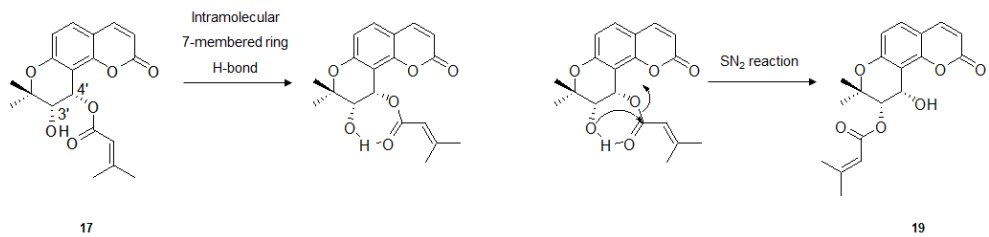

Scheme 1. Suggested mechanism of acyl migration

5.2. MS fragmentation

In the MS spectrum of khellactone esters, the cleavage at the 4’-position was observed, which was detected as a major fragmentation (Scheme 2). The MS fragmentation commonly occurred at 4’-position, but the fragment peak without a 3’-ester moiety was detected as a small peak or undetectable depending on the ionization method or energy. The MS fragmentation peaks of **1-20** revealed the position of substituents, which corresponded with the result of HMBC analysis (Table 1). Based on the MS fragmentation, the location of the 3’-and 4’-substituents could be suggested without HMBC measurement.

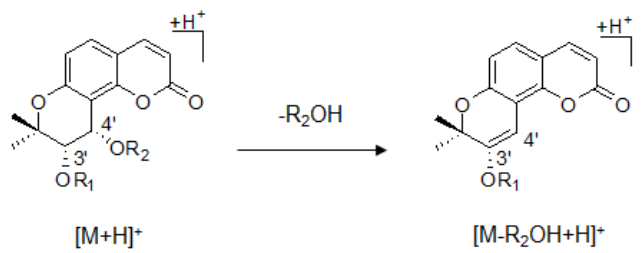

Scheme 2. Suggested fragmentation mechanism of khellactone esters

Table 1. Major ions in the mass spectra of compounds **1-20**

compound	molecular formula (m.w.)	$[M]^+$ or $[M+H]^+$ or $[M+Na]^+$	$[M-R_2OH+H]^+$	$[M-R_2OH-(R1-H)+H]^+$	$[M-R_2OH-(OR1-H)+H]^+$	Others
1[a]	$C_{23}H_{28}O_7$ (416.46)	417 (4) $[M+H]^+$	315 (100)	245 (24)	229 (21)	329 (12) $[M-R_1OH+H]^+$, 445 (14) $[M+C_2H_5]^+$
2[b]	$C_{21}H_{22}O_7$ (386.40)	409 (60) $[M+Na]^+$	287 (5)	245 (2)		425 (100) $[M+K]^+$, 795 (14) $[2M+Na]^+$, 811 (16) $[2M+K]^+$
3[a]	$C_{23}H_{28}O_7$ (416.46)	417 (2) $[M+H]^+$	329 (100)	245 (14)	229 (19)	315 (32) $[M-R_1OH+H]^+$, 445 (11) $[M+C_2H_5]^+$
4[a]	$C_{24}H_{28}O_7$ (428.47)	429 (2) $[M+H]^+$	329 (100)	245 (8)	229 (10)	327 (40) $[M-R_1OH+H]^+$, 457 (9) $[M+C_2H_5]^+$
5[a]	$C_{24}H_{28}O_7$ (428.47)	429 (5) $[M+H]^+$	327 (100)	245 (12)	229 (20)	329 (60) $[M-R_1OH+H]^+$, 457 (19) $[M+C_2H_5]^+$
6[a]	$C_{23}H_{28}O_7$ (416.46)	417 (2) $[M+H]^+$	315 (100)	245 (13)	229 (13)	445 (7) $[M+C_2H_5]^+$
7[b]	$C_{24}H_{28}O_7$ (428.47)	451 (100) $[M+Na]^+$	329 (6)			879 (75) $[2M+Na]^+$
8[b]	$C_{23}H_{28}O_7$ (416.46)	439 (100) $[M+Na]^+$	315 (4)			855 (13) $[2M+Na]^+$
9[b]	$C_{24}H_{28}O_7$ (428.47)	451 (100) $[M+Na]^+$	329 (19)			879 (5) $[2M+Na]^+$
10[a]	$C_{21}H_{24}O_8$ (404.41)	405 (2) $[M+H]^+$	287 (100)	245 (16)	229 (14)	433 (3) $[M+C_2H_5]^+$
11[a]	$C_{21}H_{24}O_8$ (404.41)	404 (4) $[M]^+$	287 (27)	245 (47)	229 (100)	
12[b]	$C_{21}H_{24}O_7$ (388.41)	411 (100) $[M+Na]^+$	287 (25)	245 (12)		799 (14) $[2M+Na]^+$
13[b]	$C_{19}H_{22}O_6$ (346.37)	369 (100) $[M+Na]^+$	329 (3)	245 (3)		
14[b]	$C_{19}H_{22}O_6$ (346.37)	369 (100) $[M+Na]^+$	245 (6)			715 (9) $[2M+Na]^+$
15[b]	$C_{20}H_{24}O_6$ (360.40)	383 (54) $[M+Na]^+$	329 (100)			
16[a]	$C_{19}H_{20}O_6$ (344.36)	345 (12) $[M+H]^+$	245 (100)		229 (21)	327 (25) $[M-R_1OH+H]^+$, 373 (10) $[M+C_2H_5]^+$
17[b]	$C_{19}H_{20}O_6$ (344.36)	367 (41) $[M+Na]^+$	245 (100)			711 (80) $[2M+Na]^+$
18[b]	$C_{19}H_{20}O_6$ (344.36)	367 (100) $[M+Na]^+$	245 (5)			711 (14) $[2M+Na]^+$
19[b]	$C_{19}H_{20}O_6$ (344.36)	367 (18) $[M+Na]^+$	327 (100)			711 (51) $[2M+Na]^+$
20[b]	$C_{19}H_{20}O_6$ (344.36)	367 (30) $[M+Na]^+$	327 (100)			711 (49) $[2M+Na]^+$

[a] Data were acquired by CIMS

[b] Data were acquired by ESIMS

*R_1 = 3'-substituent, R_2 = 4'-substituent

Chapter 6. Bioactivity of the Isolated Compounds

6.1. NO production inhibitory activity of isolated compounds

As mentioned in introduction section, the roots of *Peucedanum japonicum* were used as a traditional cold medicine. To find anti-inflammatory compound and identify structure and activity relationship, NO production inhibitory activity was evaluated in LPS-stimulated RAW264.7 cells. Compounds **1**, **3-6**, **22**, **31**, and **36-38** displayed significant inhibitory effects (IC_{50} < 20 μM) without cytotoxicity, while compounds **2**, **10**, **25-28**, **32**, **34**, **40-44**, **47-48**, **50-51**, and **53-59** showed IC_{50} > 50 μM. As a result, it was revealed that the isobutyryl, senecioyl, 2-methylbutyryl, and isovaleryl groups at 3' position played important role for NO production inhibitory activity.

Table 2. Inhibitory activity of isolated compounds on NO production in LPS-stimulated RAW 264.7 cells

compound	IC_{50} (μM)[a]	compound	IC_{50} (μM)[a]
1	11.1 ± 1.8	**35**	24.1 ± 2.6
3	3.4 ± 2.6	**36**	12.0 ± 0.5
4	13.9 ± 9.4	**37**	11.5 ± 2.6
5	19.5 ± 5.5	**38**	21.7 ± 5.0
6	18.6 ± 5.2	**45**	24.7 ± 6.0
7	35.7 ± 8.5	**46**	45.5 ± 2.1
12	35.6 ± 4.7	**49**	23.4 ± 5.8
21	28.0 ± 1.8	**52**	44.6 ± 8.2
22	8.1 ± 4.0	L-NAME[b]	34.6 ± 9.3
31	12.0 ± 2.5		

[a] Values were expressed as the means ± SD from triplicate experiments.
[b] L-NAME (L-Nitro-Arginine Methyl Ester) was used as a positive control.

Chapter 7. Experimental Section

7.1. Materials

7.1.1. Plant material

Roots of *Peucedanum japonicum* were collected in the Taean-gun, Chungcheongnam-do, Korea, in November 2012. It was identified by Prof. Je Hyun Lee, College of Oriental medicine, Dongguk university. A voucher specimen (Ref: SNUPH 2012-02/KOR) is deposited in the herbarium of Seoul National University in Korea.

7.1.2. Reagents

Column chromatography was carried out with Merck silica gel 60 (40-63 μm). Analytical TLC was performed with Merck silica gel 60 F_{254} precoated TLC plate and Merck RP-18 F_{254s} precoated TLC plate. Dae Jung first grade solvents were used for extraction, fractionation, and isolation. Fisher HPLC grade solvents were used for MPLC and HPLC. To prepare MTPA derivatives, pyridine-d_5 (Cambridge Isotope Laboratories, Inc.), (*R*)-(-)- and (*S*)-(+)-MTPA-Cl (Fluka), and DMAP (Sigma Aldrich) were used.

7.1.3. Equipments

Optical rotations were obtained using JASCO P-2000 polarimeter. UV spectra were acquired on Perkin Elmer Lambda 25 UV/Vis spectrophotometer. CD and UV spectra were recorded by an Applied photophysics Chirascan-plus CD spectrometer. IR spectra were measured on JASCO FT/IR-4200 spectrophotometer. NMR spectra were obtained using a Bruker AVANCE digital 400 or 500 spectrometer or JEOL JNM-ECA 600 spectrometer or Bruker AVANCE III HD 800 spectrometer with a 5-mm CPTCI cryoprobe. High-resolution and low-resolution CIMS were measured on

a JEOL JMS 700 Spectrometer. High-resolution and low-resolution ESIMS were acquired using AB SCIEX Q-TOF 5600 mass spectrometer or Agilent Technologies 6130 Quadrupole LC/MS spectrometer equipped with Agilent Technologies 1260 Infinity LC system and INNO C18 column (4.6 × 150 mm, S-5 μm, 12 nm). The MPLC was conducted with Teledyne Isco Combi Flash Companion and Grace Reveleris C18 Reversed-Phase 120 g Cartridge. HPLC was carried out with Gilson 321 pump, Gilson UV/VIS 151 detector, and YMC Hydrosphere C18 column (20 × 250 mm, S-5 μm, 12 nm) or INNO C18 column (20 × 250 mm, S-5 μm, 12 nm) or YMC J'sphere ODS H80 column (10 × 250 mm, S-4 μm, 8 nm) or INNO C18 column (10 × 250 mm, S-5 μm, 12 nm) or DAICEL CHIRALPAK IC column (4.6 × 250 mm, 5 μm).

7.2. Extraction and fractionation of *P. japonicum*

Peucedanum japonicum roots (30.0 kg) were extracted with 100% MeOH (200 min x 3 with 45.5 L x 3) in an ultrasonic apparatus. After removing the solvent under reduced pressure, MeOH extract (2.7 kg, yield: 8.9%) was successively fractionated with *n*-hexane (454.2 g, yield: 16.9%), $CHCl_3$ (87.9 g, yield: 3.3%), EtOAc (19.9 g, yield: 0.7%), and *n*-BuOH (97.5 g, yield: 3.6%).

Scheme 3. Extraction and fractionation of *P. japonicum*

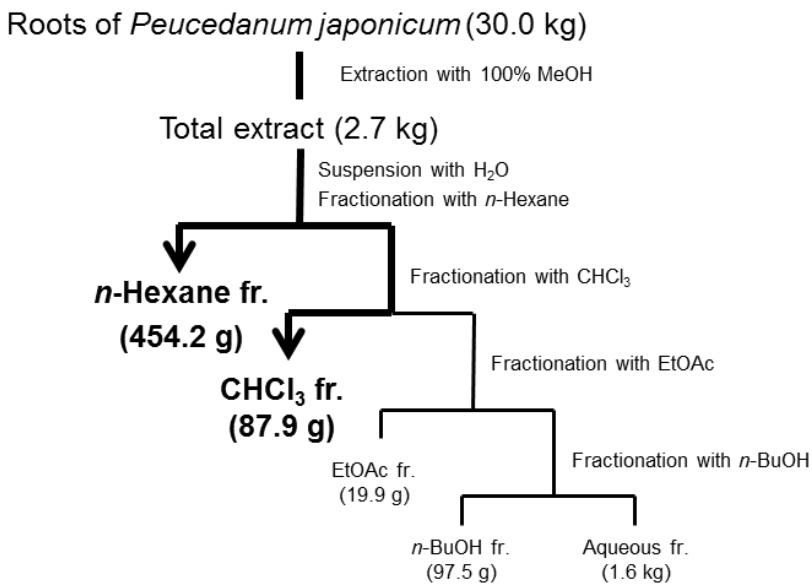

7.3. Isolation of compounds from *n*-hexane and $CHCl_3$ fr actions

Part of the *n*-hexane fraction (406.0 g) was subjected to silica gel column chromatography (CC, 34 x 15.3 cm) with step gradient mixtures of *n*-hexane-EtOAc (95:5 → 0:100) to obtain fifty one fractions (H1~H51). Fraction H24 (7.5 g) was further purified by RP-MPLC (20 ml/min) with MeOH-H_2O (75:25) to afford compound **46** (17.8 mg). Fraction H29 (3.5 g) eluted by MeOH-H_2O (70:30) mostly yielded compound **55** (257.7 mg) by RP-MPLC (40 ml/min). Fraction H32 (5.3 g) was separated on RP-MPLC eluted with MeOH-H_2O (75:25, 20 ml/min) to give sixteen subfractions (H32-1~H-32-16). Compounds **38** (8.0 mg, t_R = 23.4 min) and **59** (1.4 mg, t_R = 17.0 min) was isolated from H32-3 using RP-HPLC (CH_3CN-H_2O, 75:25, 5 ml/min). H32-4 was applied to RP-HPLC (CH_3CN-H_2O, 75:25, 5 ml/min) to acquire compound **15** (0.8 mg, t_R = 26.9 min) and sub-fration H32-4-2. Compound **39** (0.3 mg, t_R = 6.0 min) was purified from subfration H32-4-2 by chiral selective column with MeOH (1 ml/min). H32-5 was separated by RP-HPLC (CH_3CN-H_2O, 75:25, 5 ml/min) to obtain seven sub-frations (H32-5-1~H32-5-7). Compounds **1** (15.1 mg, t_R = 6.3 min), **3** (24.0 mg, t_R = 6.0 min), **6** (4.7 mg, t_R = 5.5 min), and sub-fration (H32-5-5-4) were acquired from H32-5-5 using chiral selective HPLC (1 ml/min) with MeOH. H32-5-5-4 was purified with chiral selective HPLC (1 ml/min, MeOH) to give **8** (0.6 mg, t_R = 6.6 min). Compound **9** (2.2 mg, t_R =41.6 min) was obtained from H32-6 applying RP-HPLC (CH_3CN-H_2O, 75:25, 5 ml/min). Fraction H34 (45.2 g) was subjected to RP-MPLC (MeOH-H_2O, 70:30, 40 ml/min) to yield thirteen subfractions (H34-1~H-34-13). H34-7 was purified by RP-HPLC (CH_3CN-H_2O, 75:25, 7 ml/min) to give compounds **7** (11.1 mg, t_R = 37.2 min), **32** (53.1 mg, t_R = 31.9 min), and subfrations (H34-7-2M, 2, 3, 4). Compound **21** (2.8 mg, t_R = 28.5 min) was acquired by RP-HPLC (CH_3CN-H_2O, 75:25, 7 ml/min) from H34-7-2M, while **35** (8.7 mg, t_R = 44.5 min) and **5** (2.1 mg, t_R = 45.8 min) were isolated from H34-7-2 and H34-7-4, respectively, using CH_3CN-H_2O (70:30). Compounds **4** (3.5 mg, t_R = 5.5 min) and **23** (0.9 mg, t_R = 5.9 min) were provided from subfraction H34-7-3 by chiral selective HPLC with MeOH (1 ml/min). H34-9 was applied to RP-HPLC (CH_3CN-H_2O, 85:15, 5 ml/min) to give compounds **31** (23.3 mg, t_R = 27.0

min), **36** (96.2 mg, t_R = 28.7 min), **37** (106.6 mg, t_R = 29.7 min) and **49** (4.1 mg, t_R = 17.3 min). Fraction H35 (14.7 g) was subjected to silica CC with *n*-hexane-EtOAc-MeOH (60:4:1) followed by RP-HPLC (CH_3CN-H_2O, 80:20, 5 ml/min) to provide compounds **22** (79.2 mg, t_R = 31.0 min), **34** (9.7 mg, t_R = 34.3 min), and sub-frations H35-11-1, 2. Semi-preparative HPLC was performed on ODS to isolate compounds **2** (2.8 mg, t_R = 27.4 min), **25** (168.9 mg, t_R = 28.2 min), and **26** (2.8 mg, t_R = 25.6 min) from H35-11-1 with CH_3CN-H_2O (65:35, 7 ml/min) and **12** (109.6 mg, t_R = 24.5 min) and **27** (2.3 mg, t_R = 24.0 min) from H35-11-2 with CH_3CN-H_2O (80:20, 5 ml/min), respectively. Fraction H37 (5.8 g) was applied to RP-MPLC using MeOH-H_2O (55:45, 15 ml/min) followed by RP-HPLC (CH_3CN-H_2O, 55:45, 5 ml/min) to obtain subfrations (H37-9-1, 4). Chiral selective HPLC was performed using MeOH to give compounds **30** (1.0 mg, t_R = 4.7 min) and **33** (0.6 mg, t_R = 5.5 min) from H37-9-1, and compounds **13** (6.7 mg, t_R = 5.4 min) and **14** (21.7 mg, t_R = 4.7 min) from H37-9-4. Fraction H39 (1,7 g) was subjected to RP-HPLC eluting with CH_3CN-H_2O (55:45, 5 ml/min) to acquire compounds **16** (2.5 mg, t_R = 37.8 min), **40** (11.4 mg, t_R = 34.6 min), and enantiomeric mixtures **E1** (8.1 mg, t_R = 36.6 min), **E2** (7.2 mg, t_R = 39.6 min). Enantioseparation was carried out with chiral column (MeOH, 1 ml/min) to attain compounds **17** (1.0 mg, t_R = 4.5 min) and **18** (0.5 mg, t_R = 5.9 min) from **E1**, **19** (0.8 mg, t_R = 6.3 min) and **20** (0.5 mg, t_R = 5.3 min) from **E2**. Fraction H41~43 (3.7 g) was subjected to RP-MPLC eluting with MeOH-H_2O (55:45, 10 ml/min) to yield ten sub-fractions (H41~43-1~H41~43-10). Subfraction H41~43-2 was applied to RP-HPLC (CH_3CN-H_2O, 40:60, 5 ml/min) to isolate compounds **28** (8.7 mg, t_R = 21.5 min), **51** (2.4 mg, t_R = 20.3 min), **52** (1.8 mg, t_R = 26.5 min), **62** (6.0 mg, t_R = 27.4 min), and **64** (4.1 mg, t_R = 23.6 min). Eluting with CH_3CN-H_2O (45:55), HPLC (5 ml/min) was carried out to obtain **53** (5.3 mg, t_R = 32.5 min) and **54** (4.1 mg, t_R = 29.2 min) from H41~43-4 and **10** (3.6 mg, t_R = 50.9 min), **45** (5.0 mg, t_R = 39.6 min), **48** (9.7 mg, t_R = 47.5 min), and **61** (1.4 mg, t_R = 43.4 min) from H41~43-7. Fraction 45 (4.1 g) was separated by RP-MPLC (MeOH-H_2O, 50:50, 10 ml/min) followed by ODS HPLC (5 ml/min) employing CH_3CN-H_2O (35:65) as eluent to acquire **50** (1.1 mg, t_R = 24.7 min) and **60** (2.0 mg, t_R = 33.5 min). Fraction 49 (6.0 g) was purified by RP-HPLC (5 ml/min) after applying RP-MPLC (MeOH-H_2O, 50:50, 10 ml/min) to give **57** (15.6 mg, t_R = 18.2

min) and **58** (6.3 mg, t_R = 16.2 min) from subfraction H49-2 with CH_3CN-H_2O (20:80), **56** (8.7 mg, t_R = 30.2 min) and **63** (5.1 mg, t_R = 33.6 min) from subfraction H49-3 with CH_3CN-H_2O (25:75).

The $CHCl_3$ fraction was applied to silica CC (64 x 15.3 cm) with increasingly polar mixtures of *n*-hexane-EtOAc (85:15 → 0:100) to yield thirty-six fractions (C1~C36). Fraction C20~22 (4.8 g) was separated by MPLC (20 ml/min) on ODS eluting with MeOH-H_2O (50:50) to attain sixteen subfractions (C20~22-1~C20~22-16). Subfraction C20~22-4 was applied to HPLC (5 ml/min) over ODS using CH_3CN-H_2O (40:60) to acquire **41** (5.3 mg, t_R = 38.5 min), **42** (2.9 mg, t_R = 43.8 min), **43** (7.9 mg, t_R = 45.9 min), and subfraction C20~22-4-3. Sub-fraction C20~22-4-3 was further purified by RP-HPLC (CH_3CN-H_2O, 40:60, 5 ml/min) to give **44** (2.3 mg, t_R = 25.6 min). Subfraction C20~22-5 was chromatographed by HPLC (CH_3CN-H_2O, 40:60, 5 ml/min) over ODS followed by RP-HPLC (CH_3CN-H_2O, 30:70, 5 ml/min) to obtain **24** (1.0 mg, t_R = 70.0 min) and **29** (2.6 mg, t_R = 68.4 min). Compound **47** (5.5 mg, t_R = 40.8 min) was yielded from C20~22-11 by RP-HPLC (CH_3CN-H_2O, 45:55, 5 ml/min). C20~22-12 was subjected to RP-HPLC (CH_3CN-H_2O, 45:55, 5 ml/min) to yield seven subfractions (C20~22-12-1~C20~22-12-7). Compound **11** (0.8 mg, t_R = 31.5 min) was isolated from C20~22-12-7 by semi-preparative RP-HPLC (CH_3CN-H_2O, 45:55, 2 ml/min).

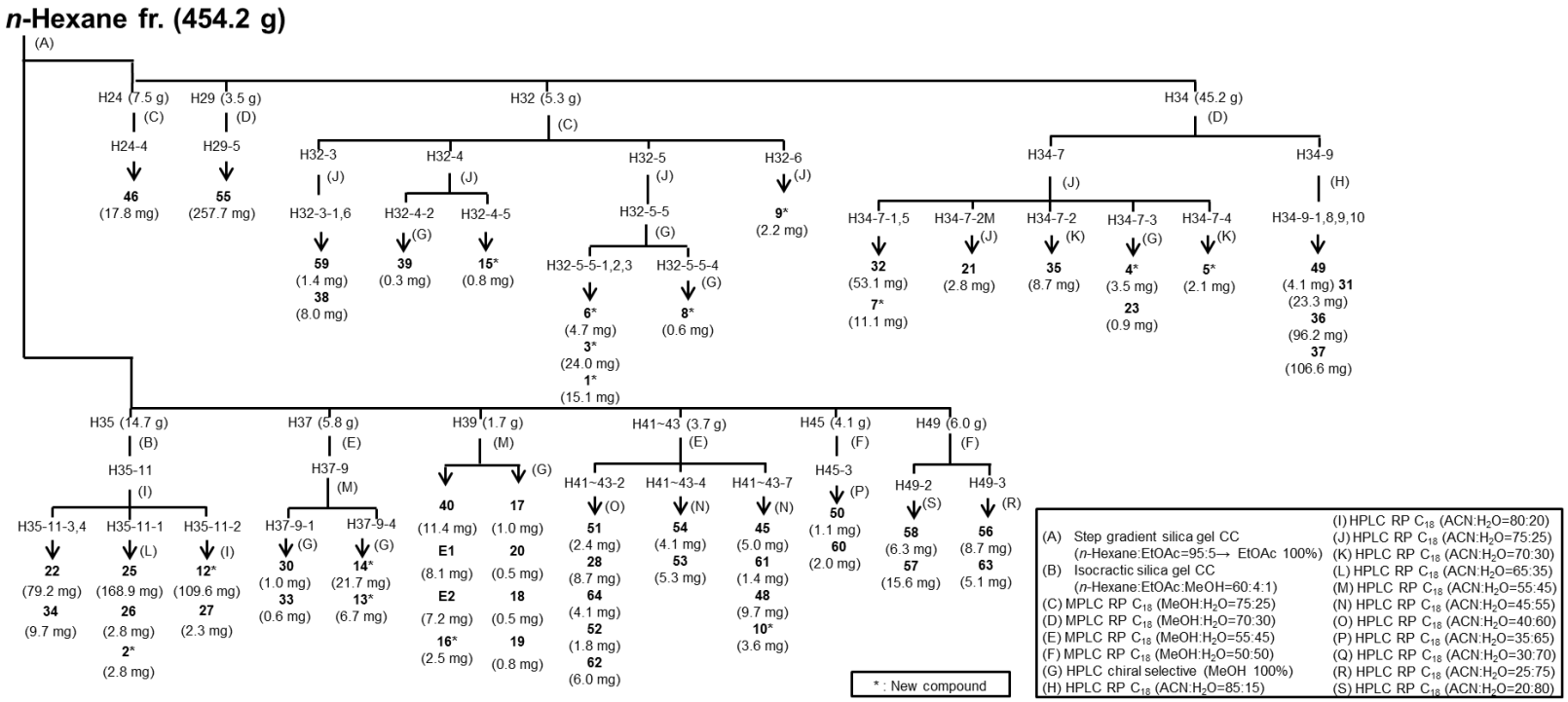

Scheme 4. Isolation of compounds from *n*-hexane fraction

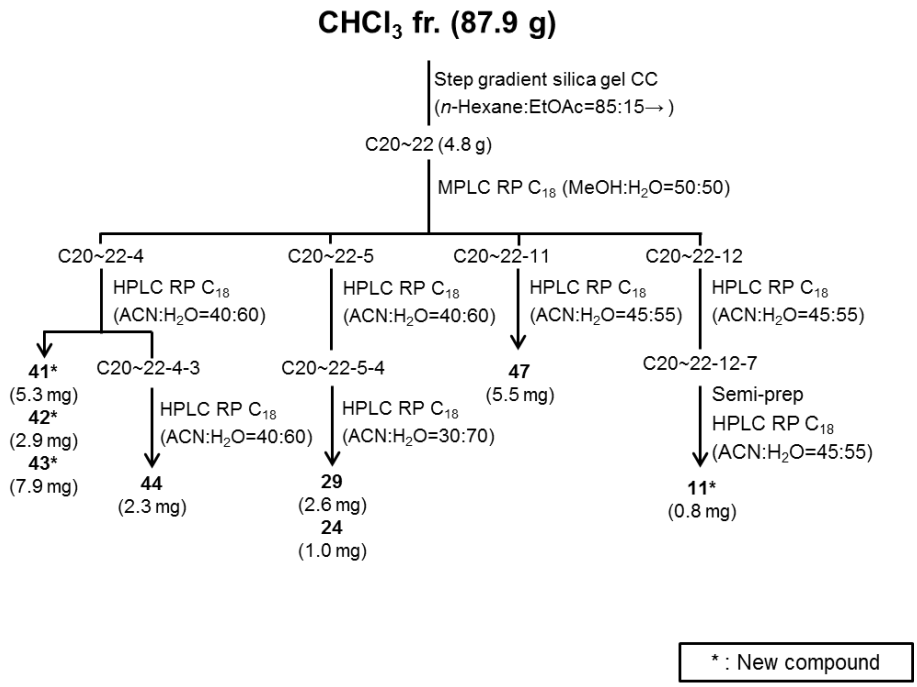

Scheme 5. Isolation of compounds from $CHCl_3$ fraction

7.4. Spectroscopic and spectrometric data of isolated com pounds

7.4.1. (3’*S*,4’*S*)-3'-*O*-isobutyryl-4'-*O*-(2-methylbutyryl)khellactone (**1**)

Colorless needles

$C_{23}H_{28}O_7$

$[\alpha]^{20}_D$ +1.4 (*c* 0.1, MeOH)

UV (MeOH) λ_{max} (log ε) 226 (3.52), 248 (3.12), 259 (2.99), 300 (3.45), 325 (3.63) nm

CD (MeOH) λ_{max} ($\Delta\varepsilon$) 224 (-3.73), 244 (+0.92), 256 (+0.73), 323 (-0.87) nm

^{1}H NMR data (400 MHz, $CDCl_3$): See Table 3

^{13}C NMR data (100 MHz, $CDCl_3$): See Table 9

CIMS *m/z* 417 $[M+H]^+$;

HRCIMS *m/z* 417.1912 $[M+H]^+$ (calcd for $C_{23}H_{29}O_7$, 417.1913)

7.4.2. (3’*S*,4’*S*)-3'-*O*-acetyl-4'-*O*-senecioylkhellactone (**2**)

Colorless needles

$C_{21}H_{22}O_7$

$[\alpha]^{20}_D$ -5.5 (*c* 1.0, MeOH)

UV (MeOH) λ_{max} (log ε) 221 (4.24), 247 (3.62), 257 (3.48), 296 (3.68), 326 (3.86) nm

CD (MeOH) λ_{max} ($\Delta\varepsilon$) 226 (-17.00), 245 (+2.86), 255 (+2.46), 319 (-2.44) nm

^{1}H NMR data (400 MHz, $CDCl_3$): See Table 3

^{13}C NMR data (100 MHz, $CDCl_3$): See Table 9

HRESIMS *m/z* 409.1258 $[M+Na]^+$ (calcd for $C_{21}H_{22}O_7Na$, 409.1258)

7.4.3. (3’*S*,4’*S*)-4'-*O*-isobutyryl-3'-*O*-(2-methylbutyryl)khellactone (**3**)

Colorless needles

$C_{23}H_{28}O_7$

$[\alpha]^{20}_D$ +51.8 (*c* 0.1, MeOH)

UV (MeOH) λ_{max} (log ε) 222 (3.98), 248 (3.46), 258 (3.38), 300 (3.82), 325 (4.00) nm

CD (MeOH) λ_{max} ($\Delta\varepsilon$) 225 (-19.43), 245 (+3.31), 256 (+2.63), 323 (-4.16) nm

IR ν_{max} 2974, 2938, 2875, 1745, 1608, 1491, 1220, 1147, 772 cm^{-1}

^{1}H NMR data (400 MHz, $CDCl_3$): See Table 3

^{13}C NMR data (100 MHz, $CDCl_3$): See Table 9

CIMS *m/z* 417 $[M+H]^+$

HRCIMS *m/z* 417.1910 ($[M+H]^+$, calcd for $C_{23}H_{29}O_7$:417.1913)

7.4.4. (3'*S*,4'*S*)-3'-*O*-(2-methylbutyryl)-4'-*O*-senecioylkhellactone (**4**)

White amorphous powder

$C_{24}H_{28}O_7$

$[\alpha]^{20}_D$ -20.4 (*c* 0.1, MeOH)

UV (MeOH) λ_{max} (log ε) 220 (4.44), 248 (3.77), 258 (3.63), 299 (3.93), 324 (4.12) nm

CD (MeOH) λ_{max} ($\Delta\varepsilon$) 225 (-29.78), 246 (+4.94), 256 (+4.21), 326 (-5.38) nm

IR ν_{max} 2976, 2938, 2877, 1741, 1608, 1491, 1221, 1144, 1074, 772 cm^{-1}

^{1}H NMR data (400 MHz, $CDCl_3$): See Table 3

^{13}C NMR data (100 MHz, $CDCl_3$): See Table 9

CIMS *m/z* 429 $[M+H]^+$

HRCIMS *m/z* 429.1909 $[M+H]^+$ (calcd for $C_{24}H_{29}O_7$, 429.1913)

7.4.5. (3'*S*,4'*S*)-4'-*O*-(2-methylbutyryl)-3'-*O*-senecioylkhellactone (**5**)

White amorphous powder

$C_{24}H_{28}O_7$

$[\alpha]^{20}_D$ +6.4 (*c* 0.1, MeOH)

UV (MeOH) λ_{max} (log ε) 226 (3.52), 248 (3.12), 258 (3.04), 300 (3.45), 322 (3.64) nm

CD (MeOH) λ_{max} ($\Delta\varepsilon$) 225 (-17.32), 246 (+3.05), 256 (+2.14), 323 (-4.93) nm

IR ν_{max} 2976, 2934, 1747, 1608, 1220, 1146, 772 cm^{-1}

^{1}H NMR data (600 MHz, $CDCl_3$): See Table 3

^{13}C NMR data (150 MHz, $CDCl_3$): See Table 9

CIMS *m/z* 429 $[M+H]^+$

HRCIMS *m/z* 429.1908 $[M+H]^+$ (calcd for $C_{24}H_{29}O_7$, 429.1913)

7.4.6. (3'*S*,4'*S*)-3'-*O*-isobutyryl-4'-*O*-isovalerylkhellactone (**6**)

White amorphous powder

$C_{23}H_{28}O_7$

$[\alpha]^{20}_D$ -8.9 (*c* 0.1, MeOH)

UV (MeOH) λ_{max} (log ε) 221 (4.05), 248 (3.51), 258 (3.43), 298 (3.86), 325 (4.05) nm

CD (MeOH) λ_{max} ($\Delta\varepsilon$) 224 (-8.79), 245 (+2.53), 255 (+1.94), 323 (-1.80) nm

^{1}H NMR data (400 MHz, $CDCl_3$): See Table 3

^{13}C NMR data (100 MHz, $CDCl_3$): See Table 9

CIMS *m/z* 417 $[M+H]^+$

HRCIMS *m/z* 417.1917 $[M+H]^+$ (calcd for $C_{23}H_{29}O_7$, 417.1913)

7.4.7. (3'*S*,4'*S*)-4'-*O*-angeloyl-3'-*O*-(2-methylbutyryl)khellactone (**7**)

White amorphous powder

$C_{24}H_{28}O_7$

$[\alpha]^{20}_D$ -58.7 (*c* 0.1, MeOH)

UV (MeOH) λ_{max} (log ε) 221 (4.30), 249 (3.65), 258 (3.57), 299 (3.93), 325 (4.11) nm

CD (MeOH) λ_{max} ($\Delta\varepsilon$) 226 (-7.15), 246 (+1.36), 254 (+1.24), 318 (-1.25) nm

^{1}H NMR data (500 MHz, $CDCl_3$): See Table 3

^{13}C NMR data (125 MHz, $CDCl_3$): See Table 9

HRESIMS *m/z* 451.1729 $[M+Na]^+$ (calcd for $C_{24}H_{28}O_7Na$, 451.1727)

7.4.8. (3'*S*,4'*S*)-3'-*O*-butyryl-4'-*O*-(2-methylbutyryl)khellactone (**8**)

Colorless needles

$C_{23}H_{28}O_7$

$[\alpha]^{20}_D$ +7.0 (*c* 0.1, MeOH)

UV (MeOH) λ_{max} (log ε) 226 (3.60), 247 (3.26), 258 (3.17), 299 (3.57), 325 (3.75) nm

CD (MeOH) λ_{max} ($\Delta\varepsilon$) 224 (-4.58), 243 (+1.03), 257 (+0.90), 326 (-1.04) nm

^{1}H NMR data (800 MHz, $CDCl_3$): See Table 3

^{13}C NMR data (200 MHz, $CDCl_3$): See Table 9

HRESIMS *m/z* 439.1719 $[M+Na]^+$ (calcd for $C_{23}H_{28}O_7Na$, 439.1727)

7.4.9. (3'*S*,4'*S*)-4'-*O*-angeloyl-3'-*O*-isovalerylkhellactone (**9**)

White amorphous powder;

$C_{24}H_{28}O_7$

$[\alpha]^{20}_D$ -40.0 (*c* 0.1, MeOH)

UV (MeOH) λ_{max} (log ε) 221 (4.29), 247 (3.70), 258 (3.58), 298 (3.84), 325 (4.01) nm

CD (MeOH) λ_{max} ($\Delta\varepsilon$) 225 (-19.19), 246 (+2.61), 256 (+2.66), 326 (-2.57) nm

^{1}H NMR data (800 MHz, $CDCl_3$): See Table 4

^{13}C NMR data (200 MHz, $CDCl_3$): See Table 9

HRESIMS *m/z* 451.1724 $[M+Na]^+$ (calcd for $C_{24}H_{28}O_7Na$, 451.1727)

7.4.10. (3'*S*,4'*S*)-3'-*O*-acetyl-4'-*O*-(3-hydroxyisovaleryl)khellactone (**10**)

White amorphous powder

$C_{21}H_{24}O_8$

$[\alpha]^{20}_D$ +23.3 (*c* 0.3, $CHCl_3$)

UV (MeOH) λ_{max} (log ε) 222 (4.03), 247 (3.58), 258 (3.47), 299 (3.85), 325 (4.02) nm

CD (MeOH) λ_{max} ($\Delta\varepsilon$) 224 (-7.73), 245 (+2.32), 255 (+1.72), 322 (-1.43) nm

^{1}H NMR data (400 MHz, $CDCl_3$): See Table 4

^{13}C NMR data (100 MHz, $CDCl_3$): See Table 9

CIMS *m/z* 405 $[M+H]^+$

HRCIMS *m/z* 405.1548 $[M+H]^+$ (calcd for $C_{21}H_{25}O_8$, 405.1549)

7.4.11. (3'*S*,4'*S*)-3'-*O*-acetyl-4'-*O*-(3-hydroxy-2-methylbutyryl)khellactone (**11**)

White amorphous powder

$C_{21}H_{24}O_8$

$[\alpha]^{20}_D$ -3.2 (*c* 0.1, MeOH)

UV (MeOH) λ_{max} (log ε) 222 (4.01), 248 (3.55), 257 (3.56), 299 (3.82), 325 (4.00) nm

CD (MeOH) λ_{max} ($\Delta\varepsilon$) 224 (-8.32), 244 (+1.98), 255 (+1.52), 321 (-1.44) nm

^{1}H NMR data (600 MHz, $CDCl_3$): See Table 4

^{13}C NMR data (150 MHz, $CDCl_3$): See Table 10

CIMS *m/z* 404 $[M]^+$

HRCIMS *m/z* 404.1466 $[M]^+$ (calcd for $C_{21}H_{24}O_8$, 404.1471)

7.4.12. (3'*S*,4'*S*)-3'-*O*-acetyl-4'-*O*-(2-methylbutyryl)khellactone (**12**)

White amorphous powder

$C_{21}H_{24}O_7$

$[\alpha]^{20}_D$ +5.1 (*c* 2.0, $CHCl_3$)

UV (MeOH) λ_{max} (log ε) 221 (3.34), 249 (2.73), 259 (2.61), 299 (3.03), 325 (3.23) nm

CD (MeOH) λ_{max} ($\Delta\varepsilon$) 224 (-11.8), 244 (+3.16), 256 (+2.24), 324 (-3.03) nm

^{1}H NMR data (400 MHz, $CDCl_3$): See Table 4

^{13}C NMR data (100 MHz, $CDCl_3$): See Table 10

HRESIMS *m/z* 411.1400 $[M+Na]^+$ (calcd for $C_{21}H_{24}O_7Na$, 411.1414)

7.4.13. (3'*S*,4'*S*)-3'-*O*-(2-methylbutyryl)khellactone (**13**)

White amorphous powder

$C_{19}H_{22}O_6$

$[\alpha]^{20}_D$ -2.8 (*c* 1.0, MeOH)

UV (MeOH) λ_{max} (log ε) 222 (4.15), 248 (3.58), 259 (3.50), 298 (3.97), 325 (4.20) nm

CD (MeOH) λ_{max} ($\Delta\varepsilon$) 224 (-6.05), 235 (+1.58), 258 (+0.67), 328 (-2.16) nm

^{1}H NMR data (800 MHz, $CDCl_3$): See Table 4

^{13}C NMR data (200 MHz, $CDCl_3$): See Table 10

HRESIMS *m/z* 369.1309 $[M+Na]^+$ (calcd for $C_{19}H_{22}O_6Na$, 369.1309)

7.4.14. (3'*S*,4'*S*)-4'-*O*-(2-methylbutyryl)khellactone (**14**)

White amorphous powder

$C_{19}H_{22}O_6$

$[\alpha]^{20}_D$ -72.6 (*c* 1.0, MeOH)

UV (MeOH) λ_{max} (log ε) 223 (4.17), 249 (3.66), 259 (3.60), 298 (4.03), 327 (4.25) nm

CD (MeOH) λ_{max} ($\Delta\varepsilon$) 225 (-4.15), 243 (+0.68), 257 (+0.53), 318 (-2.01) nm

^{1}H NMR data (400 MHz, $CDCl_3$): See Table 4

^{13}C NMR data (100 MHz, $CDCl_3$): See Table 10

HRESIMS *m/z* 369.1312 $[M+Na]^+$ (calcd for $C_{19}H_{22}O_6Na$, 369.1309)

7.4.15. (3'*S*,4'*S*)-4'-*O*-methyl-3'-*O*-(2-methylbutyryl)khellactone (**15**)

White amorphous powder

$C_{20}H_{24}O_6$

$[\alpha]^{20}_D$ +4.2 (*c* 0.1, MeOH)

UV (MeOH) λ_{max} (log ε) 220 (3.66), 247 (3.17), 259 (3.09), 300 (3.26), 326 (3.39) nm

CD (MeOH) λ_{max} ($\Delta\varepsilon$) 223 (-1.16), 248 (+0.15), 259 (+0.13), 329 (-0.33) nm

^{1}H NMR data (800 MHz, $CDCl_3$): See Table 4

^{13}C NMR data (200 MHz, $CDCl_3$): See Table 10

HRESIMS *m/z* 383.1452 $[M+Na]^+$ (calcd for $C_{20}H_{24}O_6Na$, 383.1465)

7.4.16. (3'*S*,4'*R*)-4'-*O*-senecioylkhellactone (**16**)

White amorphous powder

$C_{19}H_{20}O_6$

$[\alpha]^{20}_D$ +81.1 (*c* 0.3, $CHCl_3$)

UV (MeOH) λ_{max} (log ε) 220 (4.38), 248 (3.95), 259 (3.76), 298 (3.88), 328 (4.04) nm

CD (MeOH) λ_{max} ($\Delta\varepsilon$) 226 (+18.91), 247 (-3.39), 256 (-2.86), 324 (+2.57) nm

^{1}H NMR data (400 MHz, $CDCl_3$): See Table 4

^{13}C NMR data (100 MHz, $CDCl_3$): See Table 10

CIMS *m/z* 345 $[M+H]^+$

HRCIMS *m/z* 345.1335 $[M+H]^+$ (calcd for $C_{19}H_{21}O_6$, 345.1338)

7.4.17. (3'*S*,4'*S*)-4'-*O*-senecioylkhellactone (**17**)

White amorphous powder

$C_{19}H_{20}O_6$

$[\alpha]^{20}_D$ -52.3 (*c* 0.1, MeOH)

UV (MeOH) λ_{max} (log ε) 222 (4.28), 249 (3.60), 259 (3.49), 301 (3.78), 328 (3.98) nm

CD (MeOH) λ_{max} ($\Delta\varepsilon$) 226 (-6.38), 247 (+0.44), 255 (+0.33), 324 (-1.75) nm

^{1}H NMR data (600 MHz, $CDCl_3$): See Table 5

^{13}C NMR data (150 MHz, $CDCl_3$): See Table 10

ESIMS *m/z* 367 $[M+Na]^+$

7.4.18. (3'*R*,4'*R*)-4'-*O*-senecioylkhellactone (**18**)

White amorphous powder

$C_{19}H_{20}O_6$

$[\alpha]^{20}_D$ +38.8 (*c* 0.1, MeOH)

UV (MeOH) λ_{max} (log ε) 221 (4.13), 248 (3.47), 258 (3.37), 297 (3.60), 328 (3.82) nm

CD (MeOH) λ_{max} ($\Delta\varepsilon$) 226 (+11.74), 248 (-2.48), 257 (-2.29), 326 (+2.31) nm

^{1}H NMR data (800 MHz, $CDCl_3$): See Table 5

^{13}C NMR data (200 MHz, $CDCl_3$): See Table 10

HRESIMS *m/z* 367.1144 $[M+Na]^+$ (calcd for $C_{19}H_{20}O_6Na$, 367.1152)

7.4.19. (3'*S*,4'*S*)-3'-*O*-senecioylkhellactone (**19**)

White amorphous powder

$C_{19}H_{20}O_6$

$[\alpha]^{20}_D$ +23.8 (*c* 0.1, MeOH)

UV (MeOH) λ_{max} (log ε) 222 (4.29), 248 (3.54), 259 (3.37), 298 (3.77), 326 (4.00) nm

CD (MeOH) λ_{max} ($\Delta\varepsilon$) 226 (-4.31), 246 (+1.25), 257 (+1.63), 323 (-1.25) nm

^{1}H NMR data (600 MHz, $CDCl_3$): See Table 5

^{13}C NMR data (150 MHz, $CDCl_3$): See Table 10

ESIMS *m/z* 367 $[M+Na]^+$

7.4.20. (3'*R*,4'*R*)-3'-*O*-senecioylkhellactone (**20**)

White amorphous powder

$C_{19}H_{20}O_6$

$[\alpha]^{20}_D$ -2.2 (*c* 0.1, MeOH)

UV (MeOH) λ_{max} (log ε) 223 (4.10), 247 (3.40), 259 (3.20), 296 (3.57), 327 (3.81) nm

CD (MeOH) λ_{max} ($\Delta\varepsilon$) 224 (+0.78), 233 (-1.06), 257 (-0.36), 333 (+0.53) nm

^{1}H NMR data (800 MHz, $CDCl_3$): See Table 5

^{13}C NMR data (200 MHz, $CDCl_3$): See Table 10

ESIMS *m/z* 367 $[M+Na]^+$

7.4.21. (3'*S*,4'*S*)- 4'-*O*-angeloyl-3'-*O*-senecioylkhellactone (**21**)

White amorphous powder

$C_{24}H_{26}O_7$

$[\alpha]^{20}_D$ -16.5 (*c* 0.1, MeOH)

UV (MeOH) λ_{max} (log ε) 221 (4.37), 247 (3.70), 258 (3.53), 300 (3.82), 325 (3.99) nm

CD (MeOH) λ_{max} ($\Delta\varepsilon$) 226 (-17.99), 248 (+3.26), 258 (+2.73), 329 (-2.83) nm

^{1}H NMR data (600 MHz, $CDCl_3$): See Table 5

^{13}C NMR data (150 MHz, $CDCl_3$): See Table 11

ESIMS *m/z* 853 $[2M+H]^+$

7.4.22. (3'*S*,4'*S*)- 3',4'-di-*O*-senecioylkhellactone (**22**)

White amorphous powder

$C_{24}H_{26}O_7$

$[\alpha]^{20}_D$ -12.6 (*c* 2.0, $CHCl_3$)

UV (MeOH) λ_{max} (log ε) 220 (4.54), 248 (3.78), 259 (3.55), 299 (3.86), 326 (4.04) nm

CD (MeOH) λ_{max} ($\Delta\varepsilon$) 226 (-22.33), 248 (+5.67), 258 (+3.44), 329 (-4.31) nm

^{1}H NMR data (500 MHz, $CDCl_3$): See Table 5

^{13}C NMR data (125 MHz, $CDCl_3$): See Table 11

ESIMS *m/z* 853 $[2M+H]^+$

7.4.23. (3'*S*,4'*S*)-4'-*O*-isovaleryl-3'-*O*-senecioylkhellactone (peujaponisin) (**23**)

White amorphous powder

$C_{24}H_{28}O_7$

$[\alpha]^{20}_D$ +10.9 (*c* 0.1, MeOH)

UV (MeOH) λ_{max} (log ε) 221 (4.26), 247 (3.59), 257 (3.46), 298 (3.78), 326 (3.97) nm

CD (MeOH) λ_{max} ($\Delta\varepsilon$) 225 (-8.44), 247 (+2.94), 258 (+1.72), 328 (-2.20) nm

^{1}H NMR data (600 MHz, $CDCl_3$): See Table 5

ESIMS *m/z* 451 $[M+Na]^+$

7.4.24. (3'*S*,4'*S*)-3'-*O*-acetylkhellactone (qianhucoumarin B) (**24**)

White amorphous powder

$C_{16}H_{16}O_6$

$[\alpha]^{20}_D$ -90.5 (*c* 0.1, MeOH)

UV (MeOH) λ_{max} (log ε) 221 (4.40), 248 (3.84), 259 (3.75), 299 (4.19), 328 (4.39) nm

CD (MeOH) λ_{max} ($\Delta\varepsilon$) 224 (-7.12), 248 (+1.38), 257 (+1.36), 325 (-2.74) nm

^{1}H NMR data (300 MHz, $CDCl_3$): See Table 5

^{13}C NMR data (200 MHz, $CDCl_3$): See Table 11

ESIMS *m/z* 327 $[M+Na]^+$

7.4.25. (3'*S*,4'*S*)-3'-*O*-acetyl-4'-*O*-angeloylkhellactone (pteryxin) (**25**)

White amorphous powder

$C_{21}H_{22}O_7$

$[\alpha]^{20}_D$ +3.6 (*c* 2.0, $CHCl_3$)

UV (MeOH) λ_{max} (log ε) 220 (4.26), 248 (3.62), 258 (3.50), 297 (3.85), 325 (4.05) nm

CD (MeOH) λ_{max} ($\Delta\varepsilon$) 225 (-23.74), 248 (+3.59), 257 (+3.66), 323 (-2.85) nm

^{1}H NMR data (400 MHz, $CDCl_3$): See Table 6

^{13}C NMR data (100 MHz, $CDCl_3$): See Table 11

ESIMS *m/z* 773 $[2M+H]^+$

7.4.26. (3'*S*,4'*S*)-3'-*O*-acetyl-4'-*O*-isobutyrylkhellactone (hyuganin D) (**26**)

White amorphous powder

$C_{20}H_{22}O_7$

$[\alpha]^{20}_D$ -12.0 (*c* 1.0, MeOH)

UV (MeOH) λ_{max} (log ε) 222 (3.95), 248 (3.45), 258 (3.38), 299 (3.79), 325 (3.97) nm

CD (MeOH) λ_{max} ($\Delta\varepsilon$) 225 (-7.61), 247 (+1.31), 259 (+0.46), 328 (-1.75) nm

^{1}H NMR data (400 MHz, $CDCl_3$): See Table 6

^{13}C NMR data (100 MHz, $CDCl_3$): See Table 11

ESIMS *m/z* 749 $[2M+H]^+$

7.4.27. (3'*S*,4'*S*)-3'-*O*-acetyl-3'-*O*-isovalerylkhellactone (suksdorfin, corymbocou marin) (**27**)

White amorphous powder

$C_{21}H_{24}O_7$

$[\alpha]^{20}_D$ -2.4 (*c* 1.0, MeOH)

UV (MeOH) λ_{max} (log ε) 225 (3.64), 249 (3.19), 257 (3.17), 299 (3.50), 325 (3.67) nm

CD (MeOH) λ_{max} ($\Delta\varepsilon$) 225 (-4.16), 247 (+0.55), 256 (+0.04), 329 (-1.31) nm

^{1}H NMR data (600 MHz, $CDCl_3$): See Table 6

^{13}C NMR data (150 MHz, $CDCl_3$): See Table 11

ESIMS *m/z* 777 $[2M+H]^+$

7.4.28. (-)-*cis*-khellactone (**28**)

White amorphous powder

$C_{14}H_{14}O_5$

$[\alpha]^{20}_D$ -39.8 (*c* 1.0, MeOH)

UV (MeOH) λ_{max} (log ε) 221 (4.14), 247 (3.58), 259 (3.51), 299 (3.89), 329 (4.13) nm

CD (MeOH) λ_{max} ($\Delta\varepsilon$) 230 (+1.35), 328 (-1.66) nm

^{1}H NMR data (400 MHz, CD_3OD): See Table 6

^{13}C NMR data (100 MHz, CD_3OD): See Table 11

ESIMS *m/z* 263 $[M+H]^+$

7.4.29. (3'*S*,4'*S*)-4'-*O*-acetylkhellactone (qianhucoumarin C) (**29**)

White amorphous powder;

$C_{16}H_{16}O_6$

$[\alpha]^{20}_D$ -50.3 (*c* 0.1, MeOH)

UV (MeOH) λ_{max} (log ε) 221 (4.32), 247 (3.78), 259 (3.67), 299 (4.12), 325 (4.34) nm

CD (MeOH) λ_{max} ($\Delta\varepsilon$) 224 (-5.38), 247 (+1.56), 259 (+0.75), 326 (-2.20) nm

^{1}H NMR data (300 MHz, $CDCl_3$): See Table 6

^{13}C NMR data (200 MHz, $CDCl_3$): See Table 11

ESIMS *m/z* 305 $[M+H]^+$

7.4.30. (3'*S*,4'*S*)-3'-hydroxy-4'-*O*-angeloyloxy-3',4'-dihydroseselin (**30**)

White amorphous powder

$C_{19}H_{20}O_6$

$[\alpha]^{20}_D$ -87.6 (*c* 0.1, MeOH)

UV (MeOH) λ_{max} (log ε) 221 (4.17), 248 (3.53), 259 (3.42), 299 (3.79), 325 (4.01) nm

CD (MeOH) λ_{max} ($\Delta\varepsilon$) 226 (-16.04), 250 (+2.25), 260 (+1.72), 328 (-2.95) nm

^{1}H NMR data (800 MHz, $CDCl_3$): See Table 6

^{13}C NMR data (200 MHz, $CDCl_3$): See Table 11

ESIMS *m/z* 345 $[M+H]^+$

7.4.31. (3'*S*,4'*S*)-3'-*O*-angeloyl-4'-*O*-(2-methylbutyryl)khellactone (praeruptorin F) (**31**)

White amorphous powder

$C_{24}H_{28}O_7$

$[\alpha]^{20}_D$ +16.7 (*c* 1.0, MeOH)

UV (MeOH) λ_{max} (log ε) 221 (4.32), 247 (3.67), 258 (3.52), 297 (3.88), 325 (4.07) nm

CD (MeOH) λ_{max} ($\Delta\varepsilon$) 225 (-9.69), 247 (+2.23), 258 (+1.58), 327 (-1.95) nm

^{1}H NMR data (600 MHz, $CDCl_3$): See Table 6

^{13}C NMR data (150 MHz, $CDCl_3$): See Table 12

ESIMS *m/z* 879 $[2M+Na]^+$

7.4.32. (3'*S*,4'*S*)-3',4'-di-*O*-angeloylkhellactone (anomalin, praeruptorin B) (**32**)

White amorphous powder

$C_{24}H_{26}O_7$

$[\alpha]^{20}_D$ +58.6 (*c* 0.1, $CHCl_3$)

UV (MeOH) λ_{max} (log ε) 221 (4.31), 247 (3.62), 258 (3.46), 297 (3.76), 324 (3.95) nm

CD (MeOH) λ_{max} ($\Delta\varepsilon$) 225 (-19.68), 248 (+3.11), 257 (+3.64), 324 (-2.21) nm

^{1}H NMR data (400 MHz, $CDCl_3$): See Table 6

^{13}C NMR data (75 MHz, $CDCl_3$): See Table 12

ESIMS *m/z* 853 $[2M+H]^+$

7.4.33. (3'*S*,4'*S*)-3'-*O*-angeloyloxy-4'-hydroxy-3',4'-dihydroseselin (**33**)

White amorphous powder

$C_{19}H_{20}O_6$

$[\alpha]^{20}_D$ +12.4 (*c* 0.1, MeOH)

UV (MeOH) λ_{max} (log ε) 223 (4.07), 247 (3.39), 258 (3.27), 297 (3.66), 328 (3.89) nm

CD (MeOH) λ_{max} ($\Delta\varepsilon$) 227 (-7.96), 249 (+1.21), 260 (+0.84), 328 (-1.80) nm

^{1}H NMR data (400 MHz, $CDCl_3$): See Table 7

^{13}C NMR data (100 MHz, $CDCl_3$): See Table 12

ESIMS *m/z* 345 $[M+H]^+$

7.4.34. (3'*S*,4'*S*)-3'-*O*-angeloyl-4'-*O*-senecioylkhellactone (calipteryxin) (**34**)

White amorphous powder

$C_{24}H_{26}O_7$

$[\alpha]^{20}_D$ +16.6 (*c* 1.0, MeOH)

UV (MeOH) λ_{max} (log ε) 220 (4.34), 247 (3.65), 258 (3.49), 299 (3.72), 323 (3.90) nm

CD (MeOH) λ_{max} ($\Delta\varepsilon$) 225 (-17.20), 247 (+3.66), 259 (+2.35), 325 (-2.11) nm

^{1}H NMR data (400 MHz, $CDCl_3$): See Table 7

^{13}C NMR data (100 MHz, $CDCl_3$): See Table 12

ESIMS *m/z* 853 $[2M+H]^+$

7.4.35. (3'*S*,4'*S*)-3'-*O*-isovaleryl-4'-*O*-senecioylkhellactone (**35**)

White amorphous powder

$C_{24}H_{28}O_7$

$[\alpha]^{20}_D$ -7.5 (*c* 10.0, MeOH)

UV (MeOH) λ_{max} (log ε) 222 (4.12), 247 (3.51), 257 (3.40), 299 (3.64), 323 (3.83) nm

CD (MeOH) λ_{max} ($\Delta\varepsilon$) 226 (-16.52), 249 (+2.96), 258 (+2.33), 323 (-2.69) nm

^{1}H NMR data (600 MHz, $CDCl_3$): See Table 7

^{13}C NMR data (150 MHz, $CDCl_3$): See Table 12

ESIMS *m/z* 857 $[2M+H]^+$

7.4.36. (3'*S*,4'*S*)-3',4'-di-*O*-isovalerylkhellactone (**36**)

White amorphous powder

$C_{24}H_{30}O_7$

$[\alpha]^{20}_D$ -15.4 (*c* 1.0, MeOH)

UV (MeOH) λ_{max} (log ε) 220 (4.27), 247 (3.71), 258 (3.59), 296 (3.98), 325 (4.17) nm

CD (MeOH) λ_{max} ($\Delta\varepsilon$) 224 (-11.90), 247 (+2.34), 257 (+1.65), 324 (-2.69) nm

^{1}H NMR data (300 MHz, $CDCl_3$): See Table 7

^{13}C NMR data (75 MHz, $CDCl_3$): See Table 12

ESIMS *m/z* 883 $[2M+Na]^+$

7.4.37. (3'*S*,4'*S*)-3'-*O*-isovaleryl-4'-*O*-(2-methylbutyryl)khellactone (praeruptorin H) (**37**)

White amorphous powder

$C_{24}H_{30}O_7$

$[\alpha]^{20}_D$ +15.9 (*c* 1.0, MeOH)

UV (MeOH) λ_{max} (log ε) 220 (4.20), 248 (3.66), 258 (3.57), 296 (3.91), 327 (4.12) nm

CD (MeOH) λ_{max} ($\Delta\varepsilon$) 227 (-7.01), 247 (+1.46), 258 (+1.06), 326 (-2.29) nm

^{1}H NMR data (600 MHz, $CDCl_3$): See Table 7

^{13}C NMR data (150 MHz, $CDCl_3$): See Table 12

ESIMS *m/z* 883 $[2M+Na]^+$

7.4.38. (3'*R*)-*O*-senecioyllomatin (**38**)

White amorphous powder

$C_{19}H_{20}O_5$

$[\alpha]^{20}_D$ +85.9 (*c* 0.1, MeOH)

UV (MeOH) λ_{max} (log ε) 223 (4.31), 259 (3.39), 328 (3.98) nm

CD (MeOH) λ_{max} ($\Delta\varepsilon$) 226 (+4.78), 245 (-2.19), 257 (-1.43), 326 (+3.51) nm

^{1}H NMR data (300 MHz, $CDCl_3$): See Table 7

^{13}C NMR data (75 MHz, $CDCl_3$): See Table 12

ESIMS *m/z* 329 $[M+H]^+$

7.4.39. (3'*R*)-*O*-isovaleroyllomatin (**39**)

White amorphous powder

$C_{19}H_{22}O_5$

$[\alpha]^{20}_D$ +50.4 (*c* 0.1, MeOH)

UV (MeOH) λ_{max} (log ε) 224 (3.84), 248 (3.27), 258 (3.22), 328 (3.84) nm

CD (MeOH) λ_{max} ($\Delta\varepsilon$) 223 (+2.36), 246 (-0.40), 255 (-0.35), 325 (+1.13) nm

^{1}H NMR data (800 MHz, $CDCl_3$): See Table 7

^{13}C NMR data (200 MHz, $CDCl_3$): See Table 12

ESIMS *m/z* 331 $[M+H]^+$

7.4.40. (3'*R*,4'*R*)-3',4'-di-*O*-acetylkhellactone (qianhucoumarin D) (**40**)

White amorphous powder

$C_{18}H_{18}O_7$

$[\alpha]^{20}_D$ +1.8 (*c* 0.1, MeOH)

UV (MeOH) λ_{max} (log ε) 221 (4.13), 247 (3.61), 258 (3.51), 297 (3.90), 326 (4.08)

nm

CD (MeOH) λ_{max} ($\Delta\varepsilon$) 224 (+1.77), 245 (-0.74), 254 (-0.48), 330 (+0.17) nm

^{1}H NMR data (500 MHz, CD_3OD): See Table 7

^{13}C NMR data (125 MHz, CD_3OD): See Table 12

ESIMS *m/z* 693 $[2M+H]^+$

7.4.41. 2'-hydroxy-3'-*O*-senecioylvaginol (**41**)

White amorphous powder

$C_{19}H_{20}O_7$

$[\alpha]^{25}_D$ +3.5 (*c* 0.3, $CHCl_3$)

UV (MeOH) λ_{max} (log ε) 218 (4.42), 250 (3.92), 260 (3.81), 300 (3.93), 325 (4.10) nm

CD (MeOH) λ_{max} ($\Delta\varepsilon$) 227 (+8.76), 246 (-1.88), 305 (-1.97) nm

^{1}H NMR data (500 MHz, $CDCl_3$): See Table 8

^{13}C NMR data (125 MHz, $CDCl_3$): See Table 13

CIMS *m/z* 361 $[M+H]^+$

HRCIMS *m/z* 361.1284 $[M+H]^+$ (calcd for $C_{19}H_{21}O_7$, 361.1287)

7.4.42. 2'-hydroxy-3'-*O*-(2-methylbutyryl)vaginol (**42**)

White amorphous powder

$C_{19}H_{22}O_7$

$[\alpha]^{25}_D$ +61.5 (*c* 0.3, $CHCl_3$)

UV (MeOH) λ_{max} (log ε) 219 (4.29), 250 (3.86), 261 (3.74), 301 (4.06), 325 (4.25) nm

CD (MeOH) λ_{max} ($\Delta\varepsilon$) 225 (+7.08), 240 (-1.88), 306 (-2.69) nm

^{1}H NMR data (400 MHz, $CDCl_3$): See Table 8

^{13}C NMR data (100 MHz, $CDCl_3$): See Table 13

CIMS *m/z* 363 $[M+H]^+$

HRCIMS *m/z* 363.1450 $[M+H]^+$ (calcd for $C_{19}H_{23}O_7$, 363.1444)

7.4.43. 2'-hydroxy-3'-*O*-isovalerylvaginol (**43**)

White amorphous powder

$C_{19}H_{22}O_7$

$[\alpha]^{25}_D$ +4.5 (*c* 1.0, $CHCl_3$)

UV (MeOH) λ_{max} (log ε) 219 (4.18), 250 (3.75), 261 (3.61), 300 (3.93), 325 (4.13) nm

CD (MeOH) λ_{max} ($\Delta\varepsilon$) 225 (+3.59), 240 (-1.71), 305 (-2.35) nm

^{1}H NMR data (500 MHz, $CDCl_3$): See Table 8

^{13}C NMR data (125 MHz, $CDCl_3$): See Table 13

CIMS *m/z* 363 $[M+H]^+$

HRCIMS *m/z* 363.1448 $[M+H]^+$ (calcd for $C_{19}H_{23}O_7$, 363.1444)

7.4.44. (+)-marmesin (nodakenetin) (**44**)

White amorphous powder

$C_{14}H_{14}O_4$

$[\alpha]^{20}_D$ +37.5 (*c* 0.1, MeOH)

UV (MeOH) λ_{max} (log ε) 227 (3.92), 261 (3.42), 301 (3.63), 335 (3.93) nm

^{1}H NMR (400 MHz, CD_3OD) δ 7.83 (1H, d, *J* = 9.5 Hz, H-4), 7.39 (1H, s, H-5), 6.71 (1H, s, H-8), 6.18 (1H, d, *J* = 9.5 Hz, H-3), 4.74 (1H, dd, *J* = 9.0, 8.4 Hz, H-2'), 3.24 (2H, m, H-3'), 1.28 (3H, s, H-5'), 1.22 (3H, s, H-6').

^{13}C NMR (100 MHz, CD_3OD) δ 166.1 (C-7), 164.6 (C-2), 157.7 (C-9), 147.01 (C-4), 128.1 (C-6), 125.8 (C-5), 114.9 (C-10), 113.0 (C-3), 99.0 (C-8), 93.3 (C-2'), 73.1 (C-4'), 31.1 (C-3'), 26.2 (C-5'), 26.1 (C-6').

ESIMS *m/z* 247 $[M+H]^+$

7.4.45. 9-(2-hydroxy-3-methoxy-3-methylbutoxy)bergapten (**45**)

White amorphous powder

$C_{18}H_{20}O_7$

$[\alpha]^{20}_D$ +21.7 (*c* 0.1, MeOH)

UV (MeOH) λ_{max} (log ε) 225 (4.17), 243 (3.91), 250 (3.90), 273 (4.00), 316 (3.84) nm

^{1}H NMR (400 MHz, CD_3OD) δ 8.25 (1H, d, *J* = 9.8 Hz, H-4), 7.83 (1H, d, *J* = 2.3 Hz, H-2'), 7.23 (1H, d, *J* = 2.3 Hz, H-3'), 6.29 (1H, d, *J* = 9.8 Hz, H-3), 4.52 (1H, dd, *J* = 10.3, 2.5 Hz, H-1''a), 4.26 (1H, dd, *J* = 10.3, 8.1 Hz, H-1''b), 4.21 (3H, s, 5-

OMe), 3.94 (1H, dd, *J* = 8.1, 2.5 Hz, H-2’’), 3.23 (3H, s, 3’’-OMe), 1.24 (3H, s, H-4’’), 1.19 (3H, s, H-5’’).

^{13}C NMR (100 MHz, CD_3OD) δ 163.5 (C-2), 152.5 (C-7), 147.8 (C-2’), 146.9 (C-5), 145.8 (C-9), 142.3 (C-4), 129.3 (C-8), 117.1 (C-6), 114.0 (C-3), 109.5 (C-10), 107.2 (C-3’), 78.5 (C-3’’), 77.7 (C-2’’), 77.6 (C-1’’), 62.3 (5-OMe), 50.4 (3’’-OMe), 23.0 (C-4’’), 21.5 (C-5’’).

ESIMS *m/z* 349 $[M+H]^+$

7.4.46. isoimperatorin (**46**)

White amorphous powder

$C_{16}H_{14}O_4$

$[\alpha]^{20}_D$ +1.8 (*c* 1.0, MeOH)

UV (MeOH) λ_{max} (log ε) 223 (4.05), 253 (3.87), 312 (3.77) nm

^{1}H NMR (300 MHz, $CDCl_3$) δ 8.14 (1H, d, *J* = 9.8 Hz, H-4), 7.57 (1H, d, *J* = 2.4 Hz, H-2’), 7.13 (1H, s, H-8), 6.93 (1H, dd, *J* = 2.4, 0.9 Hz, H-3’), 6.25 (1H, d, *J* = 9.8 Hz, H-3), 5.51 (1H, t, *J* = 7.0 Hz, H-2’’), 4.90 (2H, d, *J* = 7.0 Hz, H-1’’), 1.77 (3H, s, H-4’’), 1.67 (3H, s, H-5’’).

^{13}C NMR (75 MHz, $CDCl_3$) δ 161.3 (C-2), 158.1 (C-7), 152.6 (C-9), 148.9 (C-5), 144.8 (C-2’), 139.8 (C-3’’), 139.6 (C-4), 119.0 (C-2’’), 114.1 (C-6), 112.5 (C-3), 107.4 (C-10), 105.0 (C-3’), 94.2 (C-8), 69.7 (C-1’’), 25.8 (C-4’’), 18.2 (C-5’’).

ESIMS *m/z* 271 $[M+H]^+$

7.4.47. 5-(2-hydroxy-3-methoxy-3-methylbutoxy)psoralen (**47**)

White amorphous powder

$C_{17}H_{18}O_6$

$[\alpha]^{20}_D$ +23.8 (*c* 0.1, MeOH)

UV (MeOH) λ_{max} (log ε) 224 (4.29), 252 (4.14), 312 (4.05) nm

^{1}H NMR (400 MHz, $CDCl_3$) δ 8.21 (1H, d, *J* = 9.8 Hz, H-4), 7.58 (1H, d, *J* = 2.4 Hz, H-2’), 7.15 (1H, s, H-8), 6.98 (1H, dd, *J* = 2.4, 0.8 Hz, H-3’), 6.27 (1H, d, *J* = 9.8 Hz, H-3), 4.55 (1H, dd, *J* = 10.0, 3.1 Hz, H-1’’a), 4.37 (1H, dd, *J* = 10.0, 7.8 Hz, H-1’’b), 3.92 (1H, dd, *J* = 7.8, 3.1 Hz, H-2’’), 3.25 (3H, s, 3’’-OMe), 1.25 (3H, s, H-4’’), 1.22 (3H, s, H-5’’).

^{13}C NMR (100 MHz, $CDCl_3$) δ 161.2 (C-2), 158.1 (C-7), 152.6 (C-9), 148.8 (C-5), 145.0 (C-2'), 139.4 (C-4), 114.1 (C-6), 112.9 (C-3), 107.3 (C-10), 104.9 (C-3'), 94.5 (C-8), 76.1 (C-2''), 75.9 (C-3''), 74.3 (C-1''), 49.3 (3''-OMe), 20.7 (C-4'', C-5'').
ESIMS *m/z* 319 $[M+H]^+$

7.4.48. 3'-*O*-senecioylvaginidiol ((+)-8,9-dihydro-8-(2-hydroxy propan-2-yl)-2-oxo-2*H*-furo[2,3-*h*]chromen-9-yl-3-methylbut-2-enoate) (**48**)
White amorphous powder
$C_{19}H_{20}O_6$
$[\alpha]^{20}_D$ +84.4 (*c* 0.1, MeOH)
UV (MeOH) λ_{max} (log ε) 220 (4.38), 250 (3.96), 326 (4.24) nm
CD (MeOH) λ_{max} (Δε) 224 (-14.82), 251 (+1.93), 261 (+2.21), 321 (+4.54) nm
^{1}H NMR (400 MHz, CD_3OD) δ 7.87 (1H, d, *J* = 9.6 Hz, H-4), 7.59 (1H, d, *J* = 8.5 Hz, H-5), 6.98 (1H, d, *J* = 6.6 Hz, H-3'), 6.93 (1H, d, *J* = 8.5 Hz, H-6), 6.21 (1H, d, *J* = 9.6 Hz, H-3), 5.63 (1H, s, H-2''), 4.61 (1H, d, *J* = 6.6 Hz, H-2'), 2.20 (3H, br s, H-4''), 1.90 (3H, br s, H-5''), 1.39 (3H, s, H-5'), 1.33 (3H, s, H-6').
^{13}C NMR (100 MHz, CD_3OD) δ 166.8 (C-1''), 166.4 (C-7), 162.9 (C-2), 161.4 (C-3''), 153.7 (C-9), 146.7 (C-4), 133.8 (C-5), 116.9 (C-2''), 115.6 (C-10), 115.3 (C-8), 114.1 (C-3), 109.7 (C-6), 94.4 (C-2'), 72.7 (C-4'), 69.5 (C-3'), 28.3 (C-5''), 27.3 (C-5'), 27.0 (C-6'), 21.4 (C-4'').
ESIMS *m/z* 711 $[2M+Na]^+$

7.4.49. (*S*)-(+)-decursin (**49**)
White amorphous powder
$C_{19}H_{20}O_5$
$[\alpha]^{20}_D$ +88.1 (*c* 0.1, MeOH)
UV (MeOH) λ_{max} (log ε) 221 (4.17), 261 (3.24), 296 (3.61), 331 (3.81) nm
CD (MeOH) λ_{max} (Δε) 215 (-5.34), 230 (+1.72), 247 (+1.08), 259 (+0.72), 329 (+0.43) nm
^{1}H NMR (300 MHz, $CDCl_3$) δ 7.55 (1H, d, *J* = 9.5 Hz, H-4), 7.12 (1H, s, H-5), 6.77 (1H, s, H-8), 6.20 (1H, d, *J* = 9.5 Hz, H-3), 5.64 (1H, br s, H-2''), 5.06 (1H, t, *J* = 4.8 Hz, H-3'), 3.17 (1H, dd, *J* = 17.0, 4.8 Hz, H-4'a), 2.84 (1H, dd, *J* = 17.0, 4.8 Hz,

H-4’b), 2.12 (3H, br s, H-4’’), 1.85 (3H, br s, H-5’’), 1.36 (3H, s, H-5’), 1.34 (3H, s, H-6’).

^{13}C NMR (75 MHz, $CDCl_3$) δ 165.7 (C-1’’), 161.3 (C-2), 158.4 (C-3’’), 156.4 (C-7), 154.1 (C-9), 143.1 (C-4), 128.6 (C-5), 115.9 (C-6), 115.5 (C-2’’), 113.2 (C-3), 112.8 (C-10), 104.7 (C-8), 76.7 (C-2’), 69.1 (C-3’), 27.9 (C-4’), 27.5 (C-5’’), 25.0 (C-5’), 23.2 (C-6’), 20.4 (C-4’’).

ESIMS *m/z* 329 $[M+H]^+$

7.4.50. isoarnottinin (**50**)

White amorphous powder

$C_{14}H_{14}O_4$

$[\alpha]^{20}_D$ +26.0 (*c* 0.1, MeOH)

UV (MeOH) λ_{max} (log ε) 263 (3.57), 328 (3.73) nm

^{1}H NMR (400 MHz, CD_3OD) δ 7.81 (1H, d, *J* = 9.4 Hz, H-4), 7.29 (1H, d, *J* = 8.5 Hz, H-5), 6.80 (1H, d, *J* = 8.5 Hz, H-6), 6.16 (1H, d, *J* = 9.4 Hz, H-3), 5.53 (1H, t, *J* = 7.3 Hz, H-2’), 3.89 (2H, s, H-4’), 3.56 (2H, d, *J* = 7.3 Hz, H-1’), 1.87 (3H, s, H-5’).

^{13}C NMR (100 MHz, CD_3OD) δ 164.6 (C-2), 161.4 (C-7), 155.7 (C-9), 147.3 (C-4), 137.5 (C-3’), 128.7 (C-5), 124.4 (C-2’), 117.2 (C-8), 114.4 (C-6), 114.1 (C-10), 112.7 (C-3), 69.6 (C-4’), 23.1 (C-1’), 14.7 (C-5’).

ESIMS *m/z* 247 $[M+H]^+$

7.4.51. umbelliferone (**51**)

White amorphous powder

$C_9H_6O_3$

$[\alpha]^{20}_D$ +54.7 (*c* 0.1, MeOH)

UV (MeOH) λ_{max} (log ε) 220 (3.83), 257 (3.29), 292 (3.51), 325 (3.73) nm

^{1}H NMR (500 MHz, CD_3OD) δ 9.74 (1H, s, 7-O*H*), 7.84 (1H, d, *J* = 9.4 Hz, H-4), 7.44 (1H, d, *J* = 8.5 Hz, H-5), 6.78 (1H, dd, *J* = 8.5, 2.2 Hz, H-6), 6.70 (1H, d, *J* = 2.2 Hz, H-8), 6.17 (1H, d, *J* = 9.4 Hz, H-3).

^{13}C NMR (125 MHz, CD_3OD) δ 164.5 (C-2), 164.0 (C-7), 158.1 (C-9), 146.9 (C-4), 131.5 (C-5), 115.3 (C-6), 114.0 (C-10), 113.2 (C-3), 104.2 (C-8).

ESIMS *m/z* 161 $[M-H]^-$

7.4.52. scoparone (**52**)

White amorphous powder

$C_{11}H_{10}O_4$

$[\alpha]^{20}_D$ +49.6 (*c* 0.1, MeOH)

UV (MeOH) λ_{max} (log ε) 231 (4.00), 261 (3.50), 291 (3.53), 340 (3.73) nm

^{1}H NMR (600 MHz, CD_3OD) δ 7.86 (1H, d, *J* = 9.4 Hz, H-4), 7.12 (1H, s, H-5), 6.96 (1H, s, H-8), 6.24 (1H, d, *J* = 9.4 Hz, H-3), 3.90 (3H, s, 7-OMe), 3.86 (3H, s, 6-OMe).

^{13}C NMR (150 MHz, CD_3OD) δ 162.5 (C-2), 153.5 (C-7), 150.0 (C-9), 146.8 (C-6), 144.6 (C-4), 112.2 (C-3), 111.7 (C-10), 108.7 (C-5), 99.7 (C-8), 55.5 (6-OMe, 7-OMe).

ESIMS *m/z* 207 $[M+H]^+$

7.4.53. tamarin (isosuberenol) (**53**)

White amorphous powder

$C_{15}H_{16}O_4$

$[\alpha]^{20}_D$ +3.4 (*c* 1.0, MeOH)

UV (MeOH) λ_{max} (log ε) 225 (4.28), 256 (3.65), 298 (3.93), 333 (4.19) nm

^{1}H NMR (600 MHz, CD_3OD) δ 7.83 (1H, d, *J* = 9.5 Hz, H-4), 7.36 (1H, s, H-5), 6.90 (1H, s, H-8), 6.20 (1H, d, *J* = 9.5 Hz, H-3), 4.76 (1H, br s, H-4'a), 4.72 (1H, br s, H-4'b), 4.27 (1H, dd, *J* = 7.9, 5.7 Hz, H-2'), 3.90 (3H, s, 7-OMe), 2.93 (1H, dd, *J* = 13.6, 5.7 Hz, H-1'a), 2.74 (1H, dd, *J* = 13.6, 7.9 Hz, H-1'b), 1.77 (3H, s, H-5').

^{13}C NMR (150 MHz, CD_3OD) δ 162.3 (C-2), 161.4 (C-7), 154.7 (C-9), 147.3 (C-3'), 144.6 (C-4), 129.8 (C-5), 125.1 (C-6), 112.0 (C-10), 111.8 (C-3), 110.0 (C-4'), 98.2 (C-8), 74.5 (C-2'), 55.2 (7-OMe), 35.7 (C-1'), 16.5 (C-5').

ESIMS *m/z* 261 $[M+H]^+$

7.4.54. (*Z*)-suberenol (**54**)

White amorphous powder

$C_{15}H_{16}O_4$

$[\alpha]^{20}_{D}$ +2.6 (*c* 1.0, MeOH)

UV (MeOH) λ_{max} (log ε) 227 (4.01), 256 (3.94), 298 (3.71), 335 (3.85) nm

^{1}H NMR (400 MHz, CD_3OD) δ 7.86 (1H, d, *J* = 9.4 Hz, H-4), 7.59 (1H, s, H-5), 6.91 (1H, s, H-8), 6.29 (1H, dd, *J* = 12.7, 0.6 Hz, H-1'), 6.23 (1H, d, *J* = 9.4 Hz, H-3), 5.81 (1H, d, *J* = 12.7 Hz, H-2'), 3.90 (3H, s, 7-OMe), 1.26 (6H, s, H-4', H-5').

^{13}C NMR (100 MHz, CD_3OD) δ 164.3 (C-2), 162.8 (C-7), 157.2 (C-9), 146.8 (C-4), 142.5 (C-2'), 132.1 (C-5), 126.7 (C-6), 124.0 (C-1'), 114.1 (C-3), 113.7 (C-10), 100.2 (C-8), 72.9 (C-3'), 57.4 (7-OMe), 31.5 (C-4', C-5').

ESIMS *m/z* 261 $[M+H]^+$

7.4.55. suberosin (**55**)

White amorphous powder

$C_{15}H_{16}O_3$

$[\alpha]^{20}_{D}$ +1.8 (*c* 1.0, MeOH)

UV (MeOH) λ_{max} (log ε) 225 (3.95), 246 (3.54), 255 (3.47), 298 (3.64), 329 (3.86) nm

^{1}H NMR (500 MHz, $CDCl_3$) δ 7.55 (1H, d, *J* = 9.4 Hz, H-4), 7.11 (1H, s, H-5), 6.68 (1H, s, H-8), 6.15 (1H, d, *J* = 9.4 Hz, H-3), 5.21 (1H, t, *J* = 7.4 Hz, H-2'), 3.82 (3H, s, 7-OMe), 3.23 (2H, d, *J* = 7.4 Hz, H-1'), 1.70 (3H, s, H-4'), 1.64 (3H, s, H-5').

^{13}C NMR (125 MHz, $CDCl_3$) δ 161.3 (C-2), 160.5 (C-7), 154.3 (C-9), 143.5 (C-4), 133.4 (C-3'), 127.3 (C-6), 127.2 (C-5), 121.2 (C-2'), 112.5 (C-3), 111.7 (C-10), 98.3 (C-8), 55.7 (7-OMe), 27.6 (C-1'), 25.6 (C-4'), 17.6 (C-5').

ESIMS *m/z* 245 $[M+H]^+$

7.4.56. peucedanol (**56**)

White amorphous powder

$C_{14}H_{16}O_5$

$[\alpha]^{20}_{D}$ +2.3 (*c* 1.0, MeOH)

UV (MeOH) λ_{max} (log ε) 224 (4.15), 250 (3.58), 259 (3.50), 292 (3.77), 334 (4.12) nm

^{1}H NMR (400 MHz, CD_3OD) δ 7.82 (1H, d, *J* = 9.4 Hz, H-4), 7.38 (1H, s, H-5), 6.71 (1H, s, H-8), 6.16 (1H, d, *J* = 9.4 Hz, H-3), 3.60 (1H, d, *J* = 10.4 Hz, H-2'), 3.07 (1H,

d, *J* = 14.0 Hz, H-1'a), 2.53 (1H, dd, *J* = 14.0, 10.4 Hz, H-1'b), 1.24 (6H, s, H-4', H-5').

^{13}C NMR (100 MHz, CD_3OD) δ 164.8 (C-2), 162.2 (C-7), 156.5 (C-9), 147.0 (C-4), 132.5 (C-5), 127.3 (C-6), 113.8 (C-10), 113.0 (C-3), 103.9 (C-8), 80.0 (C-2'), 74.6 (C-3'), 34.2 (C-1'), 26.4 (C-4'), 26.0 (C-5').

ESIMS *m/z* 265 $[M+H]^+$

7.4.57. peucedanol 7-*O*-β-$_D$-glucopyranoside (**57**)

White amorphous powder

$C_{20}H_{26}O_{10}$

$[\alpha]^{20}_D$ -0.3 (*c* 1.0, MeOH)

UV (MeOH) λ_{max} (log ε) 223 (3.77), 244 (3.15), 253 (3.04), 293 (3.43), 328 (3.58) nm

^{1}H NMR (400 MHz, CD_3OD) δ 7.86 (1H, d, *J* = 9.5 Hz, H-4), 7.44 (1H, s, H-5), 7.16 (1H, s, H-8), 6.25 (1H, d, *J* = 9.5 Hz, H-3), 4.96 (1H, d, *J* = 7.2 Hz, H-1''), 3.93 (1H, dd, *J* = 12.1, 2.0 Hz, H-6''a), 3.71 (1H, dd, *J* = 12.1, 5.7 Hz, H-6''b), 3.46~3.56 (4H, m, H-3'', H-2', H-5'', H-2''), 3.35~3.43 (2H, m, H-4'', H-1'a), 2.33 (1H, dd, *J* = 13.5, 10.0 Hz, H-1'b), 1.24 (3H, s, H-4'), 1.23 (3H, s, H-5').

^{13}C NMR (100 MHz, CD_3OD) δ 164.2 (C-2), 160.9 (C-7), 156.3 (C-9), 146.6 (C-4), 132.0 (C-5), 129.7 (C-6), 115.5 (C-10), 114.9 (C-3), 104.6 (C-8), 103.4 (C-1''), 79.9 (C-2'), 79.2 (C-5''), 78.5 (C-3''), 75.6 (C-2''), 75.0 (C-3'), 72.1 (C-4''), 63.2 (C-6''), 34.1 (C-1'), 28.1 (C-4'), 24.1 (C-5').

ESIMS *m/z* 427 $[M+H]^+$

7.4.58. peujaponiside (**58**)

White amorphous powder

$C_{25}H_{34}O_{14}$

$[\alpha]^{20}_D$ +2.6 (*c* 0.1, MeOH)

UV (MeOH) λ_{max} (log ε) 223 (3.48), 254 (2.80), 294 (3.13), 328 (3.26) nm

^{1}H NMR (400 MHz, CD_3OD) δ 7.88 (1H, d, *J* = 9.5 Hz, H-4), 7.45 (1H, s, H-5), 7.26 (1H, s, H-8), 6.28 (1H, d, *J* = 9.5 Hz, H-3), 4.97 (1H, d, *J* = 2.6 Hz, H-1'''), 4.90 (1H, d, *J* = 7.3 Hz, H-1''), 4.01~4.12 (3H, m, H-4'''a, H-6''a, H-2'''), 3.79 (1H, d, *J* = 9.7

Hz, H-4’’’b), 3.71 (1H, m, H-6’’b), 3.65 (2H, s, H-5’’a, H-5’’b), 3.45~3.64 (4H, m, H-2’, H-2’’, H-5’’, H-3’’), 3.32~3.40 (2H, m, H-1’a, H-4’’), 2.33 (1H, dd, *J* = 13.5, 9.9 Hz, H-1’b), 1.24 (3H, s, H-4’), 1.23 (3H, s, H-5’).

^{13}C NMR (100 MHz, CD_3OD) δ 164.5 (C-2), 160.9 (C-7), 156.3 (C-9), 146.7 (C-4), 132.0 (C-5), 129.8 (C-6), 115.6 (C-10), 114.9 (C-3), 112.1 (C-1’’’), 105.0 (C-8), 103.6 (C-1’’), 81.3 (C3’’’), 79.9 (C-2’), 79.2 (C-2’’’), 78.7 (C-5’’), 78.0 (C-3’’), 75.9 (C-4’’’), 75.7 (C-2’’), 75.0 (C-3’), 72.7 (C-4’’), 70.1 (C-6’’), 66.5 (C-5’’’), 34.2 (C-1’), 28.2 (C-4’), 24.0 (C-5’).

ESIMS *m/z* 559 $[M+H]^+$

7.4.59. eugenin (**59**)

White amorphous powder

$C_{11}H_{10}O_4$

$[\alpha]^{20}_D$ +29.5 (*c* 0.1, MeOH)

UV (MeOH) λ_{max} (log ε) 232 (3.24), 251 (3.29), 257 (3.29), 292 (2.91), 320 (2.67) nm

^{1}H NMR (400 MHz, $CDCl_3$) δ 6.34 (1H, d, *J* = 2.2 Hz, H-8), 6.32 (1H, d, *J* = 2.2 Hz, H-6), 6.01 (1H, s, H-3), 3.83 (3H, s, 7-OMe), 2.33 (3H, s, 2-Me).

^{13}C NMR (100 MHz, $CDCl_3$) δ 182.5 (C-4), 166.8 (C-2), 165.3 (C-7), 162.2 (C-5), 158.1 (C-9), 108.8 (C-3), 105.2 (C-10), 97.9 (C-6), 92.5 (C-8), 55.7 (7-OMe), 20.5 (2-Me).

ESIMS *m/z* 207 $[M+H]^+$

7.4.60. 6,*β*-dihydroxyphenethyl *trans*-ferulate (decursidate) (**60**)

White amorphous powder

$C_{18}H_{18}O_6$

$[\alpha]^{20}_D$ +43.2 (*c* 0.1, MeOH)

UV (MeOH) λ_{max} (log ε) 225 (4.26), 287 (4.06), 322 (4.14) nm

^{1}H NMR (500 MHz, CD_3OD) δ 7.59 (1H, d, *J* = 15.9 Hz, H-7), 7.24 (2H, d, *J* = 8.5 Hz, H-2’, H-6’), 7.09 (1H, d, *J* = 1.6 Hz, H-2), 7.00 (1H, dd, *J* = 8.5, 1.6 Hz, H-6), 6.79 (3H, d, *J* = 8.5, H-5, H-3’, H-5’), 6.33 (1H, d, *J* = 15.9 Hz, H-8), 4.87 (1H, m, H-7’), 4.23 (2H, m, H-8’), 3.82 (3H, s, 3-OMe).

^{13}C NMR (125 MHz, CD_3OD) δ 169.9 (C-9), 158.9 (C-4’), 151.2 (C-4), 149.9 (C-3), 147.8 (C-7), 133.7 (C-1’), 129.4 (C-2’, C-6’), 128.4 (C-1), 124.8 (C-6), 117.2 (C-5), 116.9 (C-3’, C-5’), 116.0 (C-8), 112.4 (C-2), 73.4 (C-7’), 70.8 (C-8’), 57.1 (3-OMe). ESIMS *m/z* 329 $[M-H]^-$

7.4.61. 6-hydroxyphenethyl *cis*-ferulate (**61**)

White amorphous powder

$C_{18}H_{18}O_5$

$[\alpha]^{20}_D$ +19.8 (*c* 0.1, MeOH)

UV (MeOH) λ_{max} (log ε) 224 (3.89), 288 (3.61), 326 (3.74) nm

^{1}H NMR (800 MHz, CD_3OD) δ 7.72 (1H, d, *J* = 1.9 Hz, H-2), 7.09 (1H, dd, *J* = 8.2, 1.9 Hz, H-6), 7.05 (2H, d, *J* = 8.5 Hz, H-2’, H-6’), 6.86 (1H, d, *J* = 12.8 Hz, H-7), 6.77 (1H, d, *J* = 8.2 Hz, H-5), 6.72 (2H, d, *J* = 8.5 Hz, H-3’, H-5’), 5.78 (1H, d, *J* = 12.8 Hz, H-8), 4.29 (2H, t, *J* = 7.1 Hz, H-8’), 3.86 (3H, s, 3-OMe), 2.86 (2H, t, *J* = 7.1 Hz, H-7’).

^{13}C NMR (200 MHz, CD_3OD) δ 169.1 (C-9), 157.9 (C-4’), 150.3 (C-4), 149.1 (C-3), 146.1 (C-7), 131.7 (C-2’, C-6’), 130.9 (C-1’), 128.9 (C-1), 127.4 (C-6), 117.5 (C-8), 117.0 (C-3’, C-5’), 116.4 (C-5), 115.7 (C-2), 67.1 (C-8’), 57.1 (3-OMe), 36.1 (C-7’). ESIMS *m/z* 313 $[M-H]^-$

7.4.62. (-)-pinoresinol (**62**)

White amorphous powder

$C_{20}H_{22}O_6$

$[\alpha]^{20}_D$ -13.3 (*c* 1.0, MeOH)

UV (MeOH) λ_{max} (log ε) 234 (4.13), 283 (3.82), 327 (3.27) nm

CD (MeOH) λ_{max} ($\Delta\varepsilon$) 228 (-0.74), 280 (-0.29) nm

^{1}H NMR (600 MHz, CD_3OD) δ 6.92 (2H, d, *J* = 1.8 Hz, H-2, H-2’), 6.79 (2H, dd, *J* = 8.1, 1.8 Hz, H-6, H-6’), 6.74 (2H, d, *J* = 8.1 Hz, H-5, H-5’), 4.68 (2H, d, *J* = 4.4 Hz, H-7, H-7’), 4.21 (2H, dd, *J* = 9.2, 7.0 Hz, H-9a, H-9’a), 3.83 (6H, s, 3-OMe, 3’-OMe), 3.82 (2H, dd, *J* = 9.2, 3.7 Hz, H-9b, H-9’b), 3.12 (2H, m, H-8, H-8’).

^{13}C NMR (150 MHz, CD_3OD) δ 147.8 (C-3, C-3’), 146.0 (C-4, C-4’), 132.5 (C-1, C-1’), 118.7 (C-6, C-6’), 114.8 (C-5, C-5’), 109.7 (C-2, C-2’), 86.2 (C-7, C-7’), 71.3

(C-9, C-9'), 55.1 (3-OMe, 3'-OMe), 54.0 (C-8, C-8').

ESIMS *m/z* 381 $[M+Na]^+$

7.4.63. *trans*-ferulic acid (**63**)

White amorphous powder

$C_{10}H_{10}O_4$

$[\alpha]^{20}_D$ -0.2 (*c* 1.0, MeOH)

UV (MeOH) λ_{max} (log ε) 233 (3.88), 290 (3.84), 322 (3.90) nm

^{1}H NMR (500 MHz, CD_3OD) δ 7.58 (1H, d, *J* = 15.8 Hz, H-7), 7.17 (1H, s, H-2), 7.05 (1H, d, *J* = 8.1 Hz, H-6), 6.80 (1H, d, *J* = 8.1 Hz, H-5), 6.30 (1H, d, *J* = 15.8 Hz, H-8), 3.88 (3H, s, 3-OMe).

^{13}C NMR (125 MHz, CD_3OD) δ 171.9 (C-9), 151.3 (C-4), 150.2 (C-3), 147.6 (C-7), 128.6 (C-1), 124.8 (C-6), 117.3 (C-5), 116.9 (C-8), 112.5 (C-2), 57.2 (3-OMe).

ESIMS *m/z* 195 $[M+H]^+$

7.4.64. 3-formylindole (**64**)

White amorphous powder

C_9H_7NO

$[\alpha]^{20}_D$ +3.6 (*c* 1.0, MeOH)

UV (MeOH) λ_{max} (log ε) 245 (3.83), 263 (3.75), 298 (3.80) nm

^{1}H NMR (600 MHz, CD_3OD) δ 9.86 (1H, s, 3-C*H*O), 8.13 (1H, d, *J* = 7.9 Hz, H-4), 8.07 (1H, s, H-2), 7.45 (1H, d, *J* = 7.9 Hz, H-7), 7.25 (1H, t, *J* = 7.9 Hz, H-6), 7.21 (1H, t, *J* = 7.9 Hz, H-5).

^{13}C NMR (150 MHz, CD_3OD) δ 186.1 (3-*C*HO), 138.3 (C-2), 137.6 (C-8), 124.4 (C-9), 123.7 (C-6), 122.3 (C-5), 121.0 (C-4), 118.8 (C-3), 111.8 (C-7).

ESIMS *m/z* 146 $[M+H]^+$

Table 3. ^{1}H-NMR Data of Compounds **1-8** (δ in ppm; *J* in Hz)

position	**1**[a]	**2**[a]	**3**[a]	**4**[a]	**5**[c]	**6**[a]	**7**[b]	**8**[d]
3	6.20, d (9.5)	6.19, d (9.5)	6.20, d (9.5)	6.19, d (9.5)	6.20, d (9.5)	6.20, d (9.5)	6.20, d (9.5)	6.20, d (9.5)
4	7.57, d (9.5)	7.56, d (9,5)	7.57, d (9.5)	7.56, d (9,5)	7.57, d (9.5)	7.57, d (9.5)	7.57, d (9.5)	7.57, d (9.5)
5	7.33, d (8.6)	7.32, d (8.6)	7.33, d (8.6)	7.32, d (8.6)	7.33, d (8.6)	7.33, d (8.6)	7.34, d (8.6)	7.33, d (8.6)
6	6.78, d (8.6)	6.77, d (8.6)	6.78, d (8.6)	6.77, d (8.6)	6.79, d (8.6)	6.77, d (8.6)	6.78, d (8.6)	6.78, d (8.6)
3’	5.30, d (4.8)	5.29, d (4.8)	5.31, d (4.9)	5.31, d (4.9)	5.35, d (5.0)	5.29, d (4.9)	5.36, d (4.9)	5.31, d (4.9)
4’	6.53, d (4.8)	6.56, d (4.8)	6.54, d (4.9)	6.59, d (4.9)	6.56, d (5.0)	6.55, d (4.9)	6.63, d (4.9)	6.52, d (4.9)
5’	1.38, s	1.40, s	1.38, s	1.39, s	1.40, s	1.38, s	1.41, s	1.39, s
6’	1.43, s	1.44, s	1.43, s	1.44, s	1.44, s	1.43, s	1.45, s	1.43, s
3’-ester								
2	2.55, sep (7.0)	2.07, s	2.37, sxt (7.0)	2.37, sxt (7.0)	5.65, brs	2.56, sep (7.0)	2.37, sxt (7.0)	2.30, dt (7.4, 1.7)
3	1.18, d (7.0)		1.69, m	1.68, m		1.17, d (7.0)	1.68, m	1.66, sxt (7.4)
			1.46, m	1.45, m			1.46, m	
4	1.17, d (7.0)		0.90, t (7.4)	0.89, t (7.4)	2.17, brs	1.16, d (7.0)	0.89, t (7.5)	0.95, t (7.4)
5			1.14, d (7.0)	1.14, d (7.0)	1.89, brs		1.13, d (7.0)	
4’-ester								
2	2.37, sxt (7.0)	5.62, s	2.56, sep (7.0)	5.60, s	2.38, sxt (7.0)	2.28, dd (14.4, 6.7) 2.17, m		2.38, sxt (7.0)
3	1.71, m 1.44, m		1.20, d (7.0)		1.71, m 1.43, m	2.13, m	6.00, q (7.2)	1.71, m 1.45, m
4	0.91, t (7.4)	2.21, s	1.17, d (7.0)	2.21, s	0.91, t (7.4)	0.97, d (6.3)	1.97, d (7.2)	0.92, t (7.4)
5	1.19, d (7.0)	1.87, s		1.87, s	1.20, d (7.0)	0.95, d (6.3)	1.84, s	1.19, d (7.0)

[a] Data were obtained at 400 MHz in $CDCl_3$.
[b] Data were obtained at 500 MHz in $CDCl_3$.
[c] Data were obtained at 600 MHz in $CDCl_3$.
[d] Data were obtained at 800 MHz in $CDCl_3$.

Table 4. ^{1}H-NMR Data of Compounds **9-16** (δ in ppm; *J* in Hz)

position	**9**[d]	**10**[a]	**11**[c]	**12**[a]	**13**[d]	**14**[a]	**15**[d]	**16**[a]
3	6.20, d (9.5)	6.22, d (9.5)	6.24, d (9.5)	6.15, d (9.5)	6.24, d (9.5)	6.17, d (9.5)	6.24, d (9.5)	6.21, d (9.4)
4	7.57, d (9.5)	7.58, d (9.5)	7.62, d (9.5)	7.56, d (9.5)	7.62, d (9.5)	7.56, d (9.5)	7.59, d (9,5)	7.58, d (9.4)
5	7.33, d (8.6)	7.35, d (8.7)	7.37, d (8.6)	7.33, d (8.6)	7.32, d (8.6)	7.31, d (8.6)	7.29, d (8.6)	7.32, d (8.6)
6	6.78, d (8.6)	6.79, d (8.7)	6.81, d (8.6)	6.75, d (8.6)	6.77, d (8.6)	6.75, d (8.6)	6.73, d (8.6)	6.79, d (8.6)
3’	5.36, d (4.9)	5.30, d (4.8)	5.41, d (4.9)	5.22, d (4.9)	5.11, d (4.9)	4.01, d (4.7)	5.16,d (4.6)	3.93, br s
4’	6.61, d (4.9)	6.57, d (4.8)	6.47, d (4.9)	6.44, d (4.9)	5.40, d (4.9)	6.36, d (4.7)	4.83, d (4.6)	6.08, d (3.4)
5’	1.41, s	1.40, s	1.40, s	1.36, s	1.39, s	1.45, s	1.37, s	1.46, s
6’	1.44, s	1.43, s	1.41, s	1.39, s	1.47, s	1.38, s	1.47, s	1.37, s
3’-ester								
2	2.21, d (7.4)	2.09, s	2.08, s	2.04, s	2.50, sxt		2.51, sxt	5.68, s
	2.20, d (6.9)				(7.0)		(7.0)	
3	2.08, m				1.74, m		1.76, m	
					1.51, m		1.54, m	
4	0.94, d (6.6)				0.93, t (7.5)		0.95, t (7.4)	2.21, s
5	0.93, d (6.6)				1.19, d (7.0)		1.21, d (7.0)	1.89, s
4’-ester								
1							3.70, s	
2		2.59, d	2.49, qui	2.35, sxt		2.45, sxt		
		(15.4)	(7.2)	(7.0)		(7.0)		
		2.50, d						
		(15.4)						
3	6.01, q (7.3)		3.92, m	1.66, m		1.71, m		
				1.41, m		1.47, m		
4	1.98, d (7.3)	1.34, s	1.22, d (6.3)	0.88, t (7.4)		0.91, t (7.4)		
5	1.84, s	1.33, s	1.16, d (7.2)	1.15, d (7.0)		1.21, d (7.0)		
OH			3.52, d (5.4)		3.12, br s	2.96, br s		
solvent*							3.47, s	

[a] Data were obtained at 400 MHz in $CDCl_3$.
[b] Data were obtained at 500 MHz in $CDCl_3$.
[c] Data were obtained at 600 MHz in $CDCl_3$.
[d] Data were obtained at 800 MHz in $CDCl_3$.
*solvent residual peak (MeOH)

Table 5. ^{1}H-NMR Data of Compounds **17-24** (δ in ppm; *J* in Hz)

position	**17**[c]	**18**[d]	**19**[c]	**20**[d]	**21**[c]	**22**[b]	**23**[c]	**24**[e]
3	6.20, d (9.5)	6.20, d (9.4)	6.23, d (9.5)	6.23, d (9.5)	6.20, d (9.5)	6.15, d (9.5)	6.20, d (9.5)	6.24, d (9.6)
4	7.58, d (9.5)	7.57, d (9.4)	7.62, d (9.5)	7.61, d (9.5)	7.57, d (9.5)	7.55, d (9.5)	7.57, d (9.5)	7.63, d (9.6)
5	7.32, d (8.6)	7.32, d (8.6)	7.32, d (8.6)	7.31, d (8.6)	7.33, d (8.6)	7.31, d (8.6)	7.33, d (8.6)	7.32, d (8.6)
6	6.77, d (8.6)	6.77, d (8.6)	6.78, d (8.6)	6.77, d (8.6)	6.66, d (8.6)	6.75, d (8.6)	6.78, d (8.6)	6.78, d (8.6)
3’	4.02, d (4.6)	4.02, dd (4.7, 2.3)	5.19, d (4.7)	5.20, d (4.9)	5.39, d (5.0)	5.31, d (4.8)	5.34, d (4.9)	5.18, d (5.0)
4’	6.43, d (4.6)	6.43, d (4.7)	5.42, d (4.7)	5.42, d (4.9)	6.66, d (5.0)	6.57, d (4.8)	6.58, d (4.9)	5.40, d (5.0)
5’	1.45, s	1.45, s	1.39, s	1.39, s	1.43, s	1.38, s	1.40, s	1.38, s
6’	1.43, s	1.42, s	1.48, s	1.47, s	1.45, s	1.42, s	1.44, s	1.46, s
3’-ester								
2			5.79, s	5.78, brs	5.64, br s	5.62, s	5.66, br s	2.16, s
3								
4			2.19, s	2.19, brs	2.14, br s	2.11, s	2.16, br s	
5			1.91, s	1.91, brs	1.83, br s	1.84, s	1.88, br s	
4’-ester								
2	5.71, s	5.71, brs				5.58, s	2.29, dd (14.9, 6.9) 2.20, m	
3					5.98, qd (7.2, 1.4)		2.12, m	
4	2.22, s	2.23, brs			1.97, dd (7.2, 1.4)	2.14, s	0.97, d (6.6)	
5	1.90, s	1.90, brs			1.83, br s	1.83, s	0.95, d (6.6)	
OH	2.98, br s	2.92, d (2.3)	3.16, br s	3.02, br s				
solvent*		3.47, s						

[a] Data were obtained at 400 MHz in $CDCl_3$.
[b] Data were obtained at 500 MHz in $CDCl_3$.
[c] Data were obtained at 600 MHz in $CDCl_3$.
[d] Data were obtained at 800 MHz in $CDCl_3$.
[e] Data were obtained at 300 MHz in $CDCl_3$.
*solvent residual peak (MeOH)

Table 6. ^{1}H-NMR Data of Compounds **25-32** (δ in ppm; *J* in Hz)

position	**25**[a]	**26**[a]	**27**[c]	**28**[e]	**29**[f]	**30**[d]	**31**[c]	**32**[a]
3	6.13, d (9.5)	6.21, d (9.5)	6.22, d (9.4)	6.24, d (9.5)	6.22, d (9.4)	6.20, d (9.5)	6.19, d (9.5)	6.17, d (9.5)
4	7.56, d (9.5)	7.57, d (9.5)	7.58, d (9.4)	7.86, d (9.5)	7.59, d (9.4)	7.58, d (9.5)	7.57, d (9,5)	7.57, d (9.5)
5	7.32, d (8.6)	7.33, d (8.6)	7.34, d (8.6)	7.45, d (8.6)	7.33, d (8.6)	7.34, d (8.6)	7.23, d (8.6)	7.33, d (8.7)
6	6.74, d (8.6)	6.78, d (8.6)	6.78, d (8.6)	6.77, d (8.6)	6.78, d (8.6)	6.78, d (8.6)	6.78, d (8.6)	6.78, d (8.7)
3’	5.24, d (4.9)	5.30, d (4.9)	5.30, d (4.9)	3.75, d (4.7)	3.98, d (4.6)	4.06, d (4.7)	5.37, d (4.8)	5.40, d (4.9)
4’	6.53, d (4.9)	6.51, d (4.9)	6.54, d (4.9)	5.09, d (4.7)	6.40, d (4.6)	6.47, d (4.7)	6.58, d (4.8)	6.66, d (4.9)
5’	1.35, s	1.40, s	1.41, s	1.422, s	1.43, s	1.47, s	1.42, s	1.42, s
6’	1.38, s	1.43, s	1.44, s	1.418, s	1.42, s	1.42, s	1.45, s	1.45, s
3’-ester								
2	2.01, s	2.07, s	2.09, s					
3							6.09, q (7.2)	6.08, q (7.2)
4							1.94, d (7.2)	1.94, d (7.2)
5							1.85, s	1.82, s
4’-ester								
2		2.59, sep (7.0)	2.30, dd (14.8, 7.1) 2.21, dd (14.8, 7.1)		2.21, s		2.35, sxt (7.0)	
3	5.94, q (7.2)	1.21, d (7.0)	2.14, m			6.09, q (7.3)	1.69, m 1.40, m	5.99, q (7.2)
4	1.90, d (7.2)	1.18, d (7.0)	0.99, d (6.7)			1.99, d (7.3)	0.87, t (7.5)	1.92, d (7.2)
5	1.78, s		0.97, d (6.7)			1.87, br s	1.16, d (7.0)	1.79, s
OH						2.83, s		
solvent*	3.37, s							3.44, s

[a] Data were obtained at 400 MHz in $CDCl_3$.
[b] Data were obtained at 500 MHz in $CDCl_3$.
[c] Data were obtained at 600 MHz in $CDCl_3$.
[d] Data were obtained at 800 MHz in $CDCl_3$.
[e] Data were obtained at 100 MHz in CD_3OD.
[f] Data were obtained at 300 MHz in $CDCl_3$.
*solvent residual peak (MeOH)

Table 7. ^{1}H-NMR Data of Compounds **33-40** (δ in ppm; *J* in Hz)

position	**33**[a]	**34**[a]	**35**[c]	**36**[e]	**37**[c]	**38**[e]	**39**[d]	**40**[f]
3	6.22, d (9.5)	6.18, d (9.5)	6.19, d (9.6)	6.19, d (9.5)	6.16, d (9.5)	6.21, d (9.4)	6.22, d (9.4)	6.24, d (9.5)
4	7.61, d (9.5)	7.55, d (9.5)	7.55, d (9.6)	7.57, d (9.5)	7.57, d (9.5)	7.60, d (9.4)	7.61, d (9,4)	7.86, d (9.5)
5	7.31, d (8.6)	7.32, d (8.6)	7.32, d (8.7)	7.33, d (8.7)	7.33, d (8.6)	7.23, d (8.6)	7.24, d (8.6)	7.53, d (8.7)
6	6.77, d (8.6)	6.77, d (8.6)	6.77, d (8.7)	6.76, d (8.7)	6.76, d (8.6)	6.77, d (8.6)	6.73, d (8.6)	6.84, d (8.7)
3’	5.20, d (4.8)	5.38, d (4.8)	5.31, d (4.6)	5.29, d (5.0)	5.26, d (5.1)	5.13, t (4.9)	5.12, t (5.2)	5.28, d (4.8)
4’	5.45, d (4.8)	6.63, d (4.8)	6.57, d (4.6)	6.52, d (5.0)	6.48, d (5.1)	3.18, dd (18.0, 4.9)	3.18, dd (17.8, 5.2)	6.49, d (4.8)
						2.98, dd (18.0, 4.9)	2.94, dd (17.8, 5.2)	
5’	1.41, s	1.42, s	1.39, s	1.38, s	1.37, s	1.36, s	1.35, s	1.42, s
6’	1.49, s	1.47, s	1.43, s	1.41, s	1.40, s	1.33, s	1.33, s	1.44, s
3’-ester								
2			2.20, m	2.26, m	2.19, m	5.63, br s	2.18, d (7.2)	2.07, s
			2.20, m	2.19, m	2.19, m		2.18, d (7.2)	
3	6.14, q (7.2)	6.08, q (7.3)	2.08, m	2.11, m	2.07, m		2.06, m	
4	1.97, d (7.2)	1.94, d (7.3)	0.94, d (7.1)	0.94, d (6.4)	0.94, d (6.4)	2.13, br s	0.91, d (6.7)	
5	1.91, br s	1.83, s	0.93, d (7.1)	0.94, d (6.4)	0.92, d (6.4)	1.85, br s	0.91, d (6.7)	
4’-ester								
2		5.59, s	5.61, s	2.26, m	2.34, sxt (7.0)			2.09, s
				2.19, m				
3				2.11, m	1.68, m			
					1.47, m			
4		2.16, s	2.21, s	0.94, d (6.4)	0.90, t (7.4)			
5		1.85, s	1.87, s	0.94, d (6.4)	1.16, d (7.0)			

[a] Data were obtained at 400 MHz in $CDCl_3$.
[b] Data were obtained at 500 MHz in $CDCl_3$.
[c] Data were obtained at 600 MHz in $CDCl_3$.
[d] Data were obtained at 800 MHz in $CDCl_3$.
[e] Data were obtained at 300 MHz in $CDCl_3$.
[f] Data were obtained at 500 MHz in CD_3OD.
[*]solvent residual peak (MeOH)

Table 8. ^{1}H-NMR data of compounds **41-43** (δ in ppm; *J* in Hz).

position	41[b]	42[a]	43[b]
3	6.21, d (9.6)	6.21, d (9.5)	6.21, d (9.6)
4	7.59, d (9.6)	7.59, d (9.6)	7.60, d (9.6)
5	7.38, d (8.4)	7.39, d (8.4)	7.39, d (8.4)
6	6.77, d (8.4)	6.78, d (8.2)	6.77, d (8.4)
3’	6.74, s	6.75, s	6.74, s
5’	1.36, s	1.39, s	1.38, s
6’	1.36, s	1.34, s	1.33, s
3’-ester			
2	5.73, s	2.50, sxt (6.9)	2.33, d (7.3)
			2.30, d (7.1)
3		1.76, m	2.16, m
		1.53, m	
4	2.22, s	0.95, t (7.3)	0.98, d (6.7)
5	1.91, s	1.20, d (6.9)	0.98, d (6.7)
2’-OH	4.20, br s	4.14, br s	4.20, br s

[a] Data were obtained at 400 MHz in $CDCl_3$.
[b] Data were obtained at 500 MHz in $CDCl_3$.

Table 9. ^{13}C-NMR Data of Compounds **1-10** (δ in ppm)

position	**1**[a]	**2**[a]	**3**[a]	**4**[a]	**5**[c]	**6**[a]	**7**[b]	**8**[d]	**9**[d]	**10**[a]
2	159.7	159.8	159.7	159.9	159.8	159.7	159.8	159.7	159.7	159.9
3	113.3	113.3	113.2	113.3	113.3	113.2	113.3	113.3	113.3	113.2
4	143.1	143.1	143.2	143.1	143.3	143.2	143.2	143.1	143.2	143.3
5	129.2	129.1	129.1	129.0	129.2	129.2	129.2	129.2	129.2	129.4
6	114.4	114.4	114.4	114.3	114.5	114.4	114.4	114.4	114.4	114.5
7	156.6	156.7	156.6	156.7	156.9	156.6	156.6	156.6	156.7	156.6
8	107.5	107.5	107.4	107.6	107.6	107.3	107.5	107.5	107.4	106.6
9	154.0	154.0	154.0	154.0	154.2	154.0	154.0	154.0	154.1	153.9
10	112.4	112.5	112.5	112.5	112.6	112.5	112.5	112.5	112.5	112.6
2’	77.4	77.4	77.5	77.5	77.8	77.5	77.4	77.3	77.4	77.2
3’	70.3	70.6	70.0	70.2	69.3	70.1	70.2	70.4	70.1	70.4
4’	60.4	59.6	60.5	59.5	60.7	60.4	60.1	60.3	60.2	61.0
5’	25.5	25.3	25.2	25.4	25.1	25.2	25.5	25.5	25.4	25.2
6’	22.0	22.3	22.3	22.3	22.5	22.3	22.2	22.0	22.3	22.2
3’-ester										
1	175.7	169.9	175.4	175.5	165.1	175.8	175.4	172.4	171.8	169.9
2	33.9	20.7	40.9	41.0	115.1	33.9	40.9	35.9	43.1	20.7
3	19.1		26.6	26.6	159.0	19.1	26.6	18.2	25.3	
4	18.5		11.6	11.6	20.5	18.6	11.6	13.7	22.4	
5			16.2	16.3	27.6		16.1		22.5	
4’-ester										
1	175.4	165.2	175.7	165.0	175.4	171.9	166.7	175.5	166.7	171.8
2	41.3	115.0	34.0	115.0	41.3	43.2	127.5	41.3	127.5	46.5
3	26.5	158.2	18.8	158.2	26.6	25.4	138.0	26.6	137.9	69.2
4	11.6	20.4	18.8	20.3	11.6	22.5	15.6	11.6	15.6	29.3
5	16.4	27.5		27.5	16.6	22.5	20.4	16.5	20.4	29.2

[a] Data were obtained at 100 MHz in $CDCl_3$.
[b] Data were obtained at 125 MHz in $CDCl_3$.
[c] Data were obtained at 150 MHz in $CDCl_3$.
[d] Data were obtained at 200 MHz in $CDCl_3$.

Table 10. ^{13}C-NMR Data of Compounds **11-20** (δ in ppm)

position	**11**[c]	**12**[a]	**13**[d]	**14**[a]	**15**[d]	**16**[a]	**17**[c]	**18**[d]	**19**[c]	**20**[d]
2	160.6	159.6	160.6	159.8	160.7	160.1	160.2	160.1	160.6	160.4
3	112.9	113.1	112.6	112.9	112.9	113.1	113.1	113.0	112.7	112.6
4	143.7	143.2	144.0	143.2	143.6	143.3	143.4	143.3	144.0	143.9
5	129.4	129.3	128.8	129.3	128.9	129.1	129.3	129.2	128.8	128.7
6	114.8	114.4	114.7	114.5	114.5	114.5	114.6	114.5	114.7	114.6
7	156.9	156.4	156.0	156.9	156.0	157.0	157.1	157.0	156.2	156.1
8	106.8	107.2	110.8	107.1	110.1	107.6	107.3	107.2	110.8	110.6
9	154.0	153.8	154.3	154.1	154.3	154.2	154.3	154.2	154.5	154.4
10	112.6	112.4	112.4	112.2	112.5	112.6	112.4	112.3	112.5	112.4
2’	77.5	77.0	77.5	78.5	77.7	79.3	78.8	78.7	77.9	77.8
3’	69.8	70.6	72.2	71.7	72.5	73.7	71.7	71.7	71.5	71.3
4’	61.6	60.1	59.9	63.5	69.4	67.8	63.0	63.0	60.3	60.3
5’	24.7	25.5	25.8	25.8	26.2	24.9	25.6	25.5	25.6	25.5
6’	22.6	21.6	22.3	20.6	22.2	21.0	21.3	21.2	22.7	22.6
3’-ester										
1	170.0	169.6	176.0		176.0				165.6	165.6
2	20.7	20.6	41.2		41.2				115.2	115.1
3			26.7		26.8				159.3	159.3
4			11.7		11.7				20.5	20.5
5			16.7		16.5				27.6	27.6
4’-ester										
1	174.3	175.5		178.2	61.0	167.3	167.6	167.5		
2	48.4	41.2		41.4		115.0	115.0	114.9		
3	69.1	26.5		26.7		159.6	159.8	159.8		
4	21.0	11.5		11.6		20.6	20.7	20.6		
5	13.9	16.4		16.5		27.6	27.7	27.7		
solvent*					50.9			50.9		

[a] Data were obtained at 100 MHz in $CDCl_3$.
[b] Data were obtained at 125 MHz in $CDCl_3$.
[c] Data were obtained at 150 MHz in $CDCl_3$.
[d] Data were obtained at 200 MHz in $CDCl_3$.
*solvent residual peak (MeOH)

Table 11. ^{13}C-NMR Data of Compounds **21-22** and **24-30** (δ in ppm)

position	**21**[c]	**22**[b]	**24**[d]	**25**[a]	**26**[a]	**27**[c]	**28**[e]	**29**[d]	**30**[d]
2	159.8	159.8	160.7	159.7	159.7	159.7	164.2	160.1	159.9
3	113.3	113.0	112.2	112.9	113.3	113.3	113.5	113.0	113.0
4	143.2	143.2	144.2	143.3	143.2	143.1	147.0	143.4	143.3
5	129.1	129.0	128.6	129.3	129.2	129.2	130.9	129.2	129.3
6	114.5	114.3	114.9	114.3	114.4	114.4	116.6	114.5	114.5
7	156.9	156.7	156.4	156.4	156.6	156.6	158.7	156.9	156.9
8	107.6	107.5	106.7	107.0	107.2	107.2	113.6	106.7	107.1
9	154.2	154.0	154.6	153.8	154.1	154.0	156.5	154.2	154.2
10	112.6	112.4	110.6	112.4	112.5	112.5	114.5	112.4	112.3
2’	77.7	77.6	79.0	77.0	77.2	77.4	81.0	78.7	78.6
3’	69.4	69.3	70.8	70.5	70.3	70.5	73.9	71.0	71.7
4’	60.5	59.7	61.4	59.9	60.5	60.4	62.9	63.9	63.5
5’	25.2	25.0	24.8	25.2	25.1	25.3	27.6	25.0	25.6
6’	22.6	22.5	21.9	21.8	22.3	22.2	22.3	21.7	20.9
3’-ester									
1	165.2	165.1	172.0	169.7	169.8	169.8			
2	115.3	115.24	20.9	20.5	20.7	20.7			
3	158.7	158.1							
4	22.6	20.3							
5	27.6	27.4							
4’-ester									
1	166.8	165.0		166.8	175.8	171.9		172.1	169.2
2	127.8	115.17		127.3	34.1	43.3		20.9	127.3
3	137.6	157.4		137.5	18.9	25.5			139.1
4	15.6	20.2		15.3	18.8	22.44			15.8
5	20.5	27.3		20.2		22.40			20.4
solvent*				50.3				50.9	

[a] Data were obtained at 100 MHz in $CDCl_3$.
[b] Data were obtained at 125 MHz in $CDCl_3$.
[c] Data were obtained at 150 MHz in $CDCl_3$.
[d] Data were obtained at 200 MHz in $CDCl_3$.
[e] Data were obtained at 100 MHz in CD_3OD.
*solvent residual peak (MeOH)

Table 12. ^{13}C-NMR Data of Compounds **31-40** (δ in ppm)

position	**31**[c]	**32**[e]	**33**[a]	**34**[a]	**35**[c]	**36**[e]	**37**[c]	**38**[e]	**39**[d]	**40**[f]
2	159.7	159.8	160.5	159.8	159.9	159.7	159.6	161.2	161.2	162.8
3	113.2	113.1	112.6	113.3	113.4	113.2	113.1	112.5	112.6	114.3
4	143.2	143.2	143.9	143.1	143.2	143.2	143.1	143.8	143.8	146.5
5	129.2	129.2	128.7	129.0	129.1	129.2	129.3	126.6	126.7	131.8
6	114.3	114.3	114.6	114.3	114.4	114.3	114.3	114.3	114.3	116.5
7	156.6	156.6	156.0	156.7	156.8	156.6	156.4	156.3	156.2	158.8
8	107.5	107.4	110.8	107.7	107.7	107.2	107.3	107.2	107.0	108.8
9	154.0	153.9	154.4	154.1	154.1	153.9	153.8	153.4	153.4	155.9
10	112.4	112.4	112.4	112.5	112.6	112.4	112.3	112.1	112.1	114.9
2’	77.5	77.3	77.6	77.5	77.6	77.4	77.2	77.2	76.5	79.4
3’	70.2	70.1	72.4	70.3	70.3	70.2	70.3	68.3	69.2	72.6
4’	60.5	60.1	60.0	59.5	59.7	60.4	60.2	23.1	23.1	63.1
5’	25.3	25.4	25.7	25.5	25.4	25.31	25.6	23.0	22.7	26.2
6’	22.5	22.4	22.6	22.5	22.6	22.4	21.8	24.6	24.7	23.3
3’-ester										
1	166.3	166.4	166.9	166.3	172.0	171.81	171.6	165.5	172.2	172.7
2	127.0	127.2	127.2	127.2	43.2	43.2	43.0	115.5	43.4	21.4
3	139.6	139.8	139.5	139.3	25.4	25.4	25.3	158.3	25.7	
4	15.7	15.7	15.8	15.7	22.5	22.4	22.4	20.3	22.4	
5	20.4	20.4	20.6	20.3	22.5	22.4	22.3	27.5	22.3	
4’-ester										
1	175.2	166.2		165.0	165.2	171.78	175.3			172.4
2	41.2	126.8		115.1	115.2	43.0	41.2			21.3
3	26.4	138.4		157.8	158.2	25.34	26.5			
4	11.5	15.5		20.4	20.5	22.4	11.6			
5	16.2	20.3		27.4	27.5	22.3	16.5			
solvent*		50.7								

[a] Data were obtained at 100 MHz in $CDCl_3$.
[b] Data were obtained at 125 MHz in $CDCl_3$.
[c] Data were obtained at 150 MHz in $CDCl_3$.
[d] Data were obtained at 200 MHz in $CDCl_3$.
[e] Data were obtained at 75 MHz in $CDCl_3$.
[f] Data were obtained at 125 MHz in CD_3OD.
*solvent residual peak (MeOH)

Table 13. ^{13}C-NMR data of compounds **41-43** (δ in ppm).

position	41[b]	42[a]	43[b]
2	159.9	159.6	159.7
3	113.2	113.3	113.3
4	143.5	143.4	143.4
5	131.4	131.5	131.5
6	107.1	107.1	107.1
7	162.0	161.8	161.9
8	111.3	111.1	111.1
9	151.8	151.9	151.8
10	113.4	113.4	113.4
2’	112.8	112.8	112.7
3’	67.9	68.5	68.5
4’	74.5	74.6	74.6
5’	23.8	23.8	23.7
6’	23.7	23.7	23.7
3’-ester			
1	164.4	175.0	171.3
2	114.2	41.3	43.1
3	161.1	26.8	25.8
4	20.7	11.5	22.4
5	27.6	16.6	22.3

[a] Data were obtained at 100 MHz in $CDCl_3$.
[b] Data were obtained at 125 MHz in $CDCl_3$.

7.5. Partial and total alkaline hydrolysis of 1

Compound **1** (3.2 mg) was dissolved in 1,4-dioxane (0.5 ml) and 0.5 M KOH (0.5 ml) was added at room temperature. The NP-TLC was performed with *n*-hexane and EtOAc (2:1) to confirm reaction progress. After 2 min, the reaction mixture was neutralized with 5% H_2SO_4 (~120 μl), extracted with $CHCl_3$ (1 ml), and concentrated. Hydrolysis product, **1a** (t_R = 11.0 min), **1b** (t_R = 7.1 min), and **1c** (t_R = 7.6 min), were obtained by HPLC (CH_3CN-H_2O, 75:25, 2 ml/min, 327 nm).

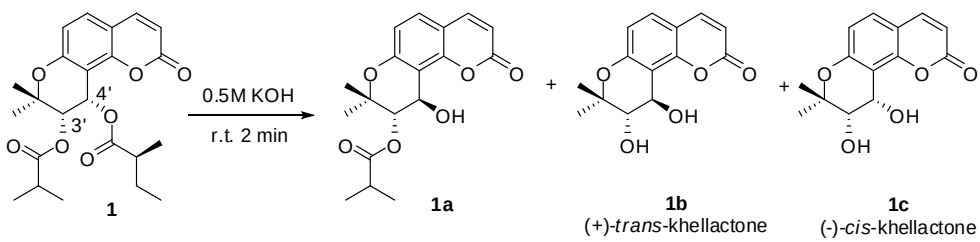

Scheme 6. Reaction of partial and total alkaline hydrolysis of **1**

7.6. Preparation of MTPA esters of 1a

Compound **1a** was dissolved in deuterated pyridine (800 μl) and (*R*)-(-)-MTPA-Cl (10 μl, 0.05 mmol) and DMAP were added. The mixture was left at room temperature overnight, evaporated, and dissolved in $CHCl_3$ (50 μl). Reaction process was confirmed by silica TLC using n-hexane and EtOAc (2:1). The resulting (*S*)-MTPA ester **1aa** (13.9 min) was purified by HPLC (CH_3CN-H_2O, 90:10, 2 ml/min) using INNO C18 column (10 × 250 mm, S-5 μm, 12 nm). Likewise, (*S*)-(+)-MTPA-Cl (10 μl, 0.05 mmol) was added to **1a** to afford (*R*)-MTPA ester **1ab** (13.1 min).

7.7. Preparation of MTPA esters of 16

Compound **16** (0.4 mg, 0.001 mmol) was resuspended in deuterated pyridine (600 μl), and reacted with (*R*)-(-)-MTPA-Cl (10 μl, 0.05 mmol) under nitrogen gas stream. The resulting mixture was subjected to silica capillary CC (7 x 0.5 cm) eluting with *n*-hexane-EtOAc (5:1). Fifty drops were collected in a vial and (*S*)-MTPA ester was attained from 15th-21st vial. The analytical NP-TLC (*n*-hexane-EtOAc, 3:1) was applied to confirm reaction progress. In the same manner, (*S*)-(+)-MTPA-Cl (10 μl, 0.05 mmol) was treated to **16** (0.5 mg, 0.002 mmol) to acquire (*R*)-MTPA ester.

7.8. Preparation of MTPA esters of 17 and 18

Enantiomeric mixture **E1** (mixture of **17** and **18**, 0.5 mg) was substituted with nitrogen gas, deuterated pyridine (800 μl), (*R*)-(-)-MTPA-Cl (10 μl, 0.05 mmol), and DMAP were added. The progress of reaction was confirmed by silica TLC using *n*-hexane and EtOAc (2:1). The resulting (*S*)-MTPA esters **17a** (53.8 min) and **18a** (49.7 min) were isolated by HPLC (CH_3CN-H_2O, 75:25. 5 ml/min) with INNO C18 column (20 × 250 mm, S-5 μm, 12 nm). To obtain (*R*)-MTPA esters **17b** (49.4 min) and **18b** (53.5 min), (*S*)-(+)-MTPA-Cl (10 μl, 0.05 mmol) was reacted with **E1** (0.4 mg). Resulting MTPA esters were confirmed by NMR and ECD spectra (Figure 95).

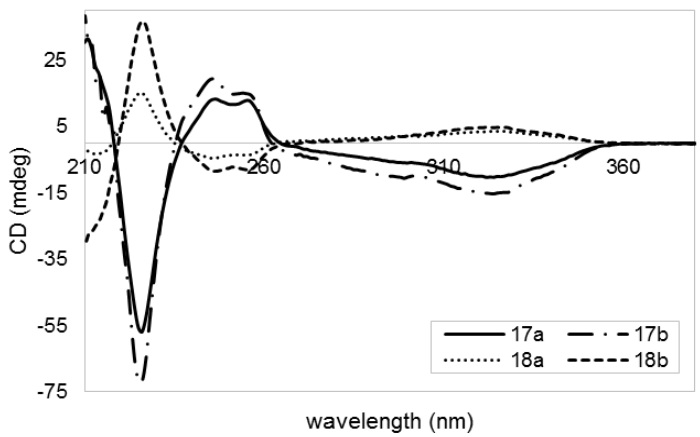

Figure 95. ECD curves of MTPA esters of **E1** (mixture of enantiomers **17** and **18**)

7.9. Preparation of MTPA esters of 19 and 20

In the same manner with **17** and **18**, (*S*)-MTPA esters **19a** (66.1 min) and **20a** (70.4 min), (*R*)-MTPA esters **20b** (66.2 min) and **19b** (70.5 min) were yielded. Obtained MTPA esters were analyzed by NMR and ECD spectra (Figure 96).

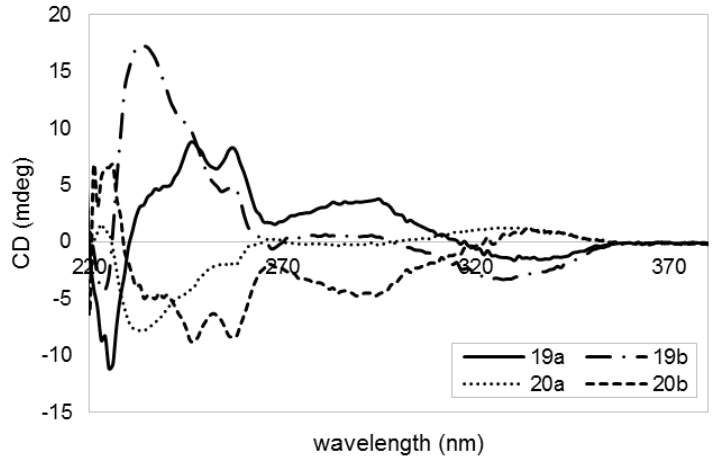

Figure 96. ECD curves of MTPA esters of **E2** (mixture of enantiomers **19** and **20**)

7.10. X-ray crystallographic analysis of 1 and 2

Diffraction data were collected by SuperNova, Dual, Cu at zero, AtlasS2 diffractometer with Cu Kα radiation (λ = 1.54184). Using Olex2, the structure was solved by direct methods with ShelXT structure solution program and refined by Least Squares minimization with ShelXL refinement package. The crystallographic data of **1** and **2** were deposited at the Cambridge Crystallographic Data Centre (CCDC deposition number, **1**: 1488681, **2**: 1474283).

7.10.1. Crystal data of **1**

colorless crystal, $C_{23}H_{28}O_7$, M = 416.45, monoclinic, crystal size 0.3 × 0.101 × 0.031 mm^3, space group $P2_1$ (no. 4), a = 24.3633(4) Å, b = 9.12727(13) Å, c = 31.0898(6) Å, β = 109.128(2)°, V = 6531.8(2) Å^3, Z = 12, T = 100(80) K, μ (Cu Kα) = 0.774 mm^{-1}, D_{calc} = 1.270 g/cm^3, 39478 reflections collected (7.274° ≤ 2Θ ≤ 153.672°), 20639 independent reflections (R_{int} = 0.0243, R_{sigma} = 0.0335), Goodness of fit on F^2 = 1.031, final R_1 0.0417 (I> 2σ (I)), 0.0464 (all data), final wR_2 0.1069 (I> 2σ (I)), 0.1107 (all data), Flack parameter = 0.08(6).

7.10.2. Crystal data of **2**

colorless crystal, $C_{21}H_{22}O_7$, M = 386.38, monoclinic, crystal size 0.2 × 0.059 × 0.024 mm^3, space group $P2_1$ (no. 4), a = 9.68785(12) Å, b = 6.62844(9) Å, c = 15.2024(2) Å, β = 103.8888(13)°, V = 947.69(2) Å^3, Z = 2, T = 100.0(2) K, μ (Cu Kα) = 0.851 mm^{-1}, D_{calc} = 1.354 g/cm^3, 19091 reflections collected (9.404° ≤ 2Θ ≤ 152.988°), 3883 independent reflections (R_{int} = 0.0347, R_{sigma} = 0.0220), Goodness of fit on F^2 = 1.062, final R_1 0.0276 (I> 2σ (I)), 0.0287 (all data), final wR_2 0.0705 (I> 2σ (I)), 0.0715 (all data), Flack parameter = -0.03(6).

7.11. ECD calculation

The ground-state geometry optimization was performed in Turbomole using def-SV(P) basis set, B3LYP functional, and density functional theory (DFT) method. The calculated ECD data were acquired by TD-DFT using the basis set def-SV(P) and B3LYP functional. Using Gaussian functions, the ECD spectra were simulated by overlapping each transition. (σ: width of the band at 1/*e* height, ΔEi : excitation energies for transition *i*, *Ri* : rotatory strengths for transition *i*, σ was 0.10 eV in this work)

$$\Delta\epsilon(E) = \frac{1}{2.297 \times 10^{-39}} \frac{1}{\sqrt{2\pi\sigma}} \sum_{i}^{A} \Delta E_i R_i \, e^{[-(E-\Delta E_i)^2/(2\sigma)^2]}$$

7.12. Evaluation of inhibitory effect on NO production in LPS-stimulated RAW264.7 cells

7.12.1. Reagents

Dulbecco's modified Eagle's media (DMEM), fetal bovine serum (FBS), and phosphate buffered saline (PBS) were purchased from Hyclone Laboratories, Inc. (Logan, UT, USA). Penicillin (10,000 units/ml)/streptomycin (10 mg/ml) and 0.25% trypsin-EDTA were obtained from Life Technologies Corporation (Grand Island, NY, USA). Lipopolysaccharides (LPS, from *Escherichia coli* 0111:B4), N_{ω}-Nitro-L-arginine methyl ester hydrochloride (L-NAME), sodium nitrite, sulfanilamide, *N*-(1-Naphthyl)ethylenediamine dihydrochloride (NEDHC), thiazolyl blue tetrazolium bromide (MTT), and dimethyl sulfoxide (DMSO, 99.9%) were purchased from Sigma-Aldrich Co. (St. Louis, MO, USA). Phosphoric acid (85.0%) and DMSO (99.5%) were obtained from Daejung Chemicals & Metals Co., Ltd. (Siheung, Korea). Multi well culture plate (48 well and 96 well) was purchased from SPL Life Sciences Co., Ltd. (Pocheon, Korea) and cell culture dish (100π) from Thermo Fisher Scientific Inc. (Waltham, MA, USA).

7.12.2. Cell cultures

RAW264.7 cells were acquired from Korean Cell Line Bank (Seoul, Korea) and maintained in DMEM with 10% FBS and 1% penicillin/streptomycin.

7.12.3. Griess assay

RAW264.7 cells were seeded at 1 x 10^6 cells/ml in 48 well plates and incubated for 24 h and treated with compounds for 1 h before adding LPS (1 ng/ml). The final DMSO concentration was maintained under 0.05%. After 16 h incubation, 100 μl of sample aliquots were transferred to a 96 well plate and mixed with 100 μl of mixture of Griess reagent A and B (A: 0.1 % NEDHC, B: 1 % sulfanilamide and 2 %

phosphoric acid). The absorbance was measured at 550 nm. The NO concentration was calculated using nitrite standard curve (Dawson et al. 1994).

7.12.4. MTT assay

After moving 100µl of sample aliquots for Griess assay, MTT solution (2 mg/ml, 20 µl) was added to each well in 48 well plate, which were incubated for 1 h 30 min. The supernatant was removed and formazan was dissolved with 200 µl of DMSO and 100 µl of solution was transferred to a 96 well plate. The absorbance was measured at 540 nm. The percent cell viability is absorbance of sample-treated well compared to that of control well.

Chapter 8. Conclusion

Sixteen new khellactone esters (**1-16**) and three new angular furanocoumarins (**41-43**) were isolated from the *n*-hexane and $CHCl_3$ fractions of the *Peucedanum japonicum* roots. Additionally, forty-five known compounds were obtained, which were identified as angular dihydropyranocoumarins (**17-40**), linear furanocoumarins (**44-47**), an angular dihydrofuranocoumarin (**48**), a linear dihydropyranocoumarin (**49**), simple coumarins (**50-58**), a chromone (**59**), ferulic acid derivatives (**60-61**), a lignan (**62**), a phenylpropanoid (**63**), and an indole alkaloid (**64**).

An angular dihydropyranocoumarin moiety was easily identified by typical chemical shift and coupling constant in ^{1}H NMR. The position of the substituents at 3' and 4' was determined by HMBC and partly with MS fragmentation. The relative configuration was elucidated by *J* value and NOESY correlation, however, it was necessary to conduct Mosher method or X-ray crystallography to determine the absolute configuration. In the case of diacyl angular dihydropyranocoumarin, partial hydrolysis was carried out to obtain a free 4'-OH prior to the Mosher method.

In addition, CD and ECD calculation could be applied to determine the absolute configuration, if these coumarins could not make single crystal. If the khellactone ester exhibited a negative first Cotton effect at 318-329 nm, a NOESY correlation between 3' and 4' protons, and *J* value (4.6 ~ 5.0 Hz) between 3' and 4' protons, the absolute configuration could be suggested as 3'(S) and 4'(S) regardless of the presence of the 3'- or 4'-substituents.

The enantiomers could exist in these angular dihydropyranocoumarins, and be isolated using chiral-selective column. Because the ratios of the major and minor MTPA reaction products and enantioseparation products were similar, HPLC analysis of MTPA reaction products could be applied to detect the enantiomers.

In the case of monoacylkhellactone, 3'- and 4'- substituents could be interconverted and the equilibrium was reached about 4 days after purification. Because of acyl migration, 3'- and 4'- positional isomers might be isolated together..

The major MS fragment peak of khellactone ester was observed without a 4'-ester moiety, which was more dominant than that without a substituent at 3'-position.

Therefore, the position of 3'- and 4'-substituents could be suggested in consideration of the MS fragmentation.

Among the isolated compounds, the NO production inhibitory activity was tested in LPS-induced RAW264.7 cells. As a result, compounds **1**, **3-6**, **22**, **31**, and **36-38** exhibited significant inhibitory activity without cytotoxicity. Based on the structure-activity relationship, it was revealed that the presence of isobutyryl, senecioyl, 2-methylbutyryl, and isovaleryl groups at 3' position was important for the activity than the acetyl and angeloyl groups.

References

Bae KH (2001) *Medicinal plants of Korea*. Kyo-Hak Publishing Corporation, Seoul, Korea p 379.

Bae YS (2002) Antifungal agent using falcarindiol extracted from *Peucedanum japonicum*. KR2002053474A.

Bergendorff O, Dekermendjian K, Nielsen M, Shan R, Witt R, Ai J, Sterner O (1997) Furanocoumarins with affinity to brain benzodiazepine receptors in vitro. *Phytochemistry* 44 (6):1121-1124.

Bohlmann F, Rode KM (1968) Natural coumarin derivatives. II. Coumarins from *Libanotis buchtormensis*. *Chem Ber* 101 (8):2741-2746

Buendia-Trujillo AI, Torrres-Valencia JM, Joseph-Nathan P, Burgueno-Tapia E (2014) The absolute configuration of angular 3'-acyloxypyranocoumarins by vibrational circular dichroism exciton chirality. *Tetrahedron: Asymmetry* 25 (20-21):1418-1423.

Chen I-S, Chang C-T, Sheen W-S, Teng C-M, Tsai I-L, Duh C-Y, Ko F-N (1996) Coumarins and antiplatelet aggregation constituents from Formosan *Peucedanum japonicum*. *Phytochemistry* 41:525-530.

Choi HC, Rho TC, Kim BY, Ko HR, Oh WK, Seong CK, Mheen TI, Ahn JS, Lee HS (1999) Inhibition of nitric oxide production by coumarins from *Peucedanum japonicum* in LPS-activated RAW 264.7 cells. *Saengyak Hakhoechi* 30:99-104

Chun J, Tosun A, Kim YS (2016) Anti-inflammatory effect of corymbocoumarin from *Seseli gummiferum* subsp. corymbosum through suppression of NF-κB signaling pathway and induction of HO-1 expression in LPS-stimulated RAW 264.7 cells. *Int Immunopharmacol* 31:207-215.

Dawson VL, Brahmbhatt HP, Mong JA, Dawson TM (1994) Expression of inducible nitric oxide synthase caused delayed neurotoxicity in primary mixed neuronal-glial cortical cultures. *Neuropharmacology* 33 (11): 1425-1430.

Duh CY, Wang SK, Wu YC (1991) Cytotoxic pyranocoumarins from the ae

rial parts of *Peucedanum japonicum*. *Phytochemistry* 30:2812-2814

Duh CY, Wang SK, Wu YC (1992) Cytotoxic pyranocoumarins from roots of *Peucedanum japonicum*. *Phytochemistry* 31:1829-1830

Elgamal MHA, Shalaby nMM, Duddeck H, Hiegemann M (1993) Coumarins and coumarin glucosides from the fruits of *Ammi majus*. *Phytochem istry* 34 (3):819-823.

Gan WS (1965) *Manual of medicinal plants in Taiwan*. National Research I nstitute of Chinese Medicine, Taichung, Taiwan Vol. 3, p 675.

Gonzalez AG, Barroso JT, Lopez-Dorta H, Luis JR, Rodriguez-Luis F (197 9) Constituents of the Umbelliferae. Part 21. Pyranocoumarin derivati ves from *Seseli tortuosum*. *Phytochemistry* 18 (6):1021-1023.

Gonzalez AG, Estevez Reyes R, Rivero Espino M (1977) New sources of n atural coumarins. Part 34. Two new coumarins from *Ruta pinnata*. *P hytochemistry* 16 (12):2033-2035.

Hisamoto M, Kikuzaki H, Nakatani N (2004) Constituents of the Leaves of *Peucedanum japonicum* Thunb. and Their Biological Activity. *J Agric Food Chem* 52:445-450.

Hisamoto M, Kikuzaki H, Ohigashi H, Nakatani N (2003) Antioxidant comp ounds from the leaves of *Peucedanum japonicum* Thunb. *J Agric Fo od Chem* 51:5255-5261.

Hsiao G, Ko F-N, Jong T-T, Teng C-M (1998) Antiplatelet action of 3',4'-di isovalerylkhellactone diester purified from *Peucedanum japonicum* Th unb. *Biol Pharm Bull* 21:688-692.

Huong DTL, Choi HC, Rho TC, Lee HS, Lee MK, Kim YH (1999) Inhibit ory activity of monoamine oxidase by coumarins from *Peucedanum j aponicum*. *Arch Pharmacal Res* 22:324-326.

Ikeshiro Y, Mase I, Tomita Y (1992) Dihydropyranocoumarins from roots of *Peucedanum japonicum*. *Phytochemistry* 31 (12):4303-4306.

Ikeshiro Y, Mase I, Tomita Y (1993) Dihydropyranocoumarins from *Peuceda num japonicum*. *Phytochemistry* 33:1543-1545.

Ikeshiro Y, Mase I, Tomita Y (1994) Coumarin glycosides from *Peucedanu m japonicum*. *Phytochemistry* 35:1339-1341.

Jang K-C, Kim S-C, Song E-Y, Um Y-C, Kim SC, Lee Y-J (2008) Isolation and identification of anticancer and anti-inflammatory substances in *Peucedanum japonicum* Thumb. *Acta Hortic* 765:49-53

Jiang H, Sugiyama T, Hamajima A, Hamada Y (2011) Asymmetric Synthesis of 2-Substituted Dihydrobenzofurans and 3-Hydroxydihydrobenzopyrans through the Enantioselective Epoxidation of O-Silyl-Protected ortho-Allylphenols. *Adv Synth Catal* 353 (1):155-162.

Jong TT, Hwang HC, Jean MY, Wu TS, Teng CM (1992) An antiplatelet aggregation principle and x-ray structural analysis of cis-khellactone diester from *Peucedanum japonicum*. *J Nat Prod* 55:1396-1401.

Juichi M, Inoue M, Ikegami M, Kajiura I, Omura M, Furukawa H (1988) Constituents of domestic citrus plants. Part VII. New coumarins from *Citrus funadoko*. *Heterocycles* 27 (6):1451-1454.

Jung S, Li C, Lee S, Ohk J, Kim S-k, Lee M-S, Moon H-I (2012) Inhibitory effect and mechanism on antiproliferation of khellactone derivatives from herbal suitable for medical or food uses. *Food Chem Toxicol* 50 (3-4):648-652.

Kaplanski G, Marin V, Montero-Julian F, Mantovani A, Farnarier C (2003) IL-6: a regulator of the transition from neutrophil to monocyte recruitment during inflammation. *Trends Immunol* 24 (1):25-29.

Kim DH, Han CS, Kim GE, Kim JH, Kim SG, Kim HK, Oh OJ, Whang WK (2009) Biological activities of isolated compounds from Peucedani Radix. *Yakhak Hoechi* 53:130-137

Kim HJ, Kim HM, Ryu B, Lee W-S, Shin J-S, Lee K-T, Jang DS (2016) Constituents of PG201 (Layla), a multi-component phytopharmaceutical, with inhibitory activity on LPS-induced nitric oxide and prostaglandin E2 productions in macrophages. *Arch Pharmacal Res* 39 (2):231-239.

Kong L-Y, Min Z-D, Li Y, Pei Y-H (1996) Qianhucoumarin I from *Peucedanum praeruptorum*. *Phytochemistry* 42 (6):1689-1691.

Kong LY, Pei YH, Li X, Wang SX, Hou BL, Zhu TR (1993) The isolation and identification of qianhucoumarin B and qianhucoumarin C from

Peucedanum praeruptorum. *Yaoxue Xuebao* 28 (10):772-776

Korhonen R, Lahti A, Kankaanranta H, Moilanen E (2005) Nitric oxide pro duction and signaling in inflammation. *Curr Drug Targets: Inflammat ion Allergy* 4 (4):471-479.

Lee G, Park H-G, Choi M-L, Kim YH, Park YB, Song K-S, Cheong C, Ba e Y-S (2000) Falcarindiol, a polyacetylenic compound isolated from *Peucedanum japonicum*, inhibits mammalian DNA topoisomerase I. *J Microbiol Biotechnol* 10:394-398

Lee J, Lee YJ, Kim J, Bang O-S (2015) Pyranocoumarins from root extracts of *Peucedanum praeruptorum* dunn with multidrug resistance reversa l and anti-inflammatory activities. *Molecules* 20 (12):20967-20978.

Lee JW, Lee C, Jin Q, Yeon ET, Lee D, Kim S-Y, Han SB, Hong JT, Lee MK, Hwang BY (2014) Pyranocoumarins from *Glehnia littoralis* inh ibit the LPS-induced NO production in macrophage RAW 264.7 cell s. *Bioorg Med Chem Lett* 24 (12):2717-2719.

Lee JW, Roh TC, Rho M-C, Kim YK, Lee HS (2002) Mechanisms of relax ant action of a pyranocoumarin from *Peucedanum japonicum* in isola ted rat thoracic aorta. *Planta Med* 68:891-895.

Lee K, Lee J-H, Boovanahalli SK, Choi Y, Choo S-J, Yoo I-d, Kim DH, Y un MY, Lee GW, Song G-Y (2010) Synthesis of (S)-(+)-decursin an d its analogues as potent inhibitors of melanin formation in B16 mur ine melanoma cells. *Eur J Med Chem* 45 (12):5567-5575.

Lee SO, Choi SZ, Lee JH, Chung SH, Park SH, Kang HC, Yang EY, Cho HJ, Lee KR (2004) Antidiabetic coumarin and cyclitol compounds fr om *Peucedanum japonicum*. *Arch Pharmacal Res* 27:1207-1210.

Li J, Shen Q, Bao C-H, Chen L-T, Li X-R (2014) A new dicoumarinyl eth er from the roots of *Stellera chamaejasme* L. *Molecules* 19 (2):1603-1607.

Lou H-x, Sun L-r, Yu W-t, Fan P-h, Cui L, Gao Y-h, Ma B, Ren D-m, Ji M (2004) Absolute configuration determination of angular dihydrocou marins from *Peucedanum praeruptorum*. *J Asian Nat Prod Res* 6 (3):177-184.

Lu M, Nicoletti M, Battinelli L, Mazzanti G (2001) Isolation of praeruptorin s A and B from *Peucedanum praeruptorum* and their general pharma cological evaluation in comparison with extracts of the drug. *Farmac o* 56 (5-6-7):417-420.

Lv H, Luo J, Wang X, Kong L (2013) Application of UPLC-Quadrupole-T OF-MS coupled with recycling preparative HPLC in isolation and pre paration of coumarin isomers with similar polarity from *Peucedanum praeruptorum*. *Chromatographia* 76:141-148.

M. Swager T, H. Cardellina Ii J (1985) Coumarins from *Musineon divaricat um*. *Phytochemistry* 24 (4):805-813.

Macias FA, Massanet GM, Rodriguez-Luis F, Salva J, Fronczek FR (1989) Carbon-13 NMR of coumarins. II. Khellactones: spectroscopic criteria to establish the relative configuration of the dihydropyran ring. *Mag n Reson Chem* 27:653-658.

Martinez-Luis S, Gomez JF, Spadafora C, Guzman HM, Gutierrez M (2012) Antitrypanosomal alkaloids from the marine bacterium *Bacillus pumil us*. *Molecules* 17:11146-11155.

Marumoto S, Miyazawa M (2012) Structure-activity relationships for naturall y occurring coumarins as β-secretase inhibitor. *Bioorg Med Chem* 20 (2):784-788.

Mohammadi M, Yousefi M, Habibi Z, Shafiee A (2010) Two new coumarin s from the chloroform extract of *Angelica urumiensis* from Iran. *Che m Pharm Bull* 58:546-548.

Molloy RG, Mannick JA, Rodrick ML (1993) Cytokines, sepsis and immuno modulation. *Br J Surg* 80 (3):289-297

Morioka T, Suzui M, Nabandith V, Inamine M, Aniya Y, Nakayama T, Ichi ba T, Mori H, Yoshimi N (2004) The modifying effect of *Peucedan um japonicum*, a herb in the Ryukyu Islands, on azoxymethane-induc ed colon preneoplastic lesions in male F344 rats. *Cancer Lett* 205:13 3-141.

Nishanbaev SZ, Bobakulov KM, Abdullaev ND, Sham'yanov ID (2015) Phen olcarboxylic Acids from *Quercus robur* Growing in Uzbekistan. *Che*

m Nat Compd 51 (3):537-539.

Ren Y, Yuan C, Deng Y, Kanagasabai R, Ninh TN, Tu VT, Chai H-B, Soejarto DD, Fuchs JR, Yalowich JC, Yu J, Douglas Kinghorn A (2015) Cytotoxic and natural killer cell stimulatory constituents of *Phyllanthus songboiensis*. *Phytochemistry* 111:132-140.

Sarkhail P (2014) Traditional uses, phytochemistry and pharmacological properties of the genus *Peucedanum*: A review. *J Ethnopharmacol* 156:235-270.

Shin KH, Kang SS, Chi HJ (1992) Analysis of the coumarin constituents in peucedanii radix. *Saengyak Hakhoechi* 23:20-23

Shul'ts EE, Ganbaatar Z, Petrova TN, Shakirov MM, Bagryanskaya IY, Taraskin VV, Radnaeva LD, Otgonsuren D, Pokrovskii AG, Tolstikov GA (2012) Plant coumarins. IX. Phenolic compounds of *Ferulopsis hystrix* growing in Mongolia. Cytotoxic activity of 8,9-dihydrofurocoumarins. *Chem Nat Compd* 48 (2):211-217.

Song Y-L, Jing W-H, Tu P-F, Wang Y-T (2014) Enantiomeric separation of angular-type pyranocoumarins from Peucedani Radix using AD-RH chiral column. *Nat Prod Res* 28 (8):545-550

Song Y-L, Zhang Q-W, Li Y-P, Ru Y, Wang Y-T (2012) Enantioseparation and absolute configuration determination of angular-type pyranocoumarins from Peucedani Radix using enzymatic hydrolysis and chiral HPLC-MS/MS analysis. *Molecules* 17:4236-4251.

Tosun A, Ozkal N, Baba M, Okuyama T (2005) Pyranocoumarins from *Seseli gummiferum* subsp. corymbosum Growing in Turkey. *Turk J Chem* 29 (3):327-334

Valencia-Islas N, Abbas H, Bye R, Toscano R, Mata R (2002) Phytotoxic Compounds from *Prionosciadium watsoni*. *J Nat Prod* 65 (6):828-834.

Vila-Nova NS, Maia de Morais S, Falcao MJC, Alcantara TTN, Ferreira PAT, Cavalcanti ESB, Vieira IGP, Campello CC, Wilson M (2013) Different susceptibilities of *Leishmania* spp. promastigotes to the *Annona muricata* acetogenins annonacinone and corossolone, and the *Platymiscium floribundum* coumarin scoparone. *Exp Parasitol* 133 (3):334-33

8.

Wang X-Y, Li J-F, Jian Y-M, Wu Z, Fang M-J, Qiu Y-K (2015) On-line comprehensive two-dimensional normal-phase liquid chromatography × reversed-phase liquid chromatography for preparative isolation of *Peucedanum praeruptorum*. *J Chromatogr A* 1387:60-68.

Whang WK, Lee SJ, Kim H, Cho H, Lee KS, Kang IH, Ham I (2001) Standardization of Peucedani radix. Saengyak Hakhoechi 32 (4):292-296

Yakabe Y, Terato M, Higa A, Yamada K, Kitamura Y (2012) Iron availability alters ascorbate-induced stress metabolism in *Glehnia littoralis* root cultures. *Phytochemistry* 74:100-104.

Yu P-J, Jin H, Zhang J-Y, Wang G-F, Li J-R, Zhu Z-G, Tian Y-X, Wu S-Y, Xu W, Zhang J-J, Wu S-G (2012) Pyranocoumarins Isolated from *Peucedanum praeruptorum* Dunn Suppress Lipopolysaccharide-Induced Inflammatory Response in Murine Macrophages Through Inhibition of NF-κB and STAT3 Activation. *Inflammation* 35 (3):967-977.

Zhao N-C, Jin W-B, Zhang X-H, Guan F-L, Sun Y-B, Adachi H, Okuyama T (1999) Relaxant effects of pyranocoumarin compounds isolated from a chinese medical plant, Bai-Hua Qian-Hu, on isolated rabbit tracheas and pulmonary arteries. *Biol Pharm Bull* 22 (9):984-987.

Znati M, Ben Jannet H, Cazaux S, Souchard JP, Skhiri FH, Bouajila J (2014) Antioxidant, 5-lipoxygenase inhibitory and cytotoxic activities of compounds isolated from the *Ferula lutea* flowers. *Molecules* 19 (10): 16959-16975.

국문초록

식방풍 (Peucedani Japonici Radix) 은 미나리과 (Umbelliferae) 에 속하는 갯기름나물 (*Peucedanum japonicum* Thunberg) 의 뿌리이다. 갯기름나물은 남부와 동부 아시아 국가들에 널리 분포되어 있으며, 식방풍은 한국과 대만 등지에서 전통적으로 감기나 통증을 치료하는데 사용되어 왔다.

식방풍에서는 coumarin, chromone, polyacetylene, sugar alcohol, steroid glycoside 등이 분리 보고되었으며, 이중에서 coumarin이 대표성분으로 알려져 있다. 식방풍의 활성으로는 항산화, 항염증, 항균작용과 림프성백혈병세포에 대한 세포독성효과가 보고된 바 있다.

본 연구에서는, 식방풍의 헥산과 클로로포름 분획물로부터 총 64종의 화합물이 분리되었고, 그 중 19종의 신규화합물은 angular dihydropyrano coumarins (**1-16**) 와 angular monohydro-monohydroxy-furano coumarins (**41-43**) 로, 각각 (3'*S*,4'*S*)-3'-*O*-isobutyryl-4'-*O*-(2-methylbutyryl)khellactone (**1**), (3'*S*,4'*S*)-3'-*O*-acetyl-4'-*O*-senecioylkhellactone (**2**), (3'*S*,4'*S*)-4'-*O*-isobutyryl-3'-*O*-(2-methylbutyryl)khellactone (**3**), (3'*S*,4'*S*)-3'-*O*-(2-methylbutyryl)-4'-*O*-senecioyl khellactone (**4**), (3'*S*,4'*S*)-4'-*O*-(2-methylbutyryl)-3'-*O*-senecioylkhellactone (**5**), (3'*S*,4'*S*)-3'-*O*-isobutyryl-4'-*O*-isovaleryl khellactone (**6**), (3'*S*,4'*S*)-4'-*O*-angeloyl-3'-*O*-(2-methylbutyryl)khellactone (**7**), (3'*S*,4'*S*)-3'-*O*-butyryl-4'-*O*-(2-methyl butyryl)khellactone (**8**), (3'*S*,4'*S*)-4'-*O*-angeloyl-3'-*O*-isovalerylkhellactone (**9**), (3'*S*,4'*S*)-3'-*O*-acetyl-4'-*O*-(3-hydroxyisovaleryl)khellactone (**10**), (3'*S*,4'*S*)-3'-*O*-acetyl-4'-*O*-(3-hydroxy-2-methylbutyryl)khellactone (**11**), (3'*S*,4'*S*)-3'-*O*-acetyl-4'-*O*-(2-methylbutyryl)khellactone (**12**), (3'*S*,4'*S*)-3'-*O*-(2-methylbutyryl)khellactone (**13**), (3'*S*,4'*S*)-4'-*O*-(2-methylbutyryl)khellactone (**14**), (3'*S*,4'*S*)-4'-*O*-methyl-3'-*O*-(2-methylbutyryl)khellactone (**15**), (3'*S*,4'*R*)-4'-*O*-senecioylkhellactone (**16**), 2'-hydroxy-3'-*O*-senecioylvaginol (**41**), 2'-hydroxy-3'-*O*-(2-methylbutyryl)vaginol (**42**), 2'-hydroxy-3'-*O*-isovalerylvaginol (**43**) 로 명명하였다. 분리된 기지화합물들의 구조는 angular dihydropyranocoumarins (**17-40**), linear furanocoumarins (**44-47**), angular dihydrofuranocoumarin (**48**), linear dihydropyranocoumarin (**49**),

simple coumarins (**50-58**), chromone (**59**), ferulic acid derivatives (**60-61**), lignan (**62**), phenylpropanoid (**63**), indole alkaloid (**64**) 로 규명되었다.

분리된 화합물 중 angular dihydropyranocoumarins (khellactones) 가 대부분을 차지하는데, 이것은 monoacyl기를 가진 형태와 diacyl기를 가진 형태 두 가지가 있다. Monoacylkhellactones의 경우에는 MTPA 반응을 통해 절대구조를 결정할 수 있지만, diacylkhellactones의 경우에는 수산기의 부재로 인하여 입체구조를 밝히는 것이 매우 어렵다. 따라서 본 연구에서는 부분 가수분해를 통하여 4'위치의 치환기를 제거 후 Mosher method를 사용하거나 X선 회절분석법을 통하여 3'과 4'위치의 절대구조를 결정하였다. 그러나 부분 가수분해와 단결정 생성은 성공률이 매우 낮기 때문에 나머지 구조들을 이용하여 ECD 측정과 계산을 통해 입체구조를 결정하는 방법 또한 제시하였다.

분리과정 중, 거울상 이성질체의 존재를 확인하였으며 카이랄 컬럼을 이용하여 분리하였다. 거울상 이성질체의 검출과 분리는 카이랄 컬럼으로 하는 것이 가장 이상적이지만 분리할 화합물에 적합한 컬럼을 찾는 것이 어렵고 컬럼이 고가라는 단점이 있다. 따라서, 거울상 이성질체 혼합물의 MTPA 유도체를 역상 HPLC 컬럼으로 분석해도 카이랄 컬럼으로 분석했을 때와 유사한 분리능을 갖는다는 점을 통해 손쉬운 거울상 이성질체의 확인방법을 제시하였다. 이외에도 *cis*형태의 monoacylkhellactones의 경우 3'과 4'위치에서 acyl기의 상호전환이 나타나서 3'과 4'의 위치이성질체가 모두 나타나는 현상도 발견했다. 또한, MS를 측정하였을 때, 4'위치의 치환기가 3'위치의 치환기보다 우세하게 이탈하는 fragmentation을 관찰하여 HMBC의 측정없이도 3'과 4'위치의 치환기를 연결하는 방법 또한 확인되었다.

분리된 화합물을 대상으로 LPS로 유도한 RAW264.7 세포주에 대해 NO 생성 저해능을 평가하였다. 화합물 중 **1**, **3-6**, **22**, **31**, **36-38**가 강한 NO생성 저해능을 나타내었다.

이상의 결과로 다양한 실험을 통해 절대구조를 결정하는 방법을

제시하였다. 이러한 방법들은 유사한 구조의 입체구조를 결정하는데 있어 유용한 길잡이가 될 것으로 전망된다. 또한 분리된 화합물들을 염증성 질환 약물 개발에 후보물질로 발전시킬 가능성도 기대된다.

주요어 : 갯기름나물, 식방풍, angular dihydropyranocoumarins, khellactone esters, 부분가수분해, X선결정학, 원편광이색성
학 번 : 2012-31116